

**ANALYTICAL APPROACH BASED GENERATION PLANNING
WITH WIND ENERGY INTEGRATION**

By

© Amir Ahadi

A thesis submitted to the School of Graduate Studies

In partial fulfilment of the requirements for the degree

of

Master of Engineering

Faculty of Engineering and Applied Science

Memorial University of Newfoundland

October 2018

St. John's

Newfoundland and Labrador

Canada

Abstract

A large power grid consists of generation, transmission, and distribution. Power system planning is to develop new and upgrade existing power grids to satisfy the future load demand. Reliability evaluation has a great importance in power system planning and is viewed from two aspects, adequacy and system security. This thesis focuses on adequacy, which concerns the existence of enough power generation in the system to satisfy load demand. The output power of a wind turbine depends on wind speed which is highly uncertain and random. Hence, the first step in generation adequacy evaluation is modeling wind speed. In this research, the wind speed was predicted using the ARMA model and artificial neural network (ANN). After this step, hourly power output of wind energy was determined. This was done by the power curve characteristics of the wind turbine. Fuzzy C-Means (FCM) was then used to reduce the number of states in the wind turbine generator model. The main objective of this thesis is to evaluate the influence of wind energy to the overall reliability of the system. In addition, megawatt (MW) capacity of wind energy system required for replacing conventional generators while maintaining the same risk criteria was investigated. In this thesis, the Roy Billinton Test System (RBTS) was adopted for generation adequacy evaluation. The St. John's International Airport was selected as the wind speed measurement site. The Vestas V90-2MW (IEC IIIA) was selected as the wind turbine for the case study. The main contributions of this thesis include modeling of generation adequacy evaluation of wind energy systems using an analytical approach; wind speed prediction by ARMA and Neural Networks; Fuzzy C means algorithm to reduce the number of wind turbine states; standalone renewable energy system design; and a procedure and guideline development for generation planning with wind power integration using the analytical approach.

Acknowledgments

I would like to express my sincere gratitude and appreciation to my supervisor, Prof. Xiaodong Liang, for her continuous guidance, support, encouragement, motivation, and patience. It has been a great pleasure doing my M.Eng under her supervision. Dr. Liang's kind guidance have helped me in all the time of research and without her precious support it would not be possible to conduct this research.

I appreciate the financial support from Memorial University of Newfoundland, Natural Sciences and Engineering Research Council (NSERC), and the Research, Development Corporation (RDC) of Newfoundland and Labrador (recently RDC was combined with another organization to form InnovateNL).

Finally, I would like to thank my family and friends for their spiritual support throughout my studies and my life.

Table of Contents

Abstract	i
Acknowledgments.....	ii
Table of Contents	iii
List of Tables	vi
List of Figures.....	viii
List of Symbols, Nomenclature and Abbreviations	xi
Chapter 1: Introduction	1
1.1. Background	1
1.2. Thesis Objectives and Outlines	5
1.3. Conclusion.....	9
Chapter 2: Literature Review	10
2.1. Transmission Planning.....	10
2.2. Generation Planning.....	15
2.3. Conclusion.....	34
Chapter 3: Analytical Approach	35
3.1. Introduction of Analytical Approach	35
3.2. Load Model	36
3.3. Methods for Wind Speed Prediction	39
3.3.1. Wind Speed Prediction by ARMA Method.....	39

3.3.1.1.	Principle of ARMA Method	39
3.3.1.2.	Case Study for Wind Speed Prediction by ARMA.....	41
3.3.2.	Wind Speed Prediction by ANN Method.....	45
3.3.2.1.	Principle of ANN Method.....	45
3.3.2.2.	Case Study for Wind Speed Prediction by ANN Method.....	49
3.4.	Generation Model.....	55
3.4.1.	COPT of Conventional Generators.....	55
3.4.2.	COPT of Wind Generation Systems.....	57
3.5.	Generation Adequacy Evaluation of Conventional Generators and Wind Farm	61
3.5.1.	An Improved Analytical Approach – Fuzzy C Means	62
3.5.2.	A Case Study for Generation Adequacy – Capacity Factor	68
3.6.	Conclusion.....	72
Chapter 4: Standalone System Design		74
4.1.	Introduction of Standalone System Design	74
4.2.	Wind Generation System Design	74
4.3.	Hybrid System.....	97
4.4.	Conclusion.....	113
Chapter 5: Proposed Guideline for Generation Planning Using Analytical Approach		115
5.1.	Proposed Guideline	115
5.2.	Cost Analysis.....	120

5.3. Conclusion.....	122
Chapter 6: Conclusion and Future Work	123
References.....	126
Appendix: List of Refereed Publications.....	142

List of Tables

Table 2.1: A Comparison between Analytical and Simulation Techniques [32].	16
Table 3.1: The weekly peak load (%) [69].	36
Table 3.2: Daily peak load (%) [69].	36
Table 3.3: Hourly peak load (%) [69].	37
Table 3.4: Technical specifications of the DFIG wind turbine [60].	42
Table 3.5: Results for Finding the Order of the ARMA.	44
Table 3.6: R-Squared Value for the Two Wind Speed Model [117].	52
Table 3.7: Conventional Generation Unit Reliability Data for RBTS [70].	56
Table 3.8: COPT of the conventional generators in the RBTS.	57
Table 3.9: COPT of 2MW wind turbine without FOR.	59
Table 3.10: COPT of 2MW wind turbine with FOR of 4%.	60
Table 3.11: Replacing conventional generator with wind energy.	61
Table 3.12: Fuzzy C Means Algorithm for Clustering Wind Energy [73].	65
Table 3.13: Comparing results for replacing 5MW conventional unit in RBTS with 8MW wind farm [73].	66
Table 3.14: LOLE (h/yr) and EENS (MWh/yr) considering different Cases [75].	70
Table 4.1: The Calculated annual O&M costs per Turbine Using the proposed Method in This Paper and the Present Practice [48].	89
Table 4.2: Weibull Shape and Scale Parameters k and c, Annual Mean Wind Speed at 140.5 m elevation and 125 m hub height at St. John's [48].	93
Table 4.3: Components failure rates for the DFIG wind turbine [49].	96
Table 4.4: The Reliability Evaluation of the Wind Turbine System [48].	97

Table 4.5: Costs and Technical specifications of the system ([101], [112]).....	106
Table 4.6: The Optimal and Non-optimal Case of the Proposed Configuration [97].....	108
Table 4.7: The Optimal Case of the Proposed Configuration [97].	109
Table 4.8: The Optimal Case of the System [97].....	112
Table 5.1: Generation adequacy evaluation.....	121
Table 5.2: Gas turbine generator additions.	122
Table 5.3: Investment comparison with WTG and gas turbines.....	122

List of Figures

Figure 1.1: An example of Uncertainty and variability of wind energy power output [17].	5
Figure 1.2: Power system reliability evaluation aspects [20].	5
Figure 2.1: Hierarchical levels [20].	10
Figure 2.2: Transmission system planning process [23].	12
Figure 2.3: Investment and customer outage costs as function of reliability [19].	13
Figure 2.4: Comprehensive overview of transmission expansion planning.	14
Figure 2.5: HL-I generation adequacy evaluation model [28].	16
Figure 2.6: Conceptual risk model for generation facilities [29].	17
Figure 2. 7: Typical risk characteristic [29].	19
Figure 2.8: Common approaches for wind speed modeling.	21
Figure 2.9: Wind speed modeling using Markov method with n states [13].	22
Figure 2.10: Probability distribution function of the wind speeds comparing with existing methods [45].	24
Figure 2.11: Generation adequacy evaluation considering methods [45].	24
Figure 2.12: Development of a wind turbine generator model using the common wind speed model [35].	25
Figure 2.13: A common wind speed model development by combining wind speed models for different sites [35].	25
Figure 2.14: Common approaches for wind turbine generator model.	26
Figure 2.15: Clustering technique for wind farm [44].	30
Figure 2.16: Uncertainty modeling methods.	34
Figure 3.17: An example of ELCC of adding a new generation system [16].	71

Figure 4.1: Component cost of a 2 MW wind turbine [86].	76
Figure 4.2: The two-step procedure for wind energy potential, reliability, and cost assessment [48].	77
Figure 4.3: The flowchart for estimating wind energy potential [48].	82
Figure 4.4: The structure of DFIG-based wind turbine [49].	82
Figure 4.5: The fault tree of a wind turbine system [48].	83
Figure 4.6: Comparison of the calculated annual O&M costs in percent of the capital investment using the proposed method and the Present Practice [48].	90
Figure 4.7: Comparison of the calculated annual O&M cost per turbine in dollars using the proposed method and the tool developed in [31]: (a) 750 W wind turbine (the initial O&M cost at Year 1 = \$7,633); (b) 1000 W wind turbine (the initial O&M cost at Year 1 = \$9,501); (c) 1500 W wind turbine (the initial O&M cost at Year 1 = \$15,683); (d) 2000 W wind turbine (the initial O&M cost at Year 1 = \$18,858); (e) 2500 W wind turbine (the initial O&M cost at Year 1 = \$23,016) [48].	92
Figure 4.8: The Weibull distribution of wind speed at St. John's at 140.5 m height and the hub height 125 m, and the actual wind measurement data at 140.5 m [48].	93
Figure 4.9: The wind power density calculated using wind speed at hub height (125 m): (a) wind power density vs. the wind speed, (b) wind power density vs. the month.	95
Figure 4.10: The wind energy curve and the chosen wind turbine power curve of the wind turbine system.	95
Figure 4.11: The annual O&M costs per turbine calculated using the proposed method and the present practice in the case study [48].	97
Figure 5.1: Generation adequacy and cost evaluation.	116

Figure 5.2: Procedure for generation adequacy and cost evaluation with wind energy. 119

List of Symbols, Nomenclature and Abbreviations

PV	Photovoltaic
NREL	National Renewable Energy Laboratory
HLI	Hierarchical Level I
HLII	Hierarchical Level II
HLIII	Hierarchical Level III
LOLE	Loss of Load Expectation
FOR	Forced Outage Rate
FTA	fault tree analysis
O&M	operation and maintenance
NPC	net present cost
LDC	Load Duration Curve
COPT	capacity outage probability table
PLCC	peak load carrying capability
ARMA	autoregressive moving average
MA	moving average
MCMC	Markov Chain Monte Carlo
FCM	Fuzzy C-means
PDF	Probability Distribution Function
LOLF	loss of load frequency
MF	membership function
IGDT	Information gap decision theory

ANN	artificial neural network
AR	autoregressive
AICc	Akaike Information Criterion Corrected
RBTS	Roy Billinton Test System
EENS	Expected Energy Not Supplied
ELCC	Effective load carrying capability
AOMC	annual O&M costs
HOMER	Hybrid Optimization of Multiple Energy Resources
CRF	capital recovery factor
BPC	blade and pitch control system
GX	gearbox
BS	brake system
YS	yaw system
GEN	generator
CON	converter
CS	control system
S	sensors
TR	transformer
AGC_i	Available generation capacity for state i
N	Number of generators
M	Number of failed generator units
A_j	Availability of unit j
FOR_j	FOR of unit j

n	number of days or hours of period under scope
p_i	probability of i_{th} outage
t_i	number of time units
SW_t	simulated wind speed at hour t
μ_t	mean observed hourly wind speed at hour t
σ_t	standard deviation of the observed hourly wind speed at hour t
$LOLE_s$	$LOLE$ for each scenario S
\overline{LOLE}	average value of $LOLE$
σ_{LOLE}	standard deviation of $LOLE$
$L(t)$	load for hour t
L_W	weekly load
L_D	Daily load
L_H	Hourly load
$e(t)$	white-noise disturbance function
$y(t)$	output at time t
n_a	Order of AR
n_c	Order of MA
q	lag operator
y_i	simulated wind speeds
y_j	Historical wind speeds
v_1	measured speed at a reference height h_1
v_2	wind speed at height h_2
α	power law exponent

$x(t)$	time series
d	past values of $x(t)$
n_p	number of past wind speed data
P_i	power output of the wind turbine
P_r	rated power output of the wind turbine
SW_{bi}	predicted wind speeds
V_{ci}	cut-in wind speed
V_r	Rated wind speed
V_{co}	Cut-out wind speed
m	Fuzziness coefficient
c_j	center of the j th cluster
μ_{ij}	degree of membership
J_m	objective function of FCM
k	shape factor of the Weibull distribution
c	scale factor of the Weibull distribution
$F(v)$	cumulative distribution function
\bar{v}	annual mean wind speeds
$P(v)$	wind power density
ρ	air density at the sea level (1.225 kg/m ³)
$W_{ED}(v_i)$	wind energy density
R_{system}	reliability of a series system with n independent components
R_i	reliability of the i th component
$R_c(t)$	reliability of the wind turbine system

λ	failure rate of a component
λ_{eq}	equivalent system failure rate
N_W	number of units of wind turbines
N_E	Number of electrolyzer
N_H	Number of hydrogen tank,
N_F	Number of fuel cell
N_{PV}	Number of PV system
N_B	Number of batteries
N_{CN}	Number of inverter
C_W	capital and replacement costs of wind turbines
C_E	capital and replacement costs of electrolyzer
C_H	capital and replacement costs of hydrogen tank
$C_F,$	capital and replacement costs of fuel cell
C_{PV}	capital and replacement costs of PV
C_B	capital and replacement costs of battery system
C_{CN}	capital and replacement costs of inverter
I	interest rate
L	life span of the project
M_C	operation and maintenance cost
C_T	minimizing total system cost
N_{PV}^{Max}	Maximum available number of units of PV panels
N_W^{Max}	Maximum available number of units of wind turbines
N_{BT}^{Max}	Maximum available number of units batteries

Chapter 1: Introduction

1.1. Background

Over the last few years, renewable energy systems, especially Photovoltaic (PV) and wind power systems, in the electricity market have gained increasing attention all over the globe due to their environmental benefits. In addition, renewable energy systems are cost-effective solutions for remote area communities that are far from an electrical grid. There have been escalating efforts for further developments of renewable energy projects in Canada from the Yukon to Newfoundland [1].

There are approximately 200,000 people who live in 280 remote communities in Canada who have no access to a main electrical grid and their primary source of power generation are fuel-based generators [2]. Operating costs are much higher in these communities because of high fuel costs. Transportation costs of the fuel also increase the total cost of fuel-based generation for communities. Furthermore, the efficiency of diesel generators is low when they operate at less than their half rated capacity [3]. Because of these reasons, utilization of conventional generators has been significantly reduced and in 2016, the capacity of renewable energy systems had its largest annual increase with about 161 gigawatts of capacity added [4]. Added capacity of PV systems and wind power generation systems in 2016 were 47% and 34%, respectively [4]. Despite the benefits of renewable energy systems, they also introduced new challenges for power system planners.

PV and wind power output depends on the availability of solar and wind resources, which can vary significantly over a period of time. This means that the power output is not constant, and it is

known as variability of renewable energy systems. This variability of PV and wind power output is not preferred by the grid, and techniques to reduce such variations have been of great interest [5]. Variability is a challenge for power system operators because of frequency and voltage fluctuations that occur from the time scale of seconds to minutes. This in return results in potential damage to the system and equipment [6].

Power system planning for conventional generators is based on the rated capacity of the generators installed at different locations in the system. However, power system planning based on the rated capacity of renewable energy systems can lead to over-investment as a result of the addition of extra transmission lines that may not be required because it is unlikely that renewable energy systems will operate at their rated power most of the time [7][8].

Renewable energy curtailment is another issue that should be taken into account. Renewable energy curtailment is defined by National Renewable Energy Laboratory (NREL) as power output reduction of a generator from what it could otherwise generate by given resource input such as wind speed or solar [9]. Even though new regulations have been introduced for renewable energy systems to ensure annual full load hours for PV and wind energy systems, curtailment is still a major challenge [4]. Renewable energy curtailment can be a result of insufficient transmission infrastructure, poor grid connections, or excessive power supply during low load demand periods. The latter was the main reason for one of the largest curtailments that occurred in north China, with more than approximately 70% of total wind generation curtailed [10].

A conventional power system is complex and difficult to analyze, as there are several uncertain parameters, such as load and transmission line constraints. Power system planners are faced with

more challenges with renewable energy integration as a result of the number of random variables, uncertainties, and renewable energy constraints, which have significantly increased the complexity of the system [11].

Renewable energy systems are non-dispatchable, which means they cannot change the power output quickly and the energy output might not be available when the system is in need to meet the load [12]. Renewable energy systems gradually replace conventional generators, thereby negatively affecting system stability and reliability. The admission requirement of wind generation systems into an existing power system is that they should provide the same characteristics, for example, stability, satisfying the frequency requirements as other conventional generators such as thermal or gas turbines [13].

Uncertainty is defined as the difference between measured, estimated, and real data including some errors in calculation or measurement [14]. Power systems should be designed to account for uncertainties by meeting reserve requirements. Power system planners need to confront uncertainties to achieve a precise decision, improve system control performance characteristics, minimize costs, and improve reliability [15]. Uncertainties in a power system generally consist of fuel cost and availability, economic growth of the country, construction time of a power system plant, load forecasting, regulatory policies, and generator outages [16].

Traditionally, uncertainties were handled by forced outage rate of conventional generators and load demand forecast error. Since wind energy is highly intermittent and non-dispatchable, uncertainty analysis has become more challenging and difficult [16]. In generation expansion planning, uncertainty and variability of wind energy are sometimes incorrectly designated the same

definitions. Variability is the variation of wind energy power output, where uncertainty is the degree of error between estimated and measured values [17]. Variability and uncertainty of wind energy power output is clarified in Figure 1.1.

Effective and innovative power system planning techniques must be developed in order to overcome the aforementioned technical challenges and integrate renewable energy systems economically and reliably in electric power systems. By using proper planning techniques, the overall system performance can be improved in terms of reduction of curtailment and cost, and enhancement of flexibility and reliability. Power system planning techniques are involved with deciding on upgrading or new system components to satisfy load demand in the future. System components can be generators, substations, transmission lines, capacitors, and cables [18].

One of the main goals of modern power systems is meeting load demand with high reliability at an acceptable installation cost. In fact, construction costs for adding new or upgrading system elements in planning will be increased, however, customers will be provided with improved reliability. This will ultimately result in decreased customer outage costs. Reliability evaluation in power system planning is of great importance to power system planners who are determining an optimum point where reliability can be increased and costs can be minimized. The reliability of electricity supply is also a major competitive factor in a deregulated market [19].

Power system reliability studies are viewed from two aspects which are generation adequacy and system security [20], as shown in Figure 1.2. System security regards the system's ability to respond to disturbances such as short circuits. Generation adequacy, which is the focus of this research, regards the existence of enough generation in a system to satisfy load demand [20].

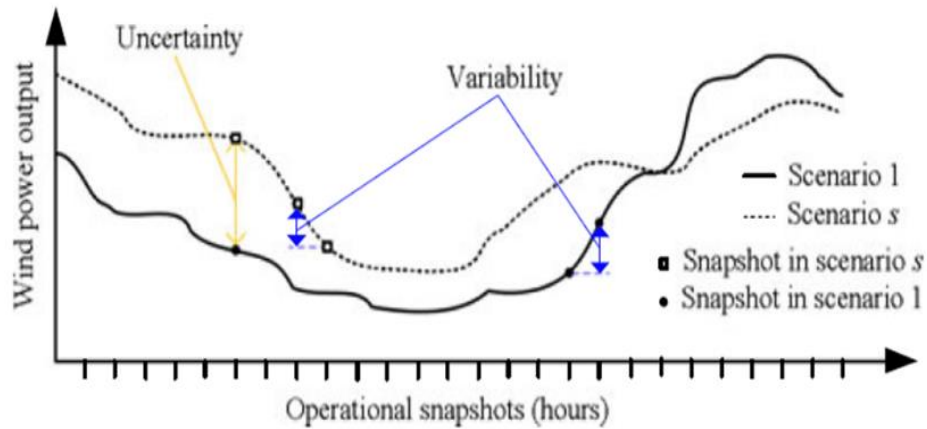


Figure 1.1: An example of uncertainty and variability of wind energy power output [17].

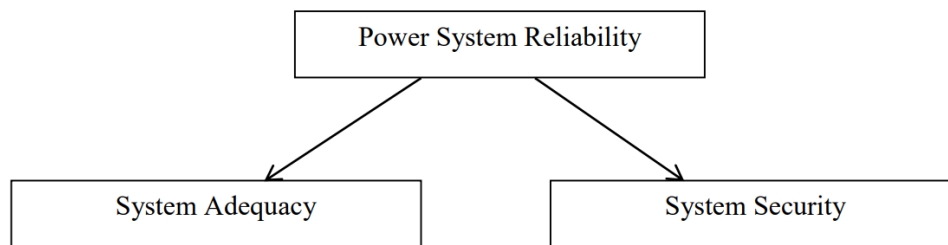


Figure 1.2: Power system reliability evaluation aspects [20].

1.2. Thesis Objectives and Outlines

This thesis is organized as follows:

In Chapter 1, the main objective of the thesis, the problem and its importance will be discussed. A general overview of power system planning will be described. A background of renewable energy systems and their importance in existing power systems will be introduced. Technical challenges of integrating renewable energy systems will also be discussed.

It will be explained why there is a need to develop effective and innovative power system planning techniques in order to overcome the technical challenges of renewable energy power generation systems and to integrate renewable energy systems economically and reliably in electric power systems. By using a proper planning technique, the overall system performance can be improved in terms of reduction of curtailment, flexibility, higher reliability, and reduction of costs.

In Chapter 2, the main objective is literature review on power system planning. Three hierarchical levels will be introduced in power system planning which are Hierarchical Level I (HLI) and it includes only generation facilities; Hierarchical Level II (HLII) which is concerned with both generation and transmission facilities; and, Hierarchical Level III (HLIII) which is involved with the complete system which is generation, transmission, and distribution. The main focus of the thesis is the generation planning.

Deterministic approaches in power system planning consider the worst case scenario of the system without considering the probability of the occurrence such as no shortage of power generation system. Probabilistic methods are based on the probability of occurrence, for instance Loss of Load Expectation (LOLE), which helps power system planners to model the past shortages of the system and include uncertainties. It will be revealed that reliability evaluation is the main key in probabilistic power system planning. Reliability has been viewed in two aspects, adequacy and security. This research is focused on adequacy evaluation. The main objective in HL-I generation adequacy evaluation is determining the ability of the generation units to satisfy total load demand, where transmission system is assumed to be 100% reliable. Different types of methods used in the literature for generation adequacy will be reviewed in Chapter 2.

In Chapter 3, the main objective is to present an analytical approach for generation planning with wind energy integration. A general modeling of generation adequacy evaluation of conventional generators and wind energy systems will be introduced. The output power of wind turbine depends on the wind speed which is highly random and uncertain.

Thus, the first step in generation adequacy evaluation is modeling wind speed. The wind speed will be predicted by two methods ARMA and Neural Networks. After modeling wind speed time series, the nonlinear relationship between wind speed and power output of wind turbine is represented by the power curve of wind turbine. Wind generator Forced Outage Rate (FOR) due to wind turbine equipment's outage is then taken into account for modeling the unavailability of wind turbine. The load model will be obtained from a standard test system and generation model will be constructed by the COPT using the predicted wind speeds by the ARMA.

The load model will be combined with generators model for generation adequacy. Generation adequacy will be evaluated by the most commonly used method called the loss of load approach. The multi-state COPT is the most commonly used model of both conventional and wind energy generation model in the literature. This model is highly suitable for generation adequacy evaluation and provides useful information for system scheduling. The number of COPT states is critical in generation adequacy evaluation because more states generally means a better modeling accuracy and a higher computation overhead.

An improved method using Fuzzy C mean algorithm will be used to obtain number of states of wind turbine. Generation adequacy will also be investigated using capacity factor method. Capacity factor is a useful technique for generation adequacy evaluation when detailed historical

wind speeds are not available. Capacity credit will also be used which is a useful technique to determine the capacity factor of a wind generation system.

In Chapter 4, the importance of using renewable energy systems in remote areas will be discussed. Standalone or remote area power supply system is aimed at supplying electricity for remote or small communities which do not have access to the main power grid due to economic and technical difficulties. Renewable energy systems have become the most popular configuration to replace diesel generators in remote areas.

The main objective of Chapter 4 is to investigate standalone system design for wind generation system design and hybrid renewable energy systems. In this Chapter, a method and a corresponding two-step procedure will be used for a wind power generation system design by wind energy potential evaluation, reliability and costs assessment. The wind energy potential will be investigated through the Weibull two-parameter model using the hourly wind speed data of a site in St. John's. An analytical method based on the fault tree analysis (FTA) and minimal cut sets will be developed for the system reliability evaluation.

A generic annual operation and maintenance (O&M) costs calculation formula will be proposed based on field data presented by NREL. Case studies will be conducted for a wind power project in St. John's, Newfoundland and Labrador, Canada. In the second section of Chapter 4, a stand-alone hybrid renewable energy system will be proposed, which consists of solar PV, wind turbine, and energy storage with the combination of battery and hydrogen.

Cost optimization which is based on the net present cost (NPC) method will be used for finding optimal sizing of individual components. The proposed stand-alone hybrid renewable energy

system is suitable to for supplying electricity in remote areas which do not have access to the main grid.

In Chapter 5, the main objective is to provide a procedure and guideline for generation planning using analytical approach. The cost analysis will also be provided in this chapter.

Chapter 6 will summarize this thesis, draw the conclusions, and recommend future works.

1.3. Conclusion

In this chapter, benefits of integrating renewable energy systems in power system planning are introduced, and the challenges in this field are discussed. Solar and wind resources vary significantly over time, power system planning based on the rated capacity of renewable energy systems without considering renewable energy's intermittent nature can lead to over-investment, renewable energy curtailment, and uncertainties. Therefore, effective and innovative power system planning techniques must be developed to overcome these technical challenges.

Chapter 2: Literature Review

2.1. Transmission Planning

A power system consists of generation, transmission, and distribution, as shown in Figure 2.1. Power system planning is generally investigated in three hierarchical levels: Hierarchical Level I (HLI) includes only generation facilities; Hierarchical Level II (HLII) is concerned with both generation and transmission facilities; and Hierarchical Level III (HLIII) is involved with the complete system which is generation, transmission, and distribution. Because of its scale and complexity, only distribution facilities are considered in HLIII [20].

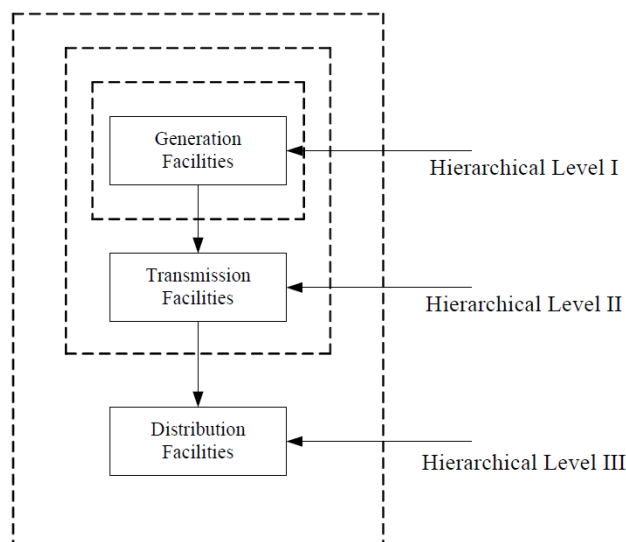


Figure 2.1: Hierarchical levels [20].

Transmission planning aims to find optimal transmission routes between generation facilities and loads. It determines when, how many, and where new transmission lines must be added in the system to meet the load demand so that the investment and operational costs are minimized and constraints are met during normal and contingency conditions [18].

Investments costs are the cost of installing new transmission lines and operational costs, and the costs due to power losses in the line. Constraints consist of limiting transfer capability and thermal limit. An N-1 contingency is widely used in transmission planning, which is the outage of a single element such as transmission line, transformer, or generator. The system should be planned so that the load can be satisfied under N-1 contingency without violating any constraints [18].

Transmission planning can be investigated using deterministic approaches or probabilistic methods [21]. Deterministic approaches consist of AC power flow, DC power flow, short-circuit analysis, and stability study. Deterministic approaches consider the worst-case scenario of the system without considering the probability of the occurrence, such as no shortage of power generation system [21]. Probabilistic methods are based on the probability of occurrence, for instance Loss of Load Expectation (LOLE), which helps power system planners to model the past shortages of the system and include uncertainties [22].

There is no conflict between deterministic and probabilistic planning approaches; since a complete transmission planning is based on considering both deterministic and probabilistic criteria. For instance, a power system planner has determined seven possible scenarios for a transmission system, as shown in Figure 2.2. Two of these scenarios can be removed because of societal, political, or environmental reasons. Deterministic approaches are applied on the remaining scenarios, and two more scenarios are removed that did not satisfy the criteria. Eventually, both probabilistic reliability evaluation and economic analysis are investigated to determine the optimal alternative [23].

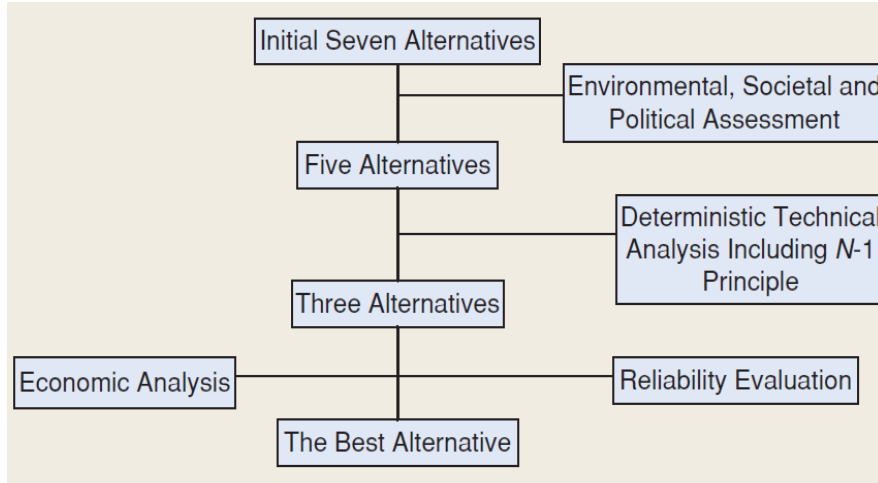


Figure 2.2: Transmission system planning process [23].

Probabilistic reliability evaluation and costs analysis are the two important keys in transmission planning, where costs must be minimized subject to reliability evaluation criteria such as LOLE. If an N-1 contingency is a mandatory factor, then deterministic approaches can also be used to determine an optimal plan in which both probabilistic and deterministic criteria are met [23]. A new method, based on probabilistic reliability criteria, was proposed in [19] to achieve an optimal transmission planning which minimized both investment and outage costs. The most frequently reliability criteria, LOLE, was used. Investment costs increase as reliability increases, as shown in Figure 2.3; Customer outage costs also increase as reliability increase. The optimum or target level is the minimum point where costs are minimized [19].

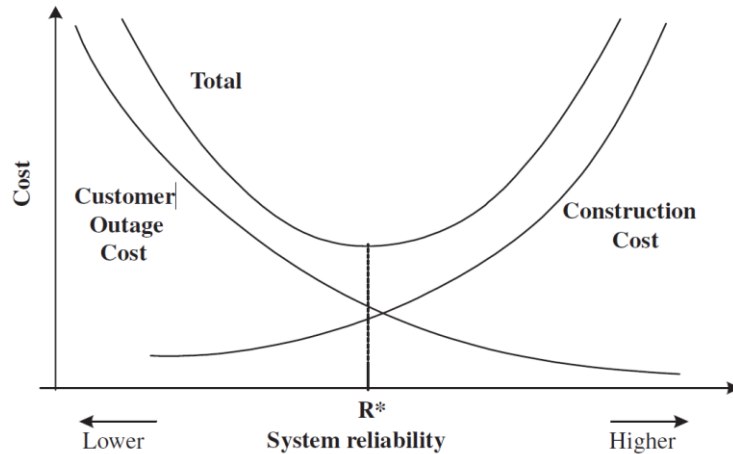


Figure 2.3: Investment and customer outage costs as function of reliability [19].

Figure 2.4 shows a comprehensive overview of transmission expansion planning. As one can see, if the contingency is mandatory, then the planning is done based on deterministic criteria which are power flow, optimal power flow, contingency analysis based on power flow, voltage stability, and transient stability. Following this, probabilistic planning based on reliability evaluation will be done. Costs analysis will also be investigated after this stage. A final alternative for planning which satisfies both reliability and costs will then be selected.

If the contingency is not the main interest, then the planning will be performed from reliability and cost evaluation in order to find the best alternative. As mentioned earlier, deterministic planning has to be done if the contingency is mandatory. One of the main tools for deterministic transmission planning is network modeling, either by deterministic power flow or probabilistic power flow. Deterministic power flow methods are DC power flow and AC power flow [18].

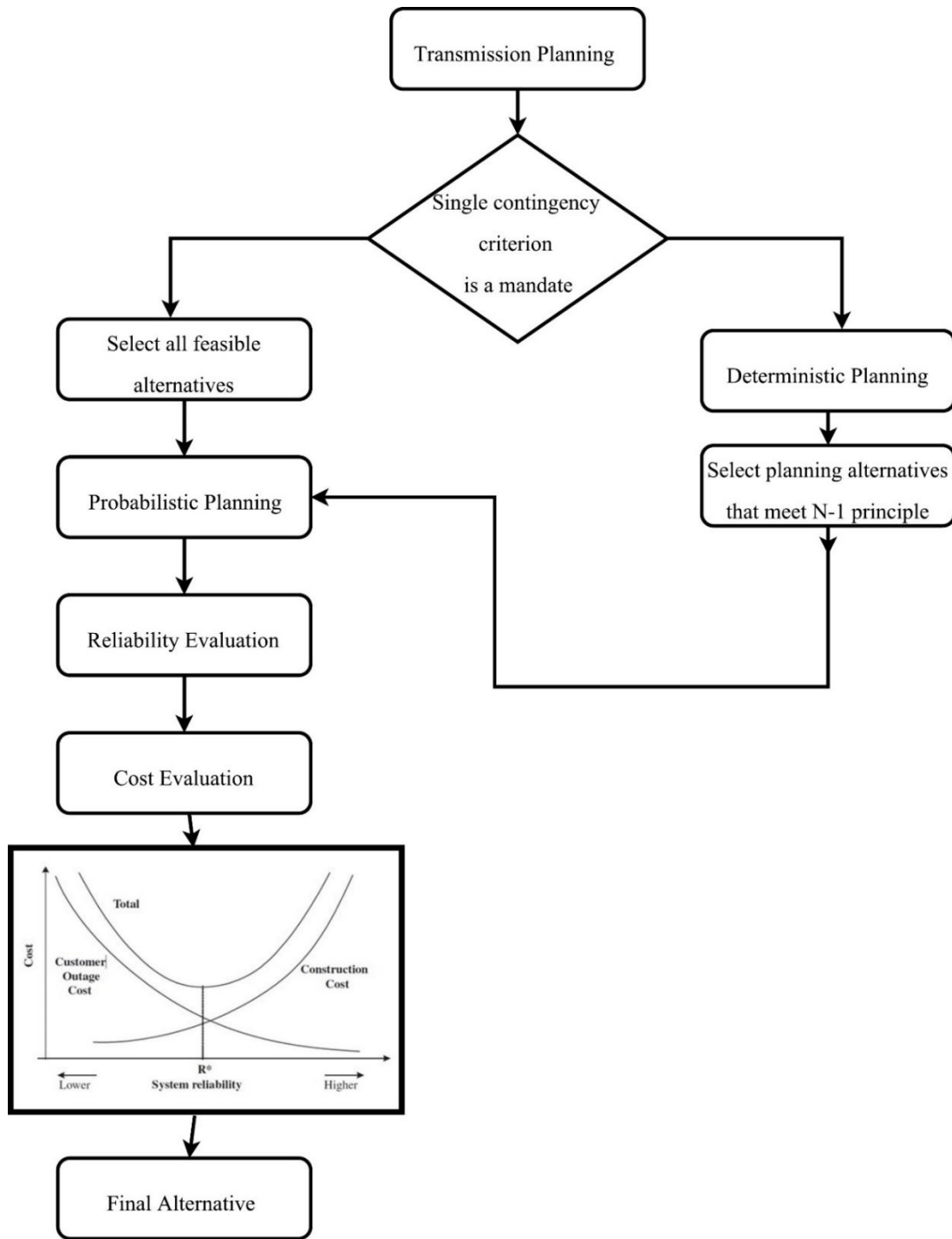


Figure 2.4: Comprehensive overview of transmission expansion planning.

2.2. Generation Planning

The main objective in HL-I generation adequacy evaluation is to determine the ability of the generation units to satisfy the total load demand, where the transmission system is assumed to be 100% reliable. Hence, generation units and loads are the two main components that have to be modeled for generation adequacy evaluation. Figure 2.6 shows the system modeling in HL-I generation adequacy assessment. All generation units are required to meet a single lumped load [28].

In this model, the generation adequacy can be evaluated for the ability of proposed or existing generation units to meet load demand. Analytical and simulations techniques are the two methods used for generation adequacy evaluation [29]-[31]. Analytical methods are based on mathematical models which are suitable for small-scale systems. A Monte Carlo simulation is the most widely used simulation technique which is more effective for large-scale systems.

It can be categorized into two groups such as non-sequential and sequential. A Non-sequential Monte Carlo simulation is complicated for considering chronological behavior of generation and load model because it is based on considering each time interval independently, and cannot model sequential events. A sequential Monte Carlo simulation is effective for considering chronological behavior of generation and load model, and it is a preferred method for multi-state systems such as wind generation system [32]. Table 2.1 compares analytical and simulation methods in a generation adequacy evaluation.

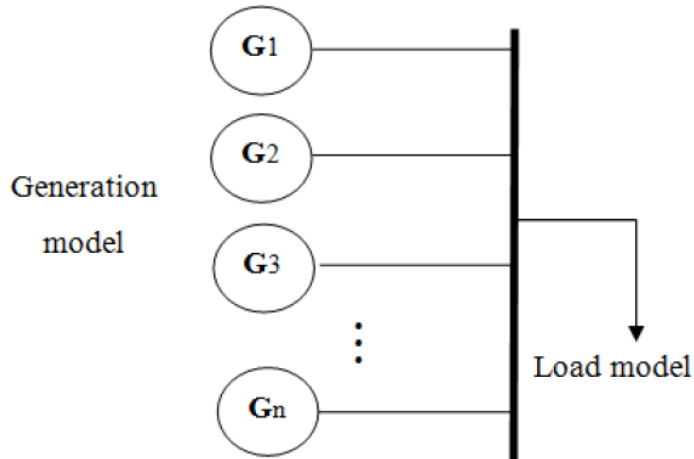


Figure 2.5: HL-I generation adequacy evaluation model [28].

Table 2.1: A Comparison between Analytical and Simulation Techniques [32].

Analytical Methods	Non-Sequential Monte Carlo	Sequential Monte Carlo
Difficult for obtaining frequency-based indices	Effective for large-scale systems with a large number of components	Effective for considering chronological behavior of generation and load model
Effective for small-scale systems such as two-state units (conventional generators)	Complicated for considering chronological behavior of generation and load model	Effective for multi-state systems such as wind generation system
Complicated for considering chronological behavior of generation and load model	Difficult for obtaining frequency-based indices	Effective for obtaining frequency-based indices
Less computational time	Less computational time	High computational time

For a generation adequacy evaluation, three models must be determined: 1) generation model, 2) load model, and 3) risk model. Generation model and load model are combined to derive the risk model [29],[33], as shown in Figure 2.7.

The load model shows the energy demand for a given period of time. Two load models are available to be used in a generation adequacy evaluation; namely, the Load Duration Curve (LDC)

and the chronological load model. The LDC, which is frequently used, represents hourly peak load variation curve by arranging the individual hourly peak loads in descending order, while the chronological load model is formed based on available hourly energy demand over a period of time. The chronological load model is used frequently due to its simplicity, but LDC is the most suitable model to approximate the load characteristics [29],[33].

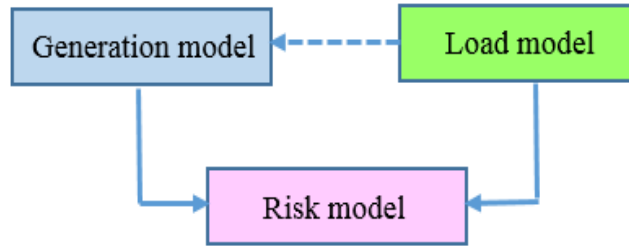


Figure 2.6: Conceptual risk model for generation facilities [29].

The most common generation model is capacity outage probability table (COPT) which represents capacity states in increasing order with their associated probability of each state [29]. The COPT is widely used in wind generation models [30],[34],[35].

A recursive algorithm is used to obtain the COPT. In this algorithm, a system consists of N generators with M failed units, and available generating capacity, AGC_i with their corresponding probability, $P\{AGC_i\}$ for state i is obtained as [36]

$$AGC_i = \sum_{j=M+1}^N G_j \quad (2.1)$$

$$P\{AGC_i\} = \prod_{j=M+1}^N A_j \times \prod_{j=1}^M FOR_j \quad (2.2)$$

where A_j , FOR_j , are the availability, and FOR of unit j , respectively.

Once generation and load models are determined, a loss of load approach can then be used to produce a risk model. In the loss of load method, the generation system is represented by the COPT and load characteristics are represented chronological load or LDC. In this method, the daily peak loads (or hourly values) are combined with the COPT. This “loss of load” index gives the information about the expected number of days (or hours) in the given time period, in which the daily peak load (or hourly load) exceeds the available capacity. The loss of load expectation (LOLE) can be expressed as follows [29]:

$$LOLE = \sum_{i=1}^n (p_i \times t_i) \quad (L_{\max} > C) \quad (\text{hrs/year}) \quad (2.3)$$

where n is the number of days or hours of period under scope, p_i is the probability of i_{th} outage which is obtained directly from the COPT, and t_i is the number of time units for which this outage cause loss of load. It is clear that if the capacity outages are less than the reserve then loss of load will not occur. Based on this approach, the maximum peak load that can be met by generation units, known as peak load carrying capability (PLCC), can be determined for a specific value of maximum risk value, as shown in Figure 2.8 [29].

There are several publications on modeling wind energy conversion system in generation adequacy evaluation studies. The two main contributions are wind speed modeling and wind generator modeling.

A) *Wind speed model:*

Various wind modeling methods are investigated in [34]: observed hourly wind speed data, mean observed hourly wind speed data, autoregressive moving average (ARMA) time series,

moving average (MA) time series, Normal distribution, and Markov chain models etc. Different wind speed models will lead to different wind speed probability distributions and affect the system's reliability indices.

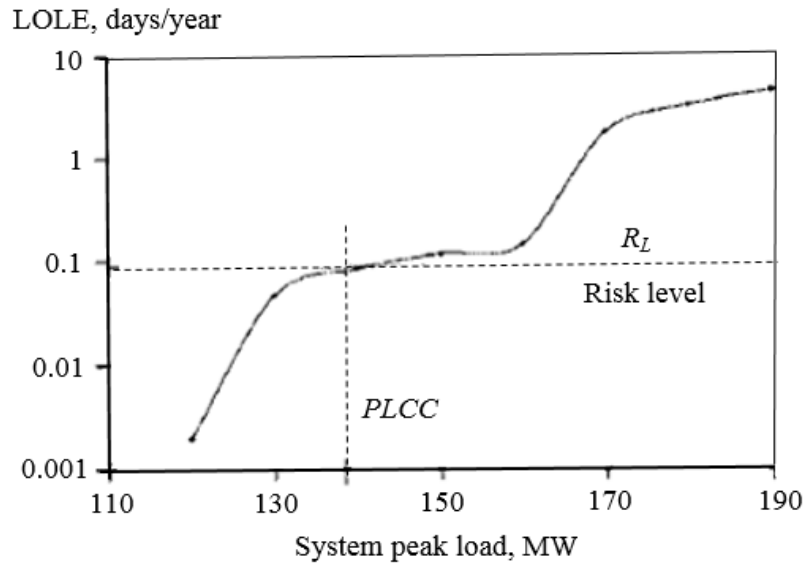


Figure 2. 7: Typical risk characteristic [29].

If a complete range of historical wind speed data is available for a site, observed hourly wind speed and mean observed hourly wind speed methods can be used, which are defined as [30],[34]:

- 1) *Observed hourly wind speed*: In this method, an observed hourly wind speed data set is used repetitively in the reliability evaluation sequential simulation process.
- 2) *Mean observed hourly wind speed*: In this method, the mean observed hourly wind speed is calculated based on different annual wind speed data sets, the mean hourly wind speed is then used repetitively in the sequential simulation process.

Wind speed data for large periods of time are not always available because of extreme weather situations or failure of wind speed measuring devices [34]. Hence, missing data must be estimated for wind speed modeling.

Two common approaches for wind speed modeling are available, probabilistic approaches [37],[38], and time series approaches [30],[34],[39], which are shown in Figure 2. 9. Probabilistic approaches are based on continuous probability distributions which rely on historical data of hourly wind speed for a site over a period of time, usually one year. In 1951, the gamma distribution was used for wind speed distribution. Since then, several distribution methods such as Gaussian, Pearson, Normal, Johnson, Rayleigh, and Weibull have been proposed. Numerous studies have shown that the Weibull distribution is the most utilized statistical function among all other statistical functions used to represent wind speed variations [40]-[42].

Time series approaches are suitable for generation adequacy evaluations, and the most frequently used models are ARMA [30], [34] and Markov Chain Monte Carlo (MCMC) [39]. MCMC approaches are based on a finite number of states for wind speed. For example, wind speed modeling considering n states with transition rate ρ between any two states is shown in Figure 2.10. Probability and the frequency of wind speeds can be obtained using this model.

Using the Markov method, it is common to consider transition rates between two states that follow Exponential distribution [43],[13]. It means that ρ is constant with respect to time. This assumption is accurate when long-term average values of wind speeds are of interest [43]. Another assumption in this approach is that wind speed states are transiting smoothly and immediately to neighboring states. This results, however, in losing some of the transitions between states, and

often in ignoring some wind speed probabilities. This drawback has been addressed in [44] by clustering the wind turbine generator output.

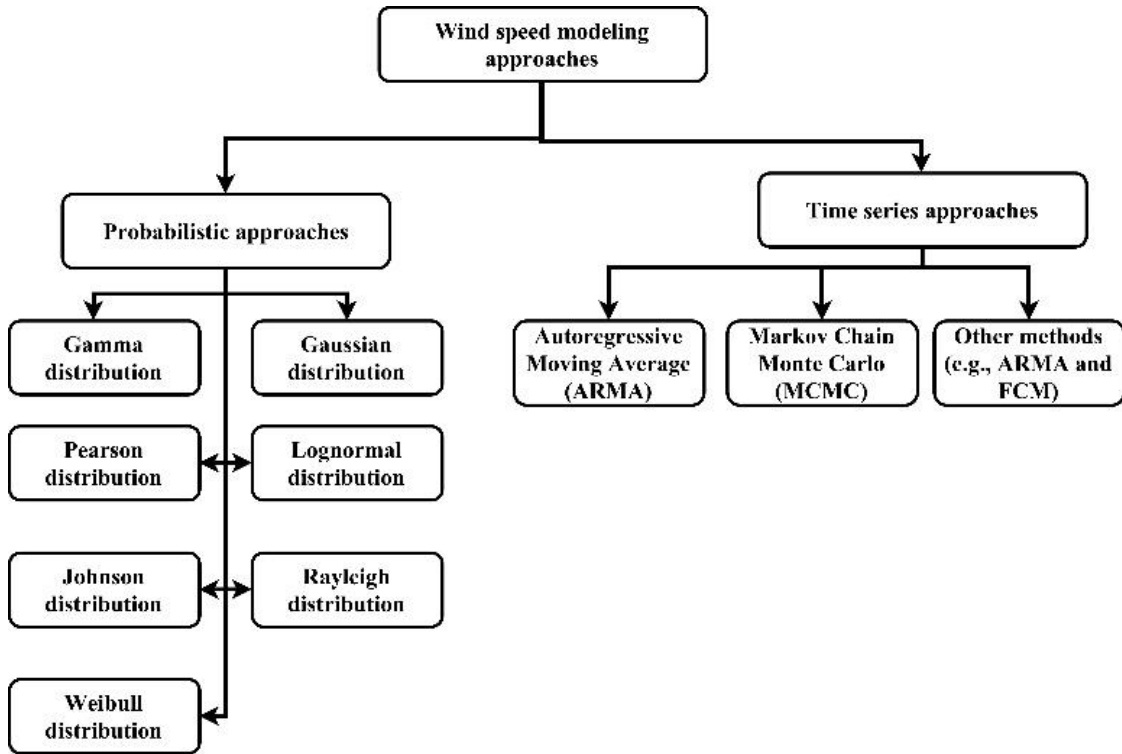


Figure 2.8: Common approaches for wind speed modeling.

3) *ARMA model*: ARMA is the most common approach for modeling wind speeds, which is briefly introduced as follows [30],[34]: The ARMA method is used to predict wind speeds. It is calculated based on the observed wind speed data and incorporates yearly wind speed variations.

This model denoted as $ARMA(p,q)$ has p autoregressive terms and q moving average terms. As an example, an ARMA model was created for the Swift Current site in Saskatchewan, Canada,

based on data from 1996 to 2003. The simulated wind speed at hour t, SW_t , in this example can be calculated as follows [30]:

$$\begin{aligned}
 SW_t &= \mu_t + \sigma_t y_t \\
 y_t &= 1.1772 y_{t-1} + 0.1001 y_{t-2} - 0.3572 y_{t-3} \\
 &+ 0.0379 y_{t-4} + \alpha_t - 0.503 \alpha_{t-1} - 0.2924 \alpha_{t-2} \\
 &+ 0.1317 \alpha_{t-3} \\
 \alpha_t &\in NID(0, 0.524760^2)
 \end{aligned}
 \tag{2.4}$$

where μ_t is the mean observed hourly wind speed at hour t, and σ_t is the standard deviation of the observed hourly wind speed at hour t.

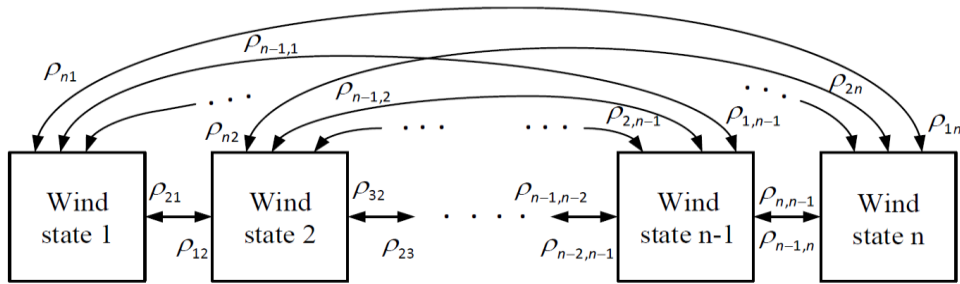


Figure 2.9: Wind speed modeling using Markov method with n states [13].

The probability distribution of an ARMA model might be a Normal distribution, which has negative wind speeds. Although, Ref. [35] suggested that these negative wind speeds be converted to zero values, this can still cause errors, and a good prediction of wind speed time series cannot be guaranteed. It is also difficult to model non-linear problems by ARMA.

Other methods are also available in the literature to overcome the drawbacks of time series models. For instance, a meteorological mining-based wind speed time series for generation adequacy applications were proposed in [45]. Path analysis method was first used to calculate the

influence weights of meteorological factors on wind power output. Meteorological data were then categorized into states using Fuzzy C-means (FCM) algorithm. Figure 2.11 shows the Probability Distribution Function (PDF) of wind speeds using four different methods.

It can be seen that simulated wind speeds using the meteorological mining-based wind speed time series are more accurate. The effectiveness of the meteorological mining-based wind speed time series was also verified by LOLE evaluation of IEEE-RTS96 comparing with the existing methods, as shown in Figure 2.12. A common wind speed model based on normal distribution of wind speeds for three different Canadian wind farm sites was developed in [35]. This model provides reasonable accuracy in wind speed modeling which is useful for wind farms that lack sufficient historical wind speed data. The only data required from which to derive the model are the annual mean wind speed μ and the standard deviation σ data at the site under study. The procedure for creating a wind turbine generator model is shown in Figure 2.13 [35].

It was shown that wind generation adequacy can be significantly simplified by using 6-step common wind speed model [35]:

$$SW_i = \mu + (i - 3) \times (5\sigma / 3) \quad \text{for } (i = 1, \dots, 6) \quad (2.5)$$

where SW_i is the simulated wind speed considering 6 steps. The common model for wind speed modeling considering three sites is shown in Figure 2.14.

Wind speed models play an important role in generation adequacy evaluations since an error in the wind speed modeling leads to cubic errors in wind power output. An accurate wind speed forecasting has technical and economic advantages. It can help power system planners develop efficient functioning hour ahead or day ahead planning in competitive market design. Wind speed

models are usually site-specific and they require a huge amount of historical data. Historical wind speed data might also not available for all potential wind sites.

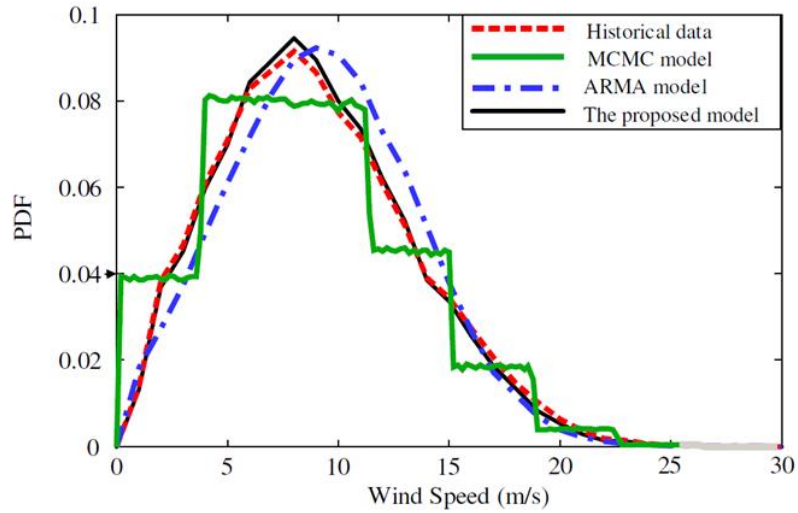


Figure 2.10: Probability distribution function of the wind speeds comparing with existing methods [45].

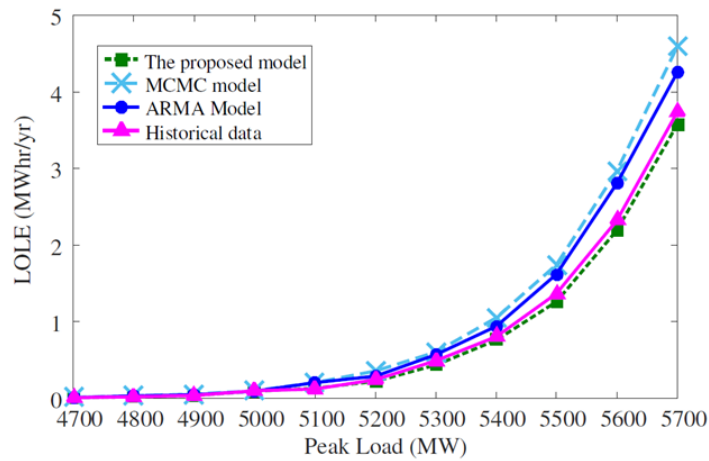


Figure 2.11: Generation adequacy evaluation considering methods [45].

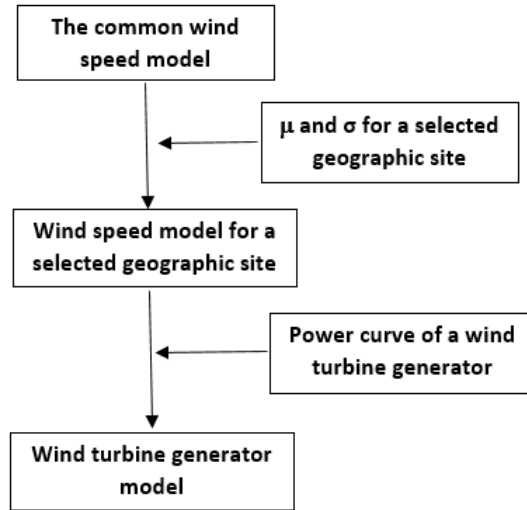


Figure 2.12: Development of a wind turbine generator model using the common wind speed model [35].

Time series models such as, ARMA, are the most frequent type of wind speed modeling methods to predict future wind speeds. Obtaining a proper ARMA time series which can accurately model wind speeds is a difficult task.

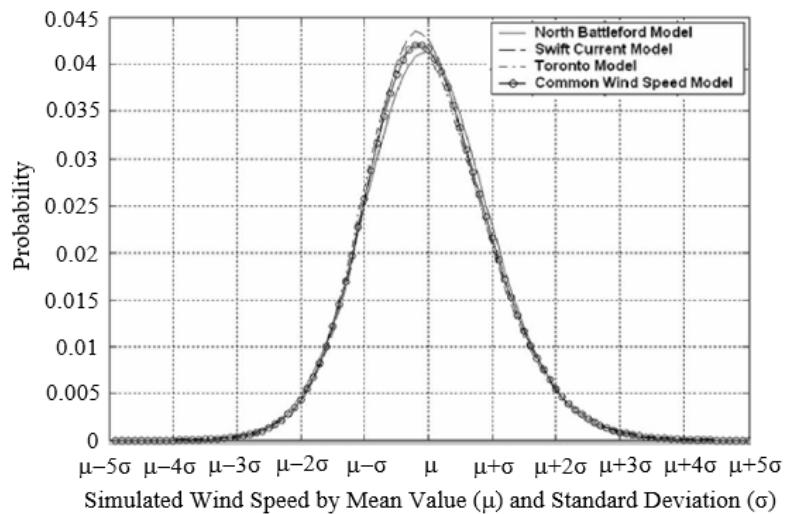


Figure 2.13: A common wind speed model development by combining wind speed models for different sites [35].

Research is continuously improving upon current wind speed models. Combining different approaches, for example time series models with FCM, are proposed to solve this problem. Using a common wind speed model that can be used for multiple wind farm sites is also another solution investigated in [35].

B) *Wind turbine generator model*: There are three main wind turbine generator models including the multi-state model, universal generating functions, and the Markov model, as depicted in Figure 2.15.

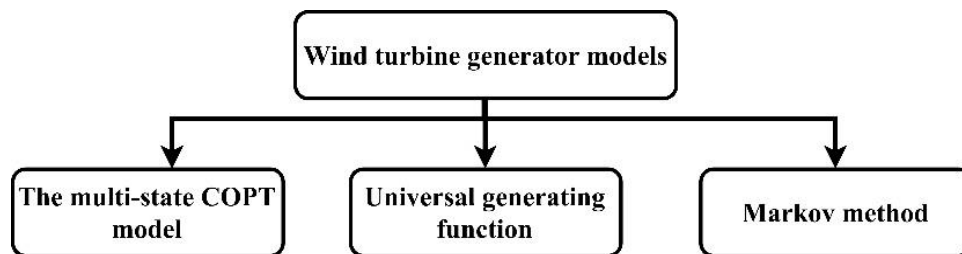


Figure 2.14: Common approaches for wind turbine generator model.

The COPT is the most common model used for wind generation systems and has been widely used in the literature [46]. The simplest WECS model using an analytical approach is an annual multi-state COPT that can be used to create the system COPT in order to calculate the LOLE index. COPT can be modified to include wind farm maintenance scheduling [30]. Both wind speed and wind turbine outage probabilities can be considered in this model. The COPT model can be obtained using the following steps [33]:

- 1) Import hourly simulated wind speeds.
- 2) Determine hourly wind turbine power output as a function of hourly simulated wind speeds using wind turbine power curve.

- 3) Divide hourly wind power output into a number of states.
- 4) Determine the total number of occurrences for each state.
- 5) Obtain the probability of each state by dividing the total number of occurrences for each output state (Step 4) by the total number of data points.
- 6) Build the wind farm COPT by multiplying power output of each single wind turbine states (Step 3) and keeping the same probability on that state.
- 7) Build another wind farm COPT that only considers FOR of wind turbines. Binominal distribution can be used for identical wind turbines. Otherwise, recursive algorithm is used for non-identical wind turbines.
- 8) Combine wind farm COPT models (Steps 6 and 7) to build the final wind farm COPT model which considers both wind speeds and FOR.
- 9) Combine wind farm COPT and load model in order to derive risk model using analytical methods.

Universal generating function models are similar to multi-state models, but they formulate wind farm generation states into clear mathematical functions that reduce complexity and computational burden compared to multi-state models [47]. Transitive relationships between generation states are not considered in the UGF and multi-state models. Hence, frequency-related indices, such as loss of load frequency (LOLF) cannot be obtained by these two methods.

This issue can be rectified by using the Markov method. Probability, frequency, duration, and transition rate of wind turbine states can be extracted [43]. The wake effects of the wind farm itself can also be included in this model. Wake effect is important in generation adequacy because it

usually creates 5%-15% losses in wind farm generation systems [48]. The main drawback of these methods is computation over-head during generation adequacy evaluation. More states generally means a better modeling accuracy and a higher computation time. For example, in a wind farm with N wind turbine generators the total number of states is 2^N . The number of states in wind turbine generator models must be reduced while maintaining the accuracy of the wind farm model [43]. The following solutions are proposed in the literature.

- 1) Data clustering is the basis of several system modeling algorithms and classifications. The main goal of clustering is to obtain data groupings from a dataset to represent a system's behavior. An analytical method based on clustering was proposed in [44]. Wind power outputs are clustered into a finite number of states based on their similarities, as shown in Figure 2.16. Every cluster belongs to only one state based on minimum Euclidean distances with the observed data points. For instance, wind speeds that result in zero power output are clustered into one state (band 1 in Figure 2.16), and wind speed which result in rated power are clustered into one state (band n in Figure 2.16).
- 2) FCM-based clustering technique was applied to obtain optimum number of states in wind farm generation for Markov chain in [49]. FCM is a popular clustering method in which a large set of data is categorized into a finite number of clusters. Each data point in the dataset belongs to a cluster with a certain degree; in fact, each data point in FCM can belong to multiple clusters with a membership grade. In FCM, cluster center is initially guessed which shows the mean location of each cluster. Following this, every datum is assigned with a membership grade for each data point. This process continues by updating cluster centers and membership grades for each cluster until the correct cluster center is obtained.

Thus, this process is based on a minimization of an objective function, which calculates distance from each cluster to each data point with a membership grade. Wind speed variation and the outage of wind turbine components such as tower, blades, and gearbox were considered.

- 3) K-means algorithm was used to determine the number of clusters in a wind speed model in [43]. It was found that only 80 states represent the wind farm model appropriately, compared to the model obtained by measurements.
- 4) An 11-state WECS model for a 20 MW wind farm with wind speed data of a particular site is created in [34]. It was found that the reliability indices, LOLE and LOEE, remain basically the same when the number of states of the model increases from 11 to 21 [34]. Dr. Rajesh Karki et. al found that a 6-state COPT model is able to achieve a trade-off between accuracy and computation overhead [46]. It was discovered that a 6-state COPT model can also serve as a default option for generation adequacy evaluation of wind energy [46].

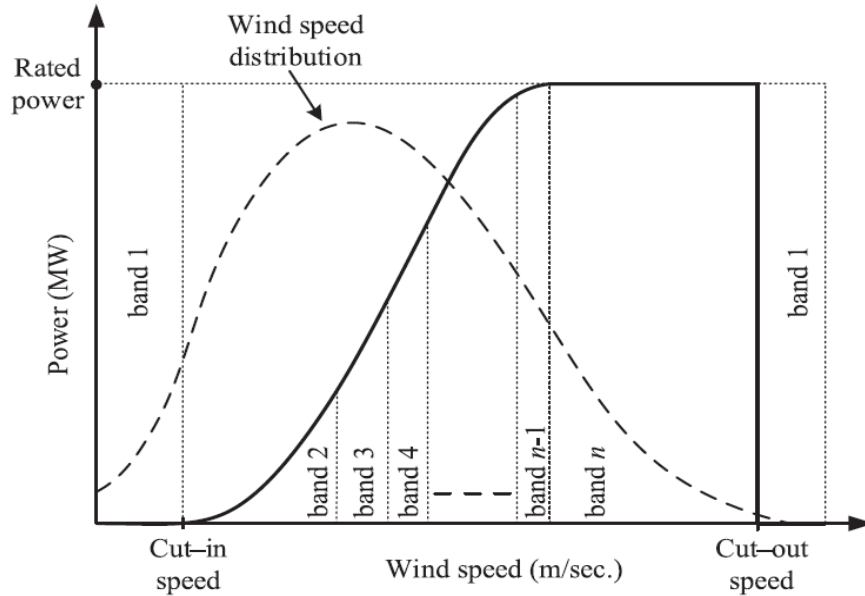


Figure 2.15: Clustering technique for wind farm [44].

- 5) In another study [35], a 6-common wind speed distribution model based on the Normal distribution was studied that can be used for generation adequacy evaluation with reasonable accuracy.

Other analyses that have been investigated in wind generation adequacy are stability and uncertainty analysis. Stability analysis in wind generation adequacy evaluation has been done in [13], which demonstrates that the reliability indices deteriorate when system security is taken into account. This has not been investigated in-depth in previous studies.

The existing uncertainty modeling methods are probabilistic, possibilistic, possibilistic-probabilistic, information gap decision theory, robust optimization, and interval analysis, as shown in Figure 2.18. The main goal of these methods is measuring the effects of uncertain inputs on a system's output. The only difference is using different types of approaches for modeling input

uncertainties. For example, probabilistic methods are based on the PDF, and the membership function (MF) is used in the fuzzy method to model uncertainties of the input parameters. These approaches are briefly explained as follows [14],[50]:

- 1) *Probabilistic approaches*: It aims to determine the PDF of the output parameters based on the PDF of input parameters. Hence, the PDF of input parameters must be known. A Monte Carlo simulation is the most commonly used method in this approach because it is system-size independent and it is highly applicable for nonlinear and complicated systems which have many uncertain parameters. Sequential, pseudo-sequential, and non-sequential Monte Carlo simulation have been used for uncertainty analysis. A Pseudo-sequential Monte Carlo is the fastest method that has the accuracy and flexibility of sequential Monte Carlo simulation with reduced computational effort. Analytical methods can also be used to model uncertainties using mathematical expressions which are categorized into groups. The first group is based on PDF linearization on input variables. Convolution method, Cumulant method, Taylor series expansion and first order second moment method are the existing methods for this approach. The second group is the most frequently used methods which are based on the PDF approximation such as point estimation and unscented transformation methods. Generating appropriate numbers of samples of input parameters to approximate the PDF of input parameters is a challenging task.
- 2) *Possibilistic approaches*: The concept of this approach was initially investigated by Zadeh, where the uncertainties of input variables are modeled using membership functions.

- 3) *Possibilistic–probabilistic approaches*: This is useful when some of input uncertainties are probabilistic and some of them are possibilistic. In fact, PDF of input parameters must be known and a membership function must be used to model uncertainties of input variables.
- 4) *Information gap decision theory (IGDT)*: This is based on non-probabilistic model of uncertainties and it is useful when historical information is not available and PDF or membership functions cannot be obtained. It also requires small information of inputs variables. This approach measures the difference between parameters from the estimate.
- 5) *Robust optimization*: This approach models random variables as uncertain parameters which belong to an uncertainty set and the system against the worst case scenario within the set must be maintained.
- 6) *Interval analysis*: In this approach, uncertain variables are selecting from a known interval. It is similar to probabilistic modeling but the PDF of input parameters have constant probability.

Uncertainties can be random or non-random parameters. Random uncertainties have high frequencies, for example, load demand variability. Non-random uncertainties have low frequencies, for example, available investment budget. Uncertainty models should take both random and non-random parameters into account. However, considering all uncertainties will increase computational time and complexity of the problem. Determining the most significant uncertainties is the first step in generation planning [17].

Wind power generation and load demand are the most uncertain parameters that have the highest influence in the planning [51],[52]. Probabilistic approaches are the most efficient modeling techniques for uncertainties because of their ability in modeling random uncertainties,

which is highly effective for wind energy uncertainties. The main drawback of this approach is their high computational burden, and even intractable. A very large number of parameters are required to achieve an accurate uncertainty modeling.

There are two main solutions for solving this problem which are using clustering techniques and scenario reduction. Clustering techniques represent the system with lower number of data compared with original set of data [17]. FCM and fuzzy k-means are the most effective methods for clustering data. If the PDF of input parameters are not available, scenarios reduction can be used which is an effective solution that reduce the computation time of uncertainty modeling. This method is based on controlling a probabilistic fitness function and it is described in the following steps [53]:

Step 1: Generating several scenarios by Monte Carlo simulation. Each scenario is the outcome of input parameter from a random variable generated by the Monte Carlo.

Step 2: Estimate $LOLE_s$ for each scenario S .

Step 3: Calculate average value of LOLE, \overline{LOLE} .

Step 4: Calculate standard deviation of LOLE, σ_{LOLE} :

$$\sigma_{LOLE} = \frac{1}{S} \sqrt{\sum_{s=1}^S \frac{(LOLE^s - \overline{LOLE})^2}{S-1}} \quad (2.6)$$

Step 5: Repeat Steps 1-4 until σ_{LOLE} is in the range of 0.01–0.05.

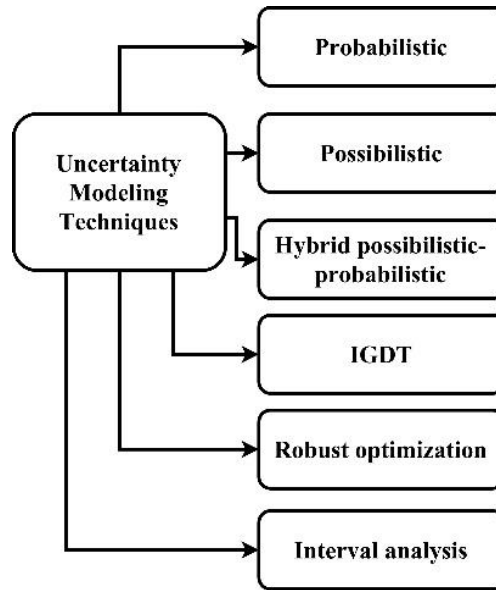


Figure 2.16: Uncertainty modeling methods.

2.3. Conclusion

In this chapter, the literature review is conducted on power system planning with wind power. It is reviewed from three different aspects, Hierarchical Levels I, II, and III. There are two general approaches reported in the literature, deterministic and probabilistic approaches. Deterministic approaches consider the worst case scenario of the system and neglect the probability of the occurrence, and probabilistic approaches consider the probability of occurrence. Reliability evaluation is an important aspect in probabilistic power system planning. There are two aspects in reliability evaluation: adequacy and security. Generation adequacy evaluation to determine the ability of the generation units to satisfy the total load demand is the main focus of this research.

Chapter 3: Analytical Approach

3.1. Introduction of Analytical Approach

A general modeling of generation adequacy evaluation of conventional generators and wind energy systems is shown in Figure 3.1. The output power of wind turbine depends on the wind speed which is highly random and uncertain. Thus, the first step in generation adequacy evaluation is modeling wind speed. After modeling wind speed time series, the nonlinear relationship between wind speed and power output of wind turbine is represented by the power curve of wind turbine. Wind generator FOR due to wind turbine equipment's outage is then taken into account for modeling the unavailability of wind turbine [28].

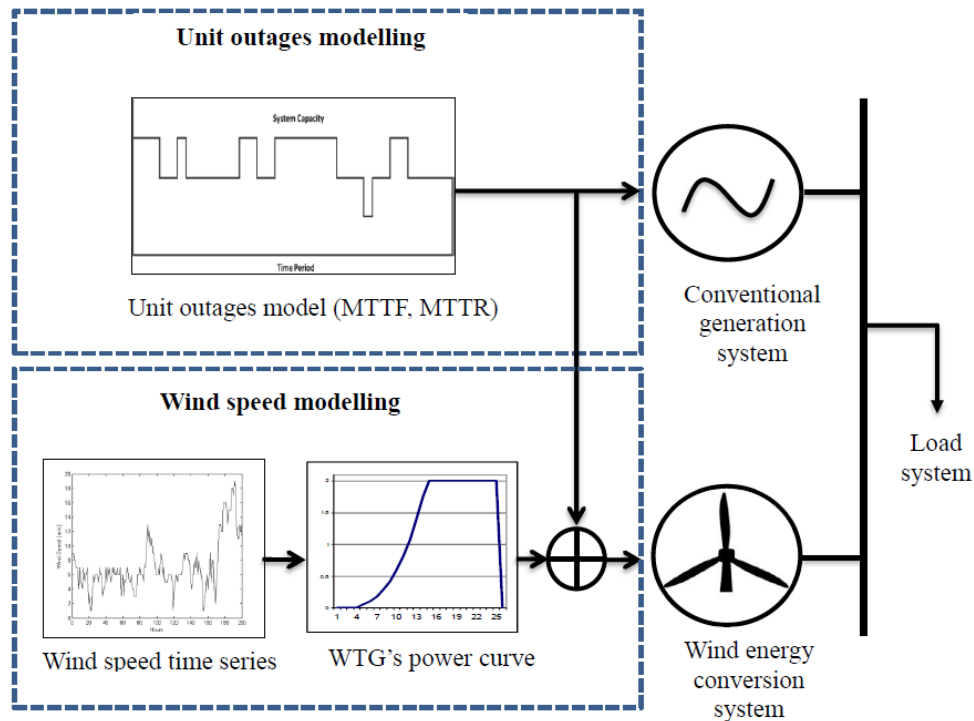


Figure 3.1: Generation adequacy evaluation of systems containing wind energy system [28].

3.2. Load Model

Before obtaining the generation model, the load model must be determined to derive the risk indices. The per-unit load model of the RBTS is used in this research which can be used to create hourly chronological loads for one year. Tables 3.1-3.3 give the per-unit load model data of the RBTS [69].

Table 3.1: The weekly peak load (%) [69].

Week	Peak load						
1	86.2	14	75.0	27	75.5	40	72.4
2	90.0	15	72.1	28	81.6	41	74.3
3	87.8	16	80.0	29	80.1	42	74.4
4	83.4	17	75.4	30	88.0	43	80.0
5	88.0	18	83.7	31	72.2	44	88.1
6	84.1	19	87.0	32	77.6	45	88.5
7	83.2	20	88.0	33	80.0	46	90.9
8	80.6	21	85.6	34	72.9	47	94.0
9	74.0	22	81.1	35	72.6	48	89.0
10	73.7	23	90.0	36	70.5	49	94.2
11	71.5	24	88.7	37	78.0	50	97.0
12	72.7	25	89.6	38	69.5	51	100.0
13	70.4	26	86.1	39	72.4	52	95.2

Table 3.2: Daily peak load (%) [69].

Day	Peak Load (%)
Monday	93
Tuesday	100
Wednesday	98
Thursday	96
Friday	94
Saturday	77
Sunday	75

The load $L(t)$ for hour t can be determined by multiplication of weekly load, daily load, and hourly peak load. The procedure for obtaining load model is explained by the following steps:

1. Step 1: Calculating hourly peak load for the first week of one year in %.

Table 3.3: Hourly peak load (%) [69].

Hour	Peak Load (%)
12-1am	67
1-2	63
2-3	60
3-4	59
4-5	59
5-6	60
6-7	74
7-8	86
8-9	95
9-10	96
10-11	96
11-noon	95
Noon-1pm	95
1-2	95
2-3	93
3-4	94
4-5	99
5-6	100
6-7	100
7-8	96
8-9	91
9-10	83
10-11	73
11-12	63

Week 1 peak load (86.2%) * Monday Peak Load * Hourly Peak Load

Week 1 peak load (86.2%) * Tuesday Peak Load * Hourly Peak Load

Week 1 peak load (86.2%) * Wednesday Peak Load * Hourly Peak Load

Week 1 peak load (86.2%) * Thursday Peak Load * Hourly Peak Load

Week 1 peak load (86.2%) * Friday Peak Load * Hourly Peak Load

Week 1 peak load (86.2%) * Saturday Peak Load * Hourly Peak Load

Week 1 peak load (86.2%) * Sunday Peak Load * Hourly Peak Load

Total= 168 hours

2. Step 2: Repeat Step 1 for Week 2 to Week 52 to obtain 8736 hours peak load in percentage.
3. Step 3: Obtain hourly peak load demand in MW by multiplying hourly peak load in % with peak load demand of the system.
4. Step 4: Sort the data from highest value to lowest value.

Figure 3.19 shows the hourly load model of the RBTS for one year which will be used to derive risk indices. The LDC over one year is also shown in Figure 3.19. The LDC is obtained by arranging the hourly load values in a descending order, where the greatest load is plotted on the left side and the smallest load is plotted on the right side. The x-axis of the LDC shows the time duration. The LDC has the exact same data as the chronological hourly load. The LDC model is adopted from [113]. This load data is for the RBTS obtained from [113].

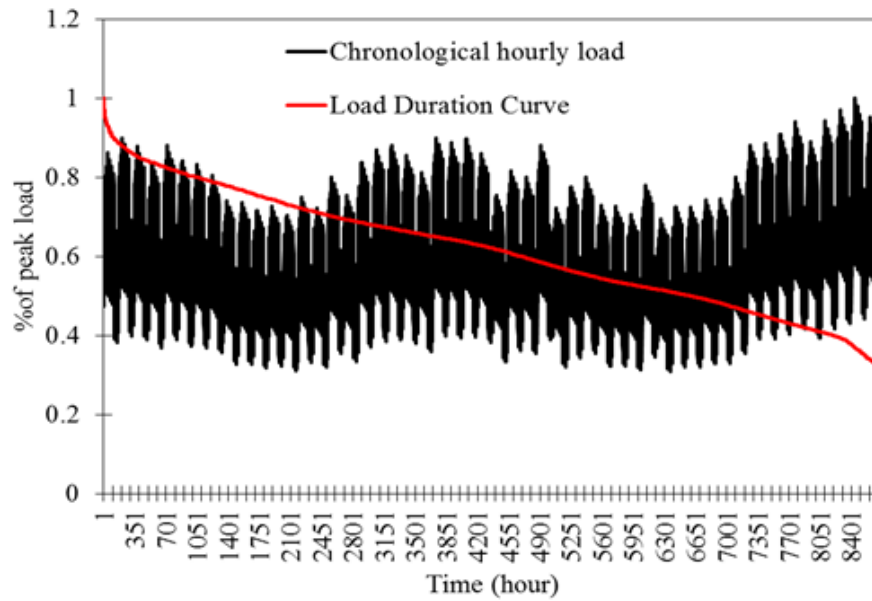


Figure 3.2: Load Model of RBTS [113].

3.3. Methods for Wind Speed Prediction

3.3.1. Wind Speed Prediction by ARMA Method

3.3.1.1. Principle of ARMA Method

ARMA model consists of two terms autoregressive (AR) and MA. AR is a linear regression curve fitting to a set of data. MA is similar to AR except the fact that the linear regression curve fitting is between the predicted data and actual data. In fact, AR predicts future data based on the past data, where MA models the errors of the previous predicted data [54].

The ARMA model is based on past data, prediction error, and a random parameter. ARMA consists of AR model which is autoregressive term with the order of n_a and MA model which is

moving average term with the order of n_c . Hence, the ARMA model is referred as ARMA (n_a, n_c).

The ARMA model for time series can be calculated by [54]

$$A(q)y(t) = C(q)e(t) \quad (3.1)$$

where $e(t)$ is white-noise disturbance function and $y(t)$ is output at time t . $A(q)$ and $C(q)$ matrices can be obtained as [54]

$$A(q) = 1 + a_1q^{-1} + \dots + a_{n_a}q^{-n_a} \quad (3.2)$$

$$C(q) = 1 + c_1q^{-1} + \dots + c_{n_c}q^{-n_c} \quad (3.3)$$

where n_a and n_c are the order of ARMA model. q is the lag operator which moves the index back one time unit. q is used to present a concise way of ARMA, which is defined as [54]

$$qy_t = y_{t-1} \quad (3.4)$$

Determining n_a and n_c is challenging because higher values increase accuracy but also increase the possibility of overfitting. It is common to approximate ARMA model for wind speed applications with ARMA ($n_a, n_a - 1$) [55]. Hence, determining n_a is sufficient for finding order of n_c , where $n_c = n_a - 1$. It is also found that the degree of n_a varies from 1 to 4 [56]. In this study, Akaike Information Criterion Corrected (AICc) is used to determine the order of ARMA which is calculated by the following steps [57]:

- 1) Insert $n_a=1$;
- 2) Obtain $n_c=n_a - 1$;
- 3) Generate wind speed time series for ARMA ($n_a, n_a - 1$);

4) Calculate AICc by

$$AIC_c = N \times \log\left(\frac{SS}{N}\right) + 2 \times (n_a + n_c + 1) \times \frac{N}{N - n_a - n_c - 2} \quad (3.5)$$

where N is the total simulated points which is 8760. SS is given as

$$SS = \sum_{i=1}^N (y_i - y_j)^2 \quad (3.6)$$

where y_i , and y_j are the simulated wind speeds, and historical data, respectively;

5) Repeat Steps 1-4 until $n_a=4$;

6) Take ARMA(n_a, n_c) with the lowest AICc.

3.3.1.2. Case Study for Wind Speed Prediction by ARMA

ARMA is the most common approach for wind speed prediction. The main contribution of this section is to use the ARMA model to predict wind speeds in St. John's. St. John's is the capital and largest city of the Canadian province of Newfoundland and Labrador. It has a total area of 446 km² and urban population of 178,427 recorded in 2016. Among other major Canadian cities, St. John's has the cloudiest (1,497 hours of sunshine), foggiest (124 days), and windiest (24.3 km/h (15.1 mph) average speed) weather [58].

The hourly wind speeds of St. John's for one year period between January 2015 and December 2015 are obtained from Historical Climate Data - Climate - Environment Canada, as shown in Figure 3.2. The St. John's International Airport at the latitude of 47°37'07.000" N, and the longitude of 52°45'09.000" W is selected as the wind speed measurement site with the station number 8403505. The elevation for wind speed measurement 140.50 m [59]. The Vestas V90-

2MW (IEC IIIA) wind turbine is selected for the case study in this research. Technical specifications of the wind turbine are shown in Table 3.4 [60]. The hub height of the IEC IIIA model of the wind turbine is 125 m.

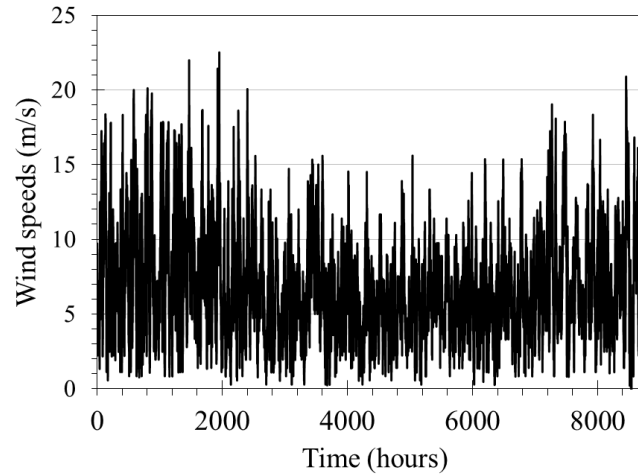


Figure 3.3: Hourly wind speed data measured at St. John’s between January and December 2015.

Table 3.4: Technical specifications of the DFIG wind turbine [60].

Rated power	IEC IIIA - 50 Hz: 2,000 kW
Cut-in wind speed	4 m/s
Rated wind speed	12 m/s
Cut-out wind speed	25 m/s
Rotor diameter	90 m
Swept area	6,362 m ²
Hub height	125 m
Lifetime	20 years

The power curve of the wind turbine is shown in Figure 3.3 [60]. The range of wind turbine operation is between the cut-in and cut-out wind speeds. The cut-in, rated, and cut-out wind speed

for the chosen wind turbine are 4 m/s, 12 m/s, and 25 m/s, respectively. The power-law wind speed model [61],[62] is used to convert measurement wind speed data at 140.5 m to wind speeds experienced by the wind turbine hub height at 125 m. The power-law wind speed model is given as [61, 62]:

$$\frac{v_2}{v_1} = \left(\frac{h_2}{h_1} \right)^\alpha \quad (3.7)$$

where v_1 denotes the measured speed at a reference height h_1 and v_2 denotes the wind speed at height h_2 . The power law exponent α varies according to many factors, and α can be taken as 1/7 [61, 62].

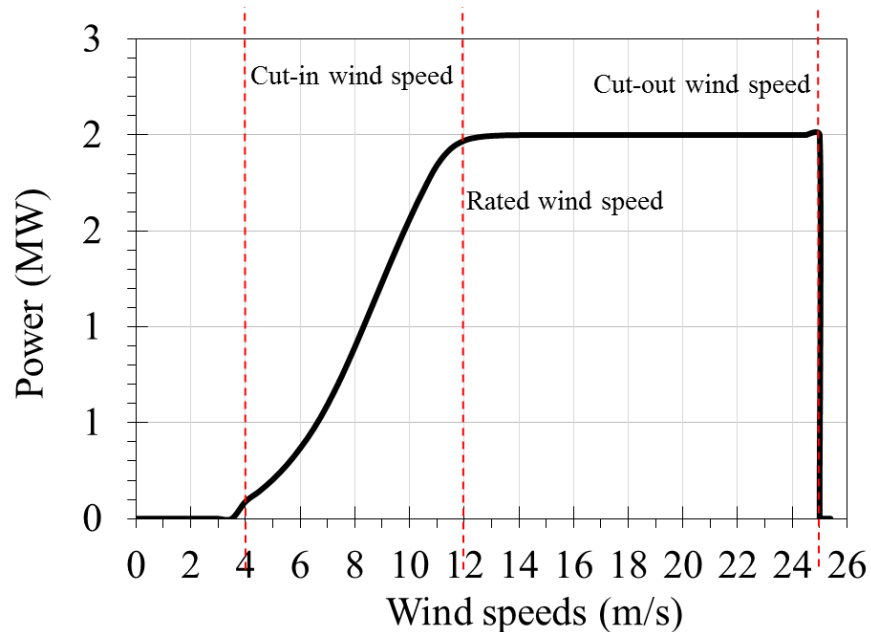


Figure 3.4: The power curve of the chosen wind turbine, Vestas V90-2MW [60].

Determining the order of the ARMA is a difficult task. In wind speed models, n_a degrees from 1 to 4 and n_c degrees from 1 to 4. Using AICs method and the steps described in previous section, AICs is calculated for predicted wind speeds using ARMA model, where n_a and n_c vary from 1 to 4. In this research, order of ARMA is obtained by AICc method. A step by step guideline of determining ARMA order by AICc method was given in Section 3.3.1.1, where n_a and n_c are varying from 1 to 4, as shown in Table 3.5. The ARMA order is determined by taking the lowest AICs as $n_a = 4, n_c = 3$. Matrices $A(q)$ and $C(q)$ are obtained using MATLAB System Identification Toolbox as

$$A(q) = 1 - 2.725q^{-1} + 2.57q^{-2} - 0.9361q^{-3} + 0.09098q^{-4} \quad (3.8)$$

$$C(q) = 1 - 1.998q^{-1} + 1.291q^{-2} - 0.2911q^{-3} \quad (3.9)$$

The noise variance is also estimated as 2.3278. Thus, $y(t)$ can be obtain using Eq. (3.1) which is predicted wind speeds for one year, as shown in Figure 3.4.

Table 3.5: Results for Finding the Order of the ARMA.

n_a, n_c	AICs
1,1	3304.111642
1,2	3305.728908
1,3	3307.044785
1,4	3308.421132
2,1	3305.756687
2,2	3307.588795
2,3	3308.883251
2,4	3310.401179
3,1	3307.341598
3,2	3210.725993
3,3	3309.733142
3,4	3313.400201

4,1	3209.357658
4,2	3211.851392
4,3	3198.168838
4,4	3218.802228

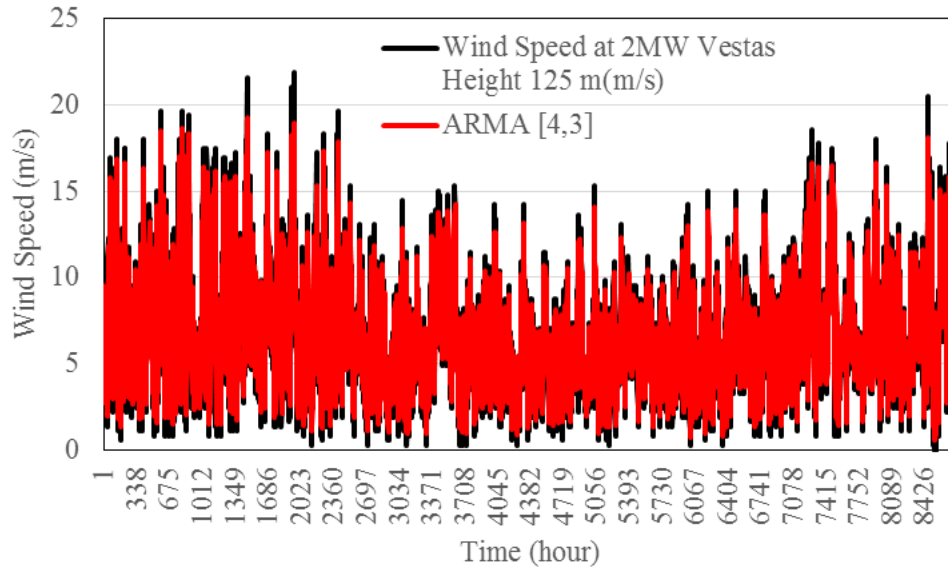


Figure 3.5: Predicted wind speed in St. John’s with ARMA model.

3.3.2. Wind Speed Prediction by ANN Method

3.3.2.1. Principle of ANN Method

An accurate estimating of wind speed is important for operational, capacity adequacy, financial, and design. There are several types of wind speed models that can be used for wind farm planning [117]. Different models result in different output power of wind turbine, thus affecting generation adequacy evaluation. In addition, an error in wind speed model results in cubic error of wind power output. In this section, the performance of ARMA model and neural network was investigated for wind speed time series prediction.

Neural networks have been commonly used for wind generation applications such as short-term and long-term wind speed predictions, wind turbine control system, reactive power control, pitch control system, maximum power point tracking, fault diagnosis, and transient stability. Neural network time series are the most applicable wind speed modeling approaches. Simplicity, less computation time, handling multivariable problems, and solving nonlinear problems are the main advantages of neural networks [63]. In this section, wind speed time series are predicted by neural network.

Three different types of training algorithms for neural network and ARMA model were used and compared with observed wind speed data. Neuron or node is the basic unit of computation in neural networks which gets input from other nodes and determine an output. Each input has its own weight factor which shows the relevance between other inputs. Calibrating all of the weight factors is called training the neural network [63].

There are generally three layers in neural networks which are input, hidden, and output. Hidden layers perform computations and link input to output. Hidden layers are not required for linear separable functions or decisions. The feedforward neural network is the simplest type of neural networks, where information is being transferred from input layer to output layers in only forward direction. Figure 3.5 shows an example of feedforward neural network. This network by considering a delay input is called focused time-delay neural network, which is highly suitable for time series predictions. Using delay inputs, information arrives at hidden layers with some time difference, thus past information can be stored in network [63].

In this study, nonlinear autoregressive time series of wind speeds are generated by focused time-delay neural network. This predicts time series $x(t)$ given d past values of $x(t)$ as follows [64]:

$$y(t) = f(x(t-1), x(t-2), \dots, x(t-n_p)) \quad (3.10)$$

where n_p is the number of past wind speed data.

Focused time-delay neural network is illustrated in Figure 3.6, where delays are involved in input layers which serve as a memory ensuring storing previous data without any feedback from output layer. In this process, n_p inputs $x(t-1), x(t-2), \dots, x(t-n_p)$ are reaching to hidden layers and response $y(t)$ is predicted. The network must be trained to adjust weight factors so that the error between estimated output and input is minimized [65].

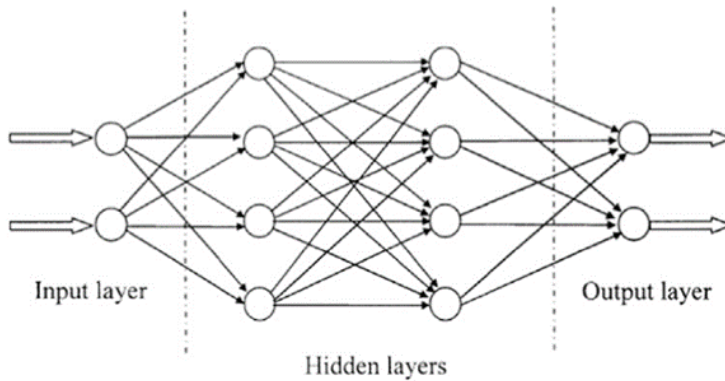


Figure 3.6: Feedforward neural network [63].

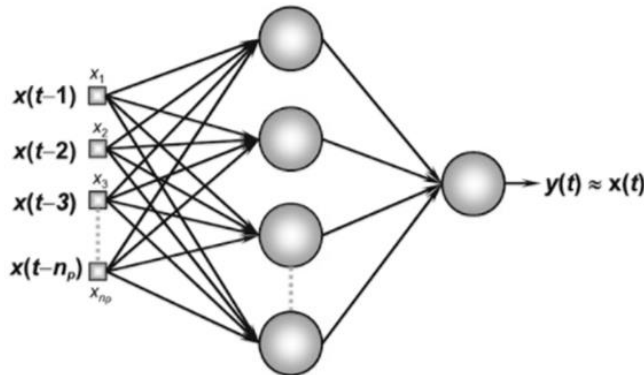


Figure 3.7: Focused time-delay neural network [65].

This error can be minimized by different types of algorithms such as Bayesian Regularization, Levenberg Marquardt, and Scaled Conjugate Gradient training, which are the most commonly used algorithms for training a neural network. They are briefly introduced as follows.

1) *Levenberg-Marquardt Backpropagation Algorithm*: This is highly recommended method because of its stability and fast convergence [65]. It is used to train the neural network which updates weight factors by Levenberg-Marquardt optimization.

2) *Bayesian Regularization Training Algorithm*: This algorithm is based on reducing the sum squared error between observed wind speeds and predicted wind speeds. Training is based on modifying weights in a repetitive steps so that the sum squared error is minimized. Hence, this process is based on a minimization of an objective function which calculates sum of squared errors [66].

3) *Scaled Conjugate Gradient Training Algorithm*: This algorithm was developed by [67] which is based on a line search for updating weight factors to avoid time-consuming process of training neural network [68].

The above three training algorithms for neural network were used to predict wind speed data by MATLAB Neural Network toolbox for the city of St. John's, Newfoundland and Labrador, Canada. The capability of wind speed prediction of each model in comparison with the observed wind speed data were evaluated by R^2 and the residual analysis.

3.3.2.2. Case Study for Wind Speed Prediction by ANN Method

Predicted hourly annual wind speeds using neural networks for St. John's are shown in Figures 3.7-3.9. Predicted hourly wind speeds for one day and two days are shown in Figures 3.10 and 3.11. It can be seen that wind speed significantly varies from hour to hour and it is a difficult task to predict wind speeds for each hour.

R^2 is used to determine the error between predicted and observed data. It can be seen from Table 3.6 that an accurate wind speed modeling is obtained using neural network time series. A high value of R^2 cannot guarantee a good fit of data. Hence, the residual analysis, which shows the difference between simulated wind speeds and the fit to the simulated wind speeds, has been performed to ensure the capability of neural network in wind speeds prediction, as shown in Figures 3.12-3.15. The distance of the data from 0 line shows the forecast error. Positive and negative points show the forecast was low and high, respectively. Values located at 0 line indicate the forecast was correct [117].

It is found that a more accurate wind speed prediction was obtained when neural network was employed than ARMA. Bayesian regularization demonstrated better accuracy of wind speed modeling than other two training algorithms, Levenberg Marquardt and Scaled Conjugate Gradient.

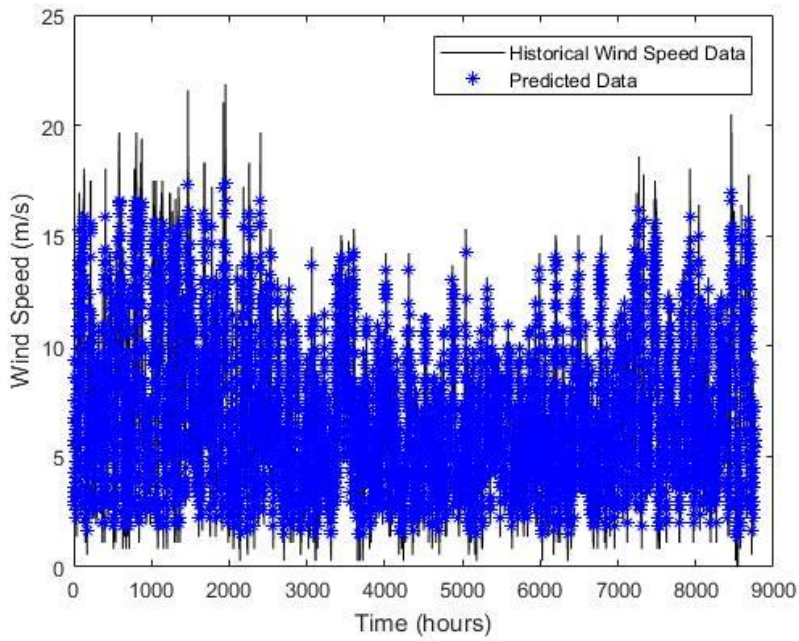


Figure 3.8: Predicted wind speed in St. John’s with neural network using Levenberg Marquardt training [117].

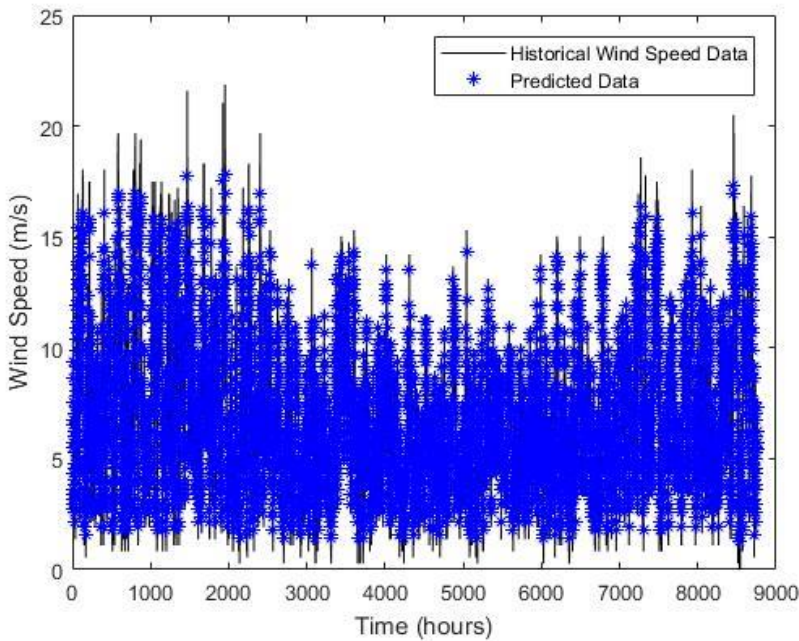


Figure 3.9: Predicted wind speed in St. John’s with neural network using Bayesian Regularization [117].

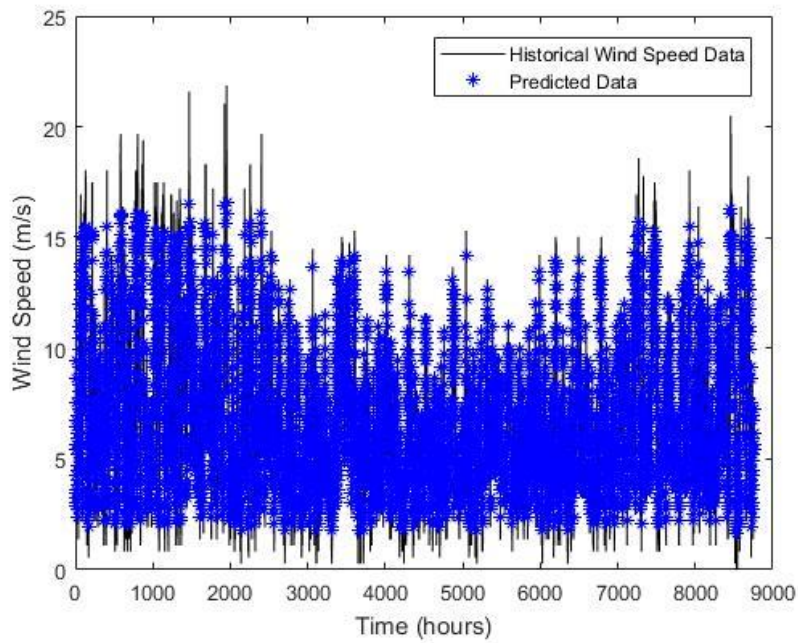


Figure 3.10: Predicted wind speed in St. John's with neural network using Scaled Conjugate Gradient [117].

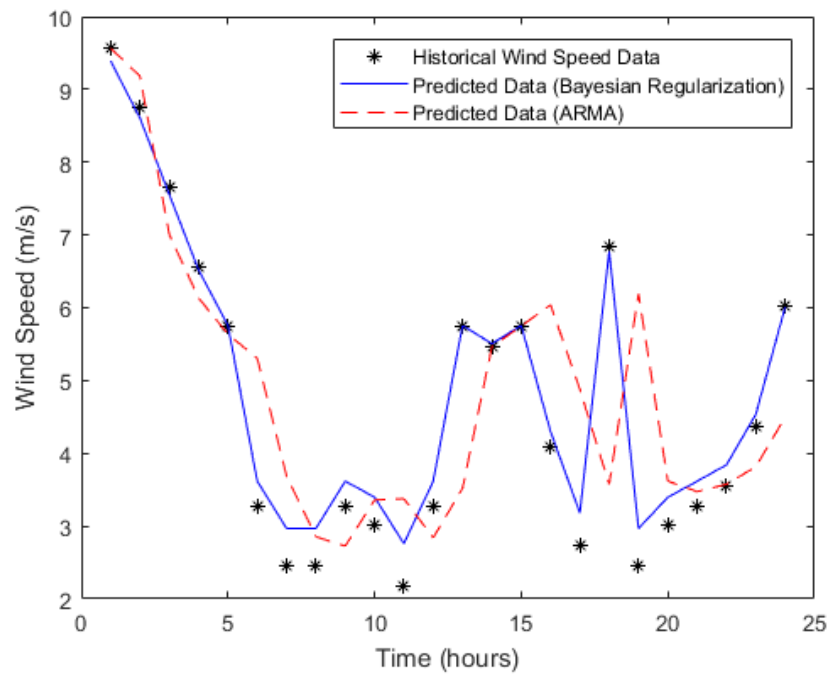


Figure 3.11: Comparison of predicted wind speeds for one day (January 1st) [117].

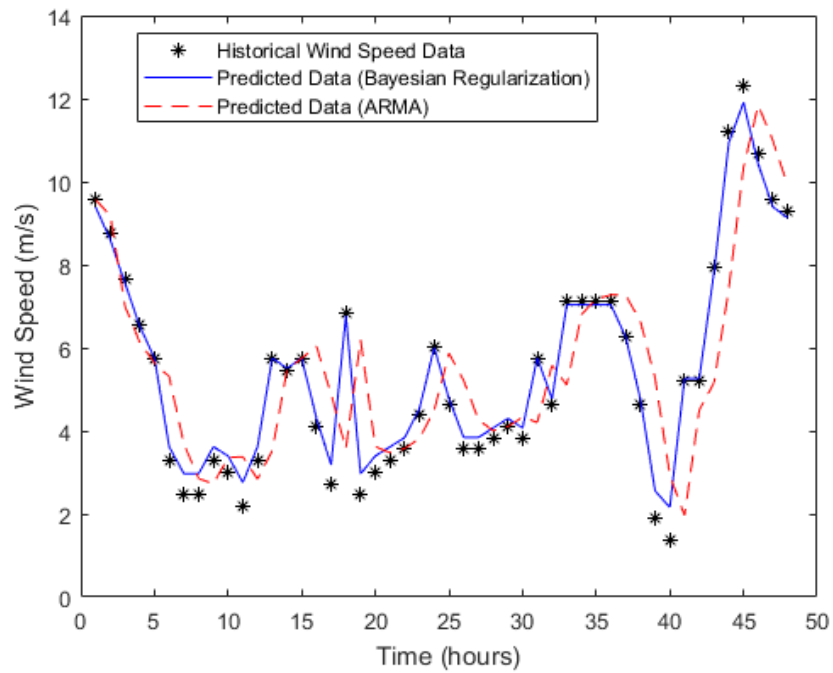


Figure 3.12: Comparison of predicted wind speeds for two days (January 1st-January 2nd) [117].

Table 3.6: R-Squared Value for the Two Wind Speed Model [117].

Wind Speed Model	R-SQUARED
ARMA	0.8071
Neural network (Levenberg Marquardt)	0.9859
Neural network (Bayesian Regularization)	0.9874
Neural network (Scaled Conjugate Gradient)	0.9824

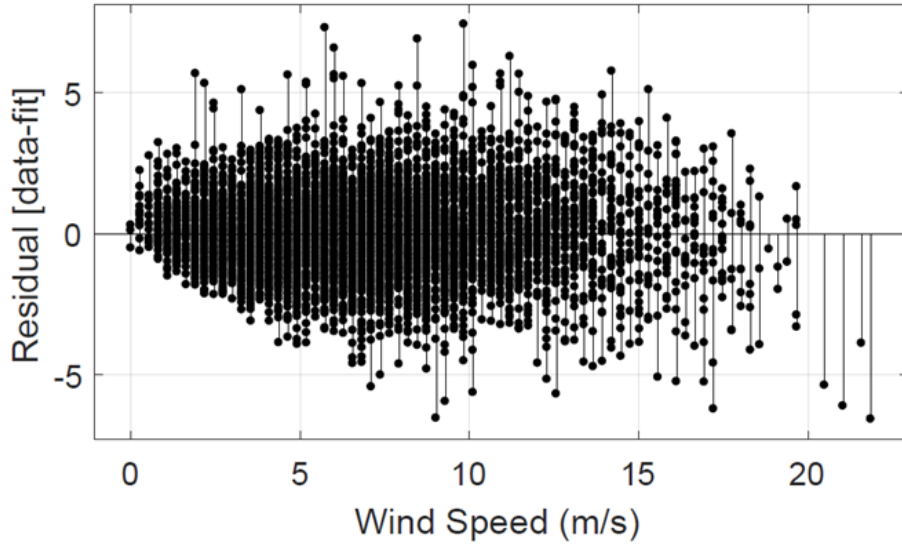


Figure 3.13: Residual analysis for ARMA time series [117].

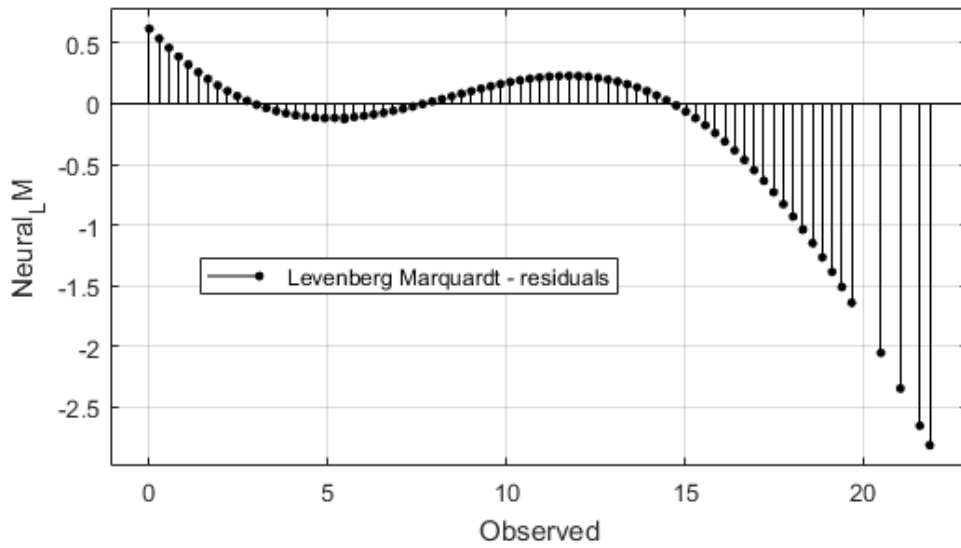


Figure 3.14: Residual analysis for neural network time series using Levenberg Marquardt training [117].

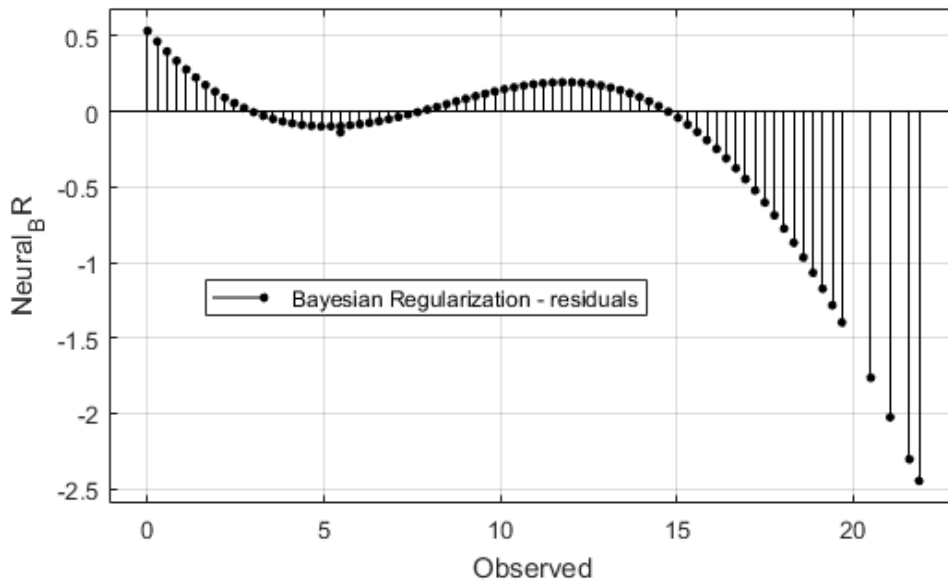


Figure 3.15: Residual analysis for neural network time series using Bayesian Regularization [117].

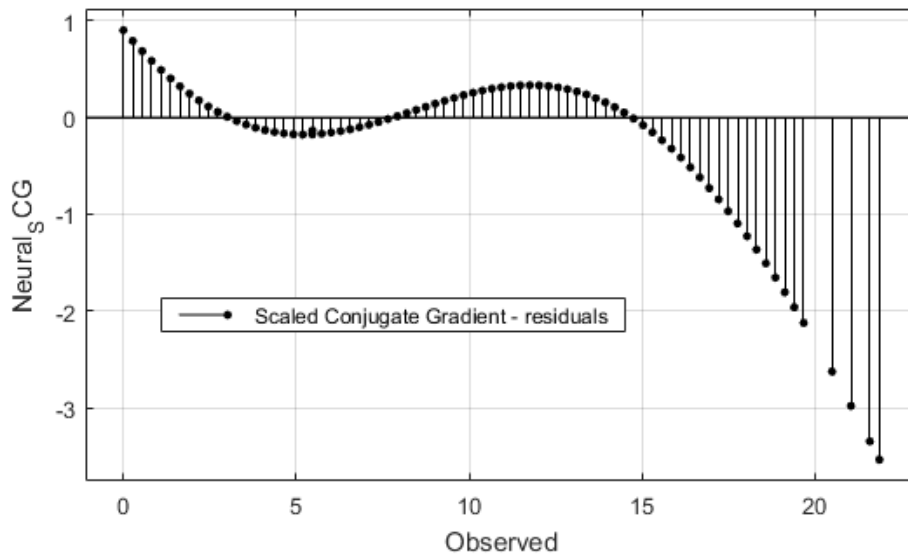


Figure 3.16: Residual analysis for neural network time series using Scaled Conjugate Gradient [117].

3.4. Generation Model

3.4.1. COPT of Conventional Generators

In generation adequacy evaluation, the generator model is represented in the form of arrays of capacity levels with the probability of each capacity level. The COPT is the most commonly used generation model. Conventional generators are generally represented by a two-state model, a up state (operating) or a down state (failed), as shown in Figure 3.16, where “Failed” refers to a generator outage due to components’ failure. In this figure, λ is the unit failure rate and μ is the unit repair rate.

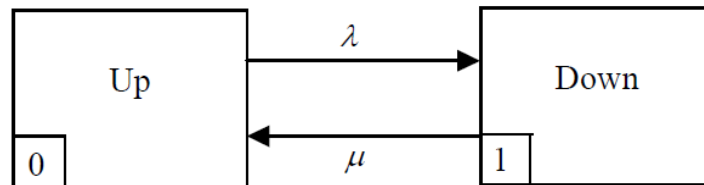


Figure 3.17: Generation unit representation by two-state model [69].

Wind energy systems are represented by a multi-state model. The COPT of a generator can be developed using a recursive technique which was introduced in previous chapter. This technique is valid for both two-state and multi-state generation systems [69].

The RBTS is adopted here. The single line diagram of RBTS is shown in Figure 3.17. Table 3.7 shows the generator ratings along with the RBTS reliability data. The system consists of a total of 6 buses with 5 load buses, 9 transmission lines, and 11 generators in buses 1 and 2 ranging from 5 MW to 40 MW. The total installed capacity of the system is 240 MW. The peak load of the

system is 185 MW. Using recursive technique, the COPT of the RBTS is obtained as shown in Table 3.8. The COPT will be used later for the generation adequacy evaluation.

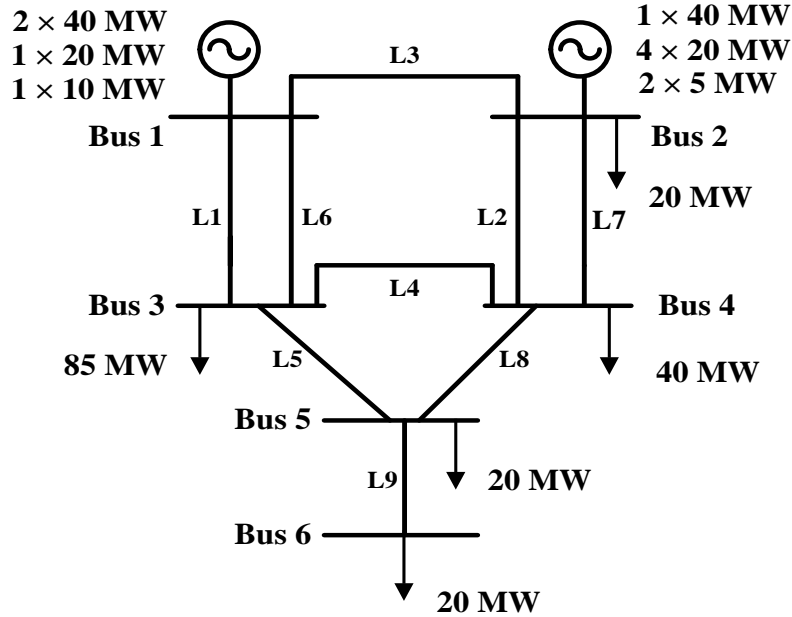


Figure 3.18: Single line diagram of the RBTS [70].

Table 3.7: Conventional Generation Unit Reliability Data for RBTS [70].

Size (MW)	Type of Unit	No of Units	FOR	MTTF/h	MTTR/h
5	Hydro	2	0.010	4380	45
10	Thermal	1	0.020	2190	45
20	Hydro	4	0.015	3650	55
20	Thermal	1	0.025	1752	45
40	Hydro	1	0.020	2920	60
40	Thermal	2	0.030	1460	45

Table 3.8: COPT of the conventional generators in the RBTS.

Capacity-out (MW)	Probability	Capacity-out (MW)	Probability
0	0.812859614	125	4.29E-07
5	0.016421406	130	4.35E-07
10	0.016671908	135	8.75E-09
15	0.000335131	140	1.46E-06
20	0.070358538	145	2.96E-08
25	0.00142135	150	3.00E-08
30	0.001443033	155	6.03E-10
35	2.90E-05	160	4.76E-08
40	0.069269729	165	9.62E-10
45	0.001399385	170	9.77E-10
50	0.001420733	175	1.96E-11
55	2.86E-05	180	7.93E-10
60	0.005828452	185	1.60E-11
65	0.000117744	190	1.63E-11
70	0.00011954	195	3.27E-13
75	2.40E-06	200	6.60E-12
80	0.002001483	205	1.33E-13
85	4.04E-05	210	1.35E-13
90	4.11E-05	215	2.72E-15
95	8.25E-07	220	2.19E-14
100	0.00015945	225	4.42E-16
105	3.22E-06	230	4.49E-16
110	3.27E-06	235	9.02E-18
115	6.57E-08	240	4.56E-20
120	2.12E-05		

3.4.2. COPT of Wind Generation Systems

Before obtaining the COPT of wind generation system, the hourly power output of wind turbine must be determined by the predicted hourly wind speeds. This is obtained by the power curve

characteristics of the wind turbine. The mathematical expression of the power curve is given by [69]

$$P_i = \begin{cases} 0, & 0 \leq SW_{bi} < V_{ci} \\ P_r (A + B \times SW_{bi} + C \times SW_{bi}^2), & V_{ci} \leq SW_{bi} < V_r \\ P_r, & V_r \leq SW_{bi} \leq V_{co} \\ 0, & V_{co} < SW_{bi} \end{cases} \quad (3.11)$$

Where P_i is the power output of the wind turbine and P_r is the rated power output of the wind turbine. SW_{bi} is the predicted wind speeds. V_{ci} , V_r , and V_{co} are cut-in wind speed, rated wind speed, and cut-out wind speed of the wind turbine characteristics, respectively. The constants A, B, and C are obtained as [69]

$$A = \frac{1}{(V_{ci} - V_r)^2} \left[V_{ci}(V_{ci} + V_r) - 4V_{ci}V_r \left(\frac{V_{ci} + V_r}{2V_r} \right)^3 \right] \quad (3.12)$$

$$B = \frac{1}{(V_{ci} - V_r)^2} \left[4(V_{ci} + V_r) \left(\frac{V_{ci} + V_r}{2V_r} \right)^3 - (3V_{ci} + V_r) \right] \quad (3.13)$$

$$C = \frac{1}{(V_{ci} - V_r)^2} \left[2 - 4 \left(\frac{V_{ci} + V_r}{2V_r} \right)^3 \right] \quad (3.14)$$

The hourly power output of the wind turbine without considering FOR of the wind turbine components are generated using the above mathematical expression of the power curve, as shown in Figure 3.18.

The COPT of the wind farm can now be obtained using the steps explained in Chapter 2.2. The COPT of the wind turbine is formed using this approach, which is shown in Table 3.9.

A wind generation unit has two parts which are wind resource (wind condition) and wind turbine components. In the previous COPT, it was assumed that all of wind turbine components are 100% reliable and there is no failed component in the components during the operation time of the wind turbine. However, a wind turbine might fail similar to any other components. FOR of the wind turbine is thus taken into account to consider the failure of wind turbine components in the COPT. The FOR of the wind turbine is considered 4% [71]. The COPT of 2MW wind turbine with FOR of 4% is shown in Table 3.10.

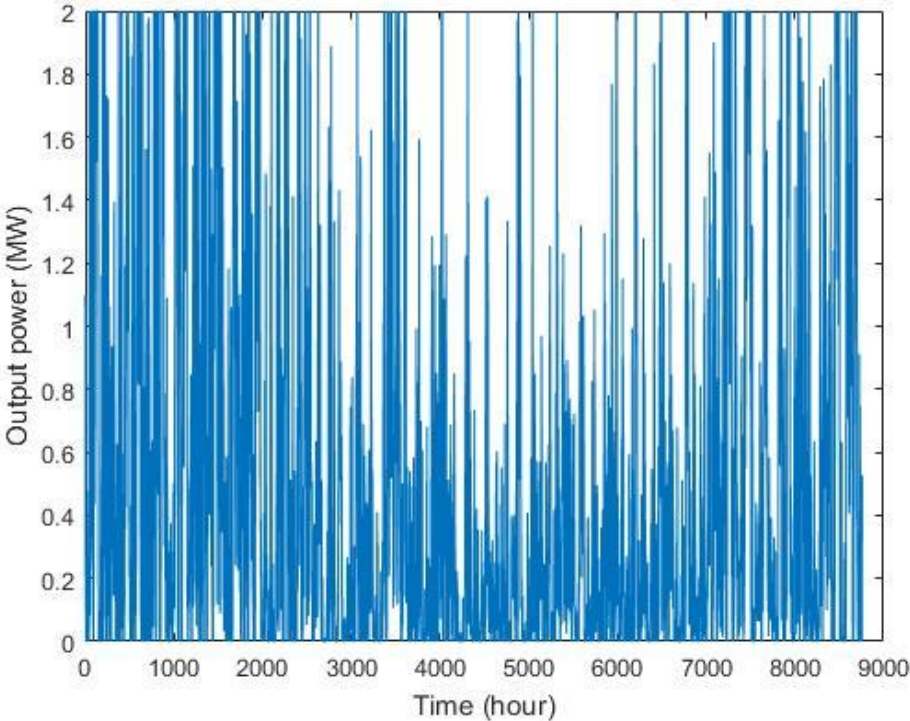


Figure 3.19: The power output of Vestas 2 MW wind turbine.

Table 3.9: COPT of 2MW wind turbine without FOR.

Capacity out (MW)	Probability	Capacity out (MW)	Probability
-------------------	-------------	-------------------	-------------

0	0.068721	1.25	0.025457
0.05	0.00411	1.35	0.031735
0.15	0.007763	1.45	0.043037
0.25	0.007306	1.55	0.047945
0.35	0.008333	1.65	0.061986
0.45	0.009361	1.75	0.071233
0.55	0.011986	1.85	0.095662
0.65	0.011644	1.95	0.137443
0.75	0.013128	2	0.265982
0.85	0.013927		
0.95	0.016667		
1.05	0.022032		
1.15	0.024543		

Table 3.10: COPT of 2MW wind turbine with FOR of 4%.

Capacity-out (MW)	Probability
0	0.072146
0.05	0.003653
0.15	0.007192
0.25	0.007991
0.35	0.007648
0.45	0.010845
0.55	0.010274
0.65	0.011416
0.75	0.014155
0.85	0.012443
0.95	0.015525
1.05	0.021119
1.15	0.022717
1.25	0.02637
1.35	0.027055
1.45	0.041781
1.55	0.046119
1.65	0.056621
1.75	0.068037
1.85	0.093493

1.95	0.13105
2	0.292352

3.5. Generation Adequacy Evaluation of Conventional Generators and Wind Farm

One event in ten years is the industry-accepted risk standard by utilities, which translates to LOLE of 0.1 days/year. This criteria means that the power electric system meets the load demand such that the demand exceeds power generation only once in ten year period [114]. The risk criteria is also expressed in hours per year, and one day in ten years risk criteria can be treated as LOLE of 2.4 h/year [114]. LOLE in hours/year is a more precise risk criteria since an event might not last 24 hours (2.4 hours/0.1days=24 hours) and it calculates outages in hours rather than days [115]. The LOLE of the RBTS considering conventional generators only is obtained as LOLE=1.05 hours/year. This matches the results obtained by the study in [72].

In this study, the risk criterion is the LOLE of 1.05 h/year [72]. In order to replace conventional generators with wind farms, the same risk level should be maintained for the system. Table 3.11 shows the wind farm capacity required to maintain the risk criteria when conventional generators are replaced with wind energy. It can be seen that it is not possible to maintain the risk criteria when 20 MW of conventional generator is replaced with wind energy. The LOLE is saturated under this condition. Ref. [72] suggested that this issue can be rectified by involving two or three independent wind sites to replace large amount of conventional generators.

Table 3.11: Replacing conventional generator with wind energy.

Conventional generator replacement (MW)	Wind farm capacity needed (MW)	LOLE (hours/year)	Ratio (wind farm capacity/conventional generator)
10	18	0.999	1.8
20	60	1.395	3

3.5.1. An Improved Analytical Approach – Fuzzy C Means

The multi-state COPT is a commonly used model of wind energy generation model. The number of states is critical in generation adequacy evaluation because more states generally means a better modeling accuracy and a higher computation overhead. It was found in [46] that a 6-state COPT model is able to achieve a trade-off between accuracy and computation overhead. A FCM algorithm can be applied to obtain optimal number of states in wind farm generation for Markov chain [49].

In this section, wind generation adequacy is evaluated for the city of St. John’s, Newfoundland and Labrador, Canada. The FCM method is applied to determine optimal number of states in wind farm’s COPT. The main contribution is to obtain a reduced number of states while maintaining accurate modeling. The Loss of Load Approach, which is the most widely used in the analytical technique, is adopted for generation adequacy assessment in this case study. The LOLE is used to quantify reliability. The RBTS is used as a test platform [73].

Data clustering is the basis of several system modeling algorithms and classification. The main goal of clustering is to obtain data groupings from a dataset to represents system’s behavior. FCM is a popular clustering method where a large set of data is categorized into a finite number of clusters with every data in the dataset belongs to a cluster with a certain degree. In fact, FCM allows every data belongs to multiple clusters with a membership grade [49].

In FCM, cluster center is initially guessed which shows the mean location of each cluster. Following this, every data is assigned with a membership grade for each data point. This process continues by updating cluster center and membership grade for each cluster until the right cluster center is obtained. Thus, this process is based on a minimization of an objective function which calculates distance from each cluster to each data point with membership grade. The objective function J_m is given by [74]

$$J_m = \sum_{i=1}^D \sum_{j=1}^N \mu_{ij}^m \|x_i - c_j\|^2 \quad (3.15)$$

where D is the number of data points. N is the number of clusters. m is Fuzziness coefficient, with $m > 1$. This value determines how much the clusters can overlap with one another. The higher the value of m , the larger the overlap between clusters.

In other words, the higher the fuzziness coefficient the algorithm uses, a larger number of data points will fall inside a ‘fuzzy’ band where the degree of membership is neither 0 nor 1, but somewhere in between. By default, $m=2$. x_i is the i th data point. c_j is the center of the j th cluster. μ_{ij} is the degree of membership of x_i in the j th cluster. For a given data point, x_i , the sum of the membership values for all clusters is one.

Clustering technique based on FCM is obtained by the following steps [74]:

1. Randomly initialize the cluster membership values, μ_{ij} .
2. Calculate the cluster centers by

$$C_j = \frac{\sum_{i=1}^D \mu_{ij}^m x_i}{\sum_{i=1}^D \mu_{ij}^m} \quad (3.16)$$

3. Update μ_{ij} by

$$\mu_{ij} = \frac{1}{\sum_{k=1}^N \left(\frac{\|x_i - c_j\|}{\|x_i - c_k\|} \right)^{\frac{2}{m-1}}} \quad (3.17)$$

4. Calculate the objective function, J_m .

5. Repeat steps 2–4 until J_m improves by less than a specified minimum threshold or until after a specified maximum number of iterations.

The stopping criteria in this process is by considering minimum improvement in objective function between two iterations. In this study, the interactions in the FCM will be stopped if the objective function is improved by less than 0.001 between two iterations. In this section, the ARMA model is used to predict future time series wind speed using historical wind speed data in St. John's. MATLAB System Identification Toolbox was used, where the hourly wind speeds of St. John's for one year period between January and December 2015 was input in the toolbox to predict wind speeds using the ARMA model.

Table 3.12 shows the required number of states of wind energy states based on Fuzzy C-Means clustering algorithm. It can be seen that after 6-state, there is not much decreasing compared to the prior states. The LOLE risk index for the RBTS is calculated as 1.05 hours/year. The wind

farm capacity for replacing conventional generators with wind turbines while maintaining the same LOLE risk criteria is evaluated as 8MW (4 wind turbines×2MW).

The effectiveness of the FCM method in reducing COPT states of wind farm is evaluated and compared with non-optimal states. Results are demonstrated for replacing 5 MW conventional unit in RBTS with 8 MW wind farm, as shown in Table 3.13 and Figure 3.20. The following conclusions can be made by the study results [73].

When replacing a 5 MW conventional generator in RBTS by the 8 MW wind farm, the base LOLE risk criteria must be maintained at 1.05. The results indicate that the 8 MW wind farm can replace the 5 MW conventional generator with 1.05 LOLE maintained if a 6 states wind turbine generator model is created using the FCM method. The corresponding LOLE considering 6 states without the FCM method is 1.39 hours/year. The analysis in [46] also shows that a 6-state model is realistic for wind power generation in the reliability analysis.

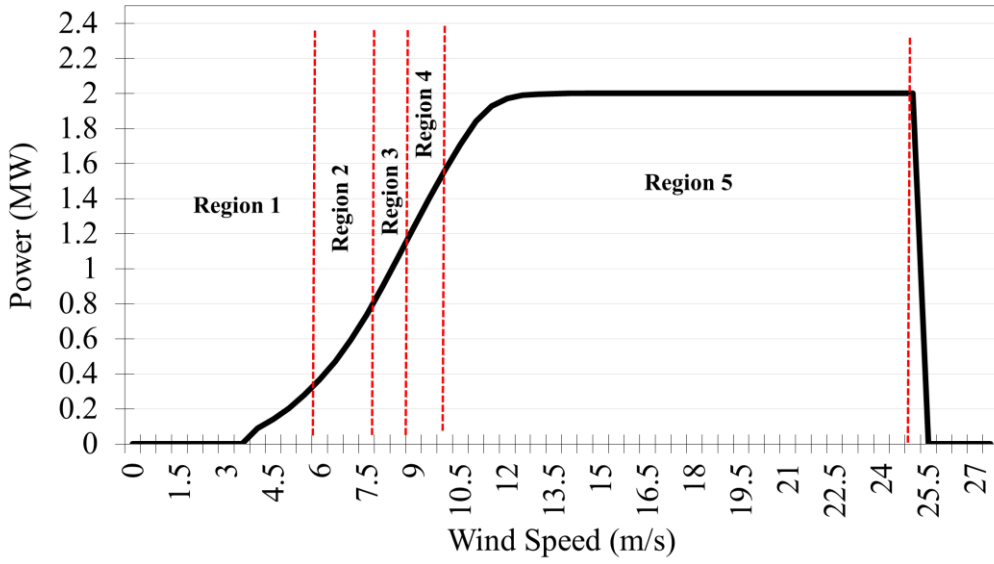
Therefore, 6 states are chosen for the LOLE calculation by the FCM method in this study. The results from the existing method indicate that the 8 MW wind farm cannot replace a 5 MW conventional generator; while the results from the FCM indicate the opposite. It is hoped that the results of this study could help planners and financial investigators to make good decisions for wind power projects in St. John's.

Table 3.12: Fuzzy C Means Algorithm for Clustering Wind Energy [73].

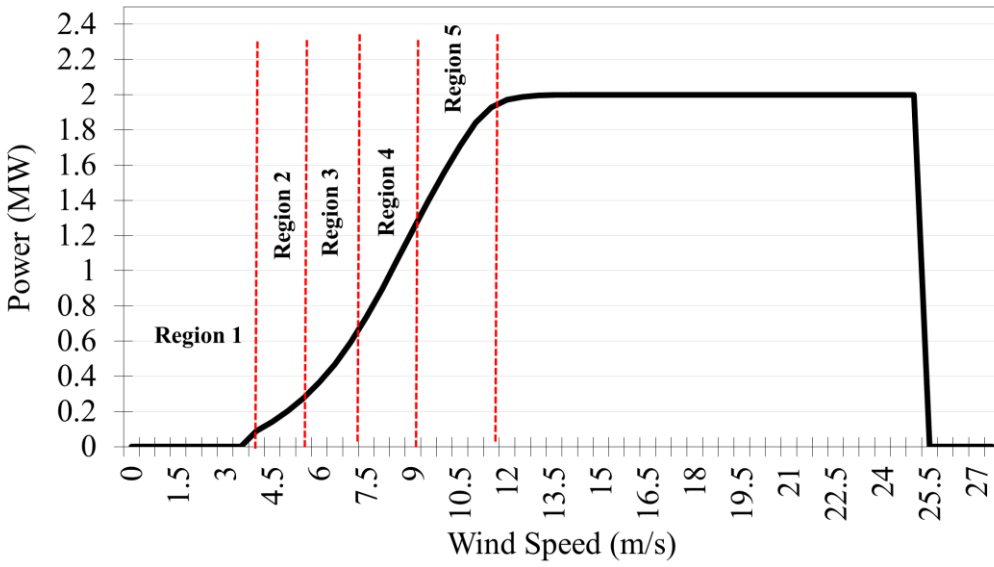
Number of Clusters	Number of Iterations	Objective Function
2	16	564.91
3	24	195.84
4	20	95.4
5	54	56.11
6	53	36.1
7	62	25.75
8	64	18.55
9	50	14.54
10	67	11.2
11	39	9.14

Table 3.13: Comparing results for replacing 5MW conventional unit in RBTS with 8MW wind farm [73].

Number of States	LOLE (hours/year)	
	Non-Optimal States	FCM
3	1.57	1.15
4	1.39	1.10
5	1.43	1.07
6	1.39	1.05
7	1.39	1.04
8	1.33	1.03
9	1.33	1.02
10	1.33	1.02
11	1.26	1.02



(a)



(b)

Figure 3.20: States of the wind turbine generator with a 6 state model: (a) non-optimal case; (b) FCM [73].

3.5.2. A Case Study for Generation Adequacy – Capacity Factor

The power output of renewable energy systems depends on the resource availability, technology choice, and design characteristics. These are considered in determining a capacity factor, which is defined as the ratio of real power output of generator over a period of time, to the rated power output [76]. When the detailed data of resource such as wind speed and solar radiation are not available, capacity factor can be used to calculate the power output of renewable energy systems directly [77]. In this section, the reliability improvements made by renewable energy sources and conventional generators with the analytical loss of load method is conducted.

The following two cases are considered [75]: 1) the RBTS plus a hybrid PV and wind generation system with the capacity of 80.5 MW (50×810 kW PV and WT 20×2 MW); 2) the RBTS plus an 80.5 MW thermal unit (2×40.25 MW). Figure 3.21 shows the system configuration for Case 1. 20 wind turbines of Vestas V90-2MW were considered which make the total capacity of wind farm as 40 MW (20×2 MW = 40 MW). The solar PV system is rated at 810 kW per one array (by assembling 900 groups of 30 series Canrom 30 Wp modules with 4% FOR). The total PV capacity is 40.5 MW considering 50 arrays (50×810 kW = 40.5 MW). The total capacity of the added thermal units to the RBTS in case 2 is 80.5 MW (two thermal units with 40.25 MW capacity) with 4% FOR [75].

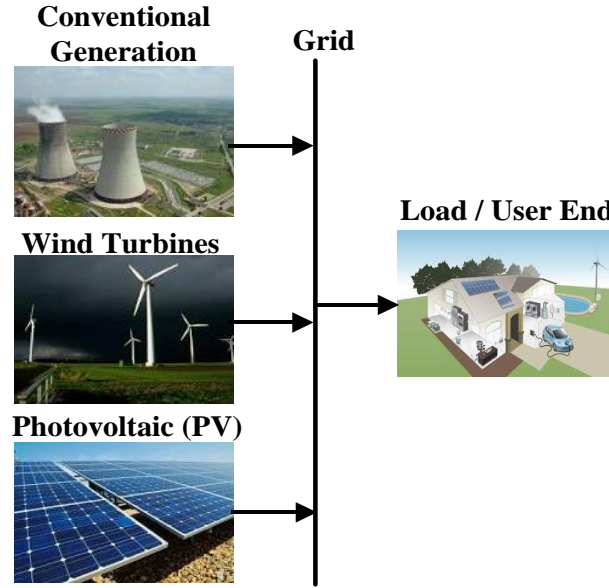


Figure 3.21: The system configuration for Case 1 [75].

Energy sale is another main objective of power system companies, hence, another important and essential reliability index is the Expected Energy Not Supplied (EENS) which can be calculated as follows [75]:

$$EENS = \sum_{i=1}^n (ENS_i \times p_i) (L_{\max} > C) \text{ (MWh/yr)} \quad (3.18)$$

According to the NREL report [78], the maximum capacity factor for wind turbines and PV systems that can be achieved in any region is 50.6%, and 28%, respectively. Therefore, the power output of one unit of wind turbines and one array of PV systems using this criteria is obtained as 1.012 MW (2MW×0.506), and 0.2268 W (0.810MW×0.28), respectively.

Thus, the total power output of wind farm and solar panel is 20.24 MW, and 11.34 MW, respectively [75]. Table 3.14 shows the result of this study for the two cases. The LOLE (hr/year)

for the RBTS, and cases 1 and 2, are 11.13, 0.61 and 0.45, respectively. It can be seen that the LOLE for Case 2 is the lowest, which indicates that the system in Case 2 is most reliable than the system in other cases. Similarly, the EENS for Case 2 is also the lowest (4.67 MWh/yr) among other cases, Case 1 (5.60 MWh/yr) and base case (116.68 MWh/yr). As it was expected, the hybrid renewable energy system can improve the reliability of the system in Case 1, however, reliability is much more improved when conventional generators in Case 2 are used even though the same capacity and FOR of the system in Case 1 is used for Case 2.

Table 3.14: LOLE (h/yr) and EENS (MWh/yr) considering different Cases [75].

Reliability indices	Base case	Case 1	Case 2
LOLE (h/yr)	11.13	0.61	0.44
EENS (MWh/yr)	116.68	5.60	4.67

The capacity credit method can be used to determine the capacity factor of wind generation for the generation adequacy evaluation, it allows to determine the maximum capacity of conventional generators that can be replaced with wind power generation while maintaining the same level of the risk of the system.

The effective load carrying capability (ELCC) is the most efficient method for the capacity credit evaluation of wind generation systems [16]. This method determines the amount of extra load demand that can be met while maintaining the same risk level. A graphical illustration of this method is shown in Figure 3.17.

To determine the amount of extra load, the system peak load is gradually increased until the system's reliability of original system with wind energy is the same as the original system without

wind energy. In this example, addition of 400 MW load is possible while keeping the same LOLE when a new generation system is added in the original system [16].

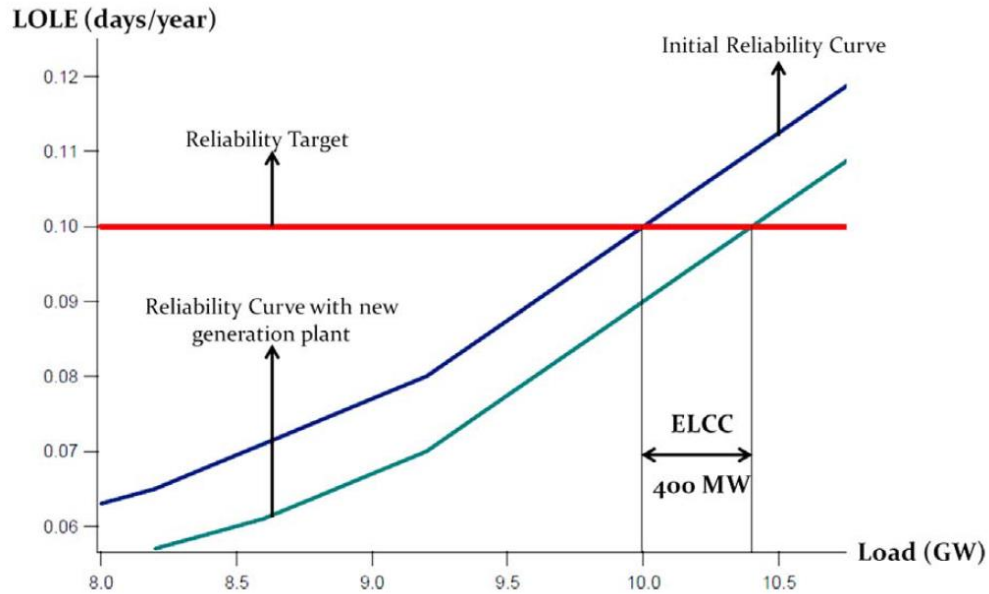


Figure 3.17: An example of ELCC of adding a new generation system [16].

The ELCC is the most popular and commonly used method for wind capacity credit assessment. This method is based on gradually increasing the system peak load meanwhile the reliability improvement by the wind energy is the same as original system without considering the wind energy. In this section, capacity credit of wind energy is determined for St. John’s. The LOLE without the wind energy for the RBTS is 1.05 hrs/yr.

As it can be seen from Figure 3.22, the maximum allowable peak load at a risk level of 1.05 hrs/yr in the RBTS with the 20 MW wind farm addition is 189.4029 MW. The increase in peak load carrying capability of 4.4029 MW (189.4029-185) is the capacity credit of the wind power.

It means, 20 MW wind farm can replace 4.4029 MW of conventional unit in RBTS. Wind capacity factor St. John's = maximum (limit) amount of conventional generator replacement is 22.01%.

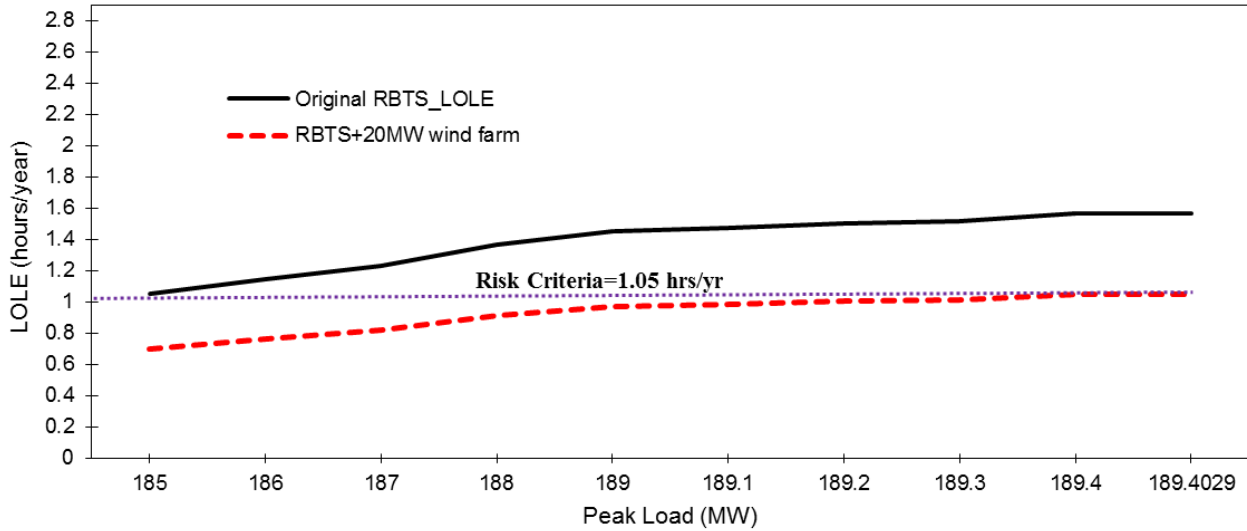


Figure 3.22: Wind capacity credit value of 20 MW wind farm in St. John's.

3.6. Conclusion

In this Chapter, the main objective is to develop an analytical approach for generation planning with wind energy integration. A general modeling of generation adequacy evaluation for conventional generators and wind energy systems is introduced.

The first step is to predict and model wind speed, which can be done by two methods, ARMA and Neural Networks. The power curve characteristics of wind turbine is used to represent power output of wind turbine. Wind generator Forced Outage Rate (FOR) is used to model unavailability of wind turbine. Generation model is constructed by the COPT using the predicted wind speeds by the ARMA.

The load model of the Roy Billinton Test System is considered, and it is combined with generators model. As a most commonly used model of both conventional and wind energy generation model in the literature, the Loss of load approach is adopted in this thesis. The number of COPT states is critical in generation adequacy evaluation because more states generally means a better modeling accuracy and a higher computation overhead. An improved method using Fuzzy C mean algorithm is used to obtain the number of states of wind turbine. Generation adequacy is also investigated using the capacity factor method, which is an effective technique for generation adequacy evaluation when the detailed historical wind speeds are not available. Capacity credit is also used to determine the capacity factor of a wind generation system.

Chapter 4: Standalone System Design

4.1. Introduction of Standalone System Design

Electricity in some remote areas in the world is still unavailable. It is estimated that 1.3 billion people worldwide currently do not have access to electricity [2]. Standalone power supply system is aimed to supply electricity to remote communities, which do not have access to the main power grid due to economic or technical difficulties [79].

Standalone power supply system can be in the form of a single based energy source (such as diesel-only, PV-only, or wind-only) or in a hybrid configuration (such as diesel-wind, diesel-PV, diesel-PV-wind etc). The energy storage system can be used to mitigate the fluctuations of renewable energy power output. The diesel-only configuration is a main generation form in remote areas due to high reliability. However, the operating cost of diesel generators is high due to high diesel price, and increased transportation cost of the diesel. Diesel generators are also being declined because of their environmental effect and greenhouse gas emissions [3]. Thus, renewable energy systems are a preferred choice in remote areas.

4.2. Wind Generation System Design

In this section, wind energy potential is firstly investigated using the Weibull distribution. An analytical method based on the FTA and minimal cut sets are used to estimate the reliability of the system. A generic formula for calculating annual O&M costs is then proposed based on the real data available from NREL. A case study for a wind energy project in St. John's, Newfoundland and Labrador, Canada is presented [58].

Three important steps are involved in a successful wind energy project which are wind energy potential, reliability, and costs [58]. The first step in designing a wind power plant is wind energy potential assessment for a site which can be obtained by analyzing statistical characteristics of wind resource [61,62]. Wind speed distribution must be accurately predicted in order to reduce wind energy potential uncertainties [58].

Reliability and costs are highly correlated and the cost or benefit analysis from renewable energy is not complete without reliability evaluation [71]. This fact is emphasized by reference [71] which states reliability of renewable energy systems must be evaluated in addition to the costs benefits. Methods for reliability and costs evaluation for small remote area systems are proposed in [71, 80]. An approach for determining optimal installation of wind energy considering costs and power system reliability performance is presented in [81] which is based on an optimization problem with nonlinear nondifferentiable objective function considering capital costs, O&M costs, and costumer interruption costs [81].

A wind energy project is planned for the operational time of 20-25 years. However, the lifetime of a wind energy project can be shorter, for instance, according to a study of United Kingdom's wind farms it was found that only a few wind farms will operate for more than 12-15 years [82]. Wind turbine components can fail because of wind variations, component aging, and power system disturbance. These failures cause extra maintenance and repair costs [83].

For such case, estimating of O&M costs is financially essential for a successful planning of wind energy projects [83]. Reliability, O&M costs, and average failure rate of a wind energy project based on an analytical method was investigated in [83]. Cost evaluation of a wind energy

project is an important step for achieving a successful financial planning and determining the feasibility of the potential site [84]. However, it is a difficult challenge due to the unpredictability and variability of wind resource [85].

Figure 4.1 shows cost distribution of a typical 2 MW wind turbine [86]. There are two aspects of costs evaluation of a wind energy project which are: 1) based on focusing on site characteristics, for example, foundations and ground conditions [87]-[88], and 2) focused on costs evaluation of wind energy during its life span [85], which is considered in this study. Two-step procedure is proposed in this study as shown in Figure 4.2. These two steps are: 1) wind energy potential evaluation; and 2) reliability and costs assessment.

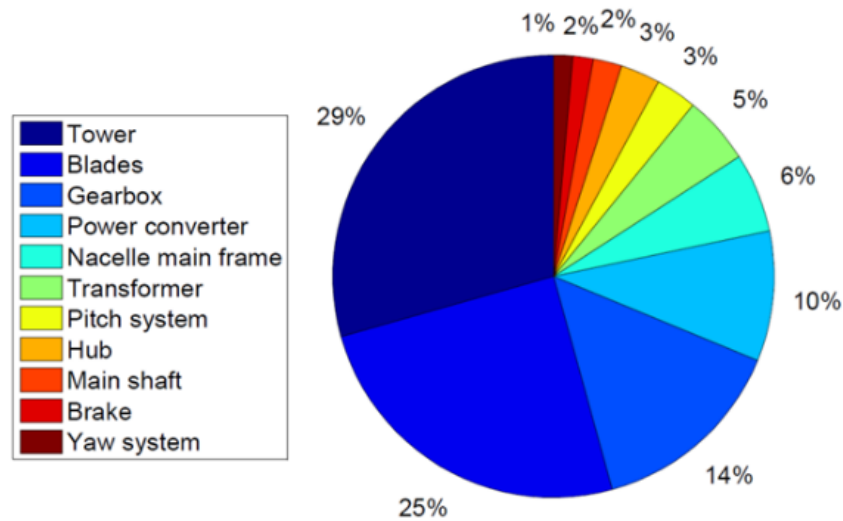


Figure 4.1: Component cost of a 2 MW wind turbine [86].

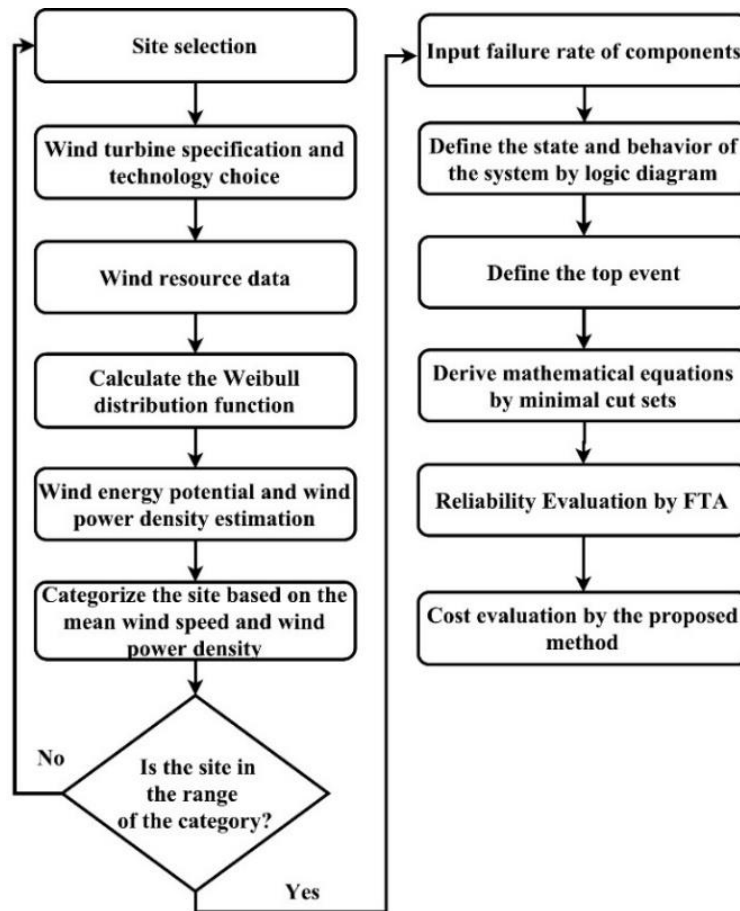


Figure 4.2: The two-step procedure for wind energy potential, reliability, and cost assessment [48].

Weibull distribution is most commonly used to predict wind speed distribution based on historical wind speed data. Weibull distribution has two parameters, the shape (k) and scale (c) factors, these factors can be calculated using several methods such as maximum likelihood method, graphical method, moment method, and probability weighted moments based on power density method [61].

In this study, the graphic method is used to calculate the Weibull distribution parameters. After the wind speed distribution is determined, the wind energy potential can be estimated by the

wind power density and annual mean wind speeds [48]. The process of wind energy potential assessment is shown in Figure 4.3.

The Weibull distribution is given as [61, 89]:

$$f(v) = \frac{k}{c} \left(\frac{v}{c} \right)^{k-1} e^{-\left(\frac{v}{c} \right)^k} \quad (4.1)$$

where, v is the hourly wind speed, k and c are shape and scale factor of the Weibull distribution, respectively. The graphic method is used for calculation of k and c parameters which is based on the cumulative distribution function $F(v)$ given by [61, 89]:

$$F(v) = 1 - e^{-\left(\frac{v}{c} \right)^k} . \quad (4.2)$$

Taking a logarithmic transformation twice for Equation (4.2), the cumulative distribution function becomes

$$\ln(-\ln(1 - F(v))) = k \times \ln(v) - k \times \ln(c). \quad (4.3)$$

Let $x = \ln(v)$, and $y = \ln\{-\ln[1 - F(v)]\}$, Equation (4.3) can be put under the form $y = ax + b$ in which $a = k$ and $b = -k \ln(c)$. The slope a and the intercept b are calculated through the standard least squares regression. Hence, k and c parameters are obtained by [61]:

$$k = a \quad (4.4)$$

$$c = e^{\frac{-b}{a}} . \quad (4.5)$$

The annual mean wind speeds for a region using the Weibull distribution (\bar{v}) can be given by:

$$\underline{v} = \frac{\sum_{i=1}^n F_D(\tau) \times v}{\sum_{i=1}^n F_D(\tau)}. \quad (4.6)$$

The wind power density $P(v)$, which describes how powerful wind speeds are during a period of a time, can be estimated using the annual mean wind speed by [41-90]

$$P(v) = \frac{1}{2} \times \rho \times \underline{v}^3 \quad (4.7)$$

where, ρ denotes the air density at the sea level (1.225 kg/m^3), \underline{v} is the annual mean wind speed.

The wind energy density, $W_{ED}(v_i)$, can also be estimated by multiplication of wind power density $P(v_i)$ and the Weibull distribution of the wind speed $f(v_i)$ as follows:

$$W_{ED}(v_i) = P(v_i) \times f(v_i). \quad (4.8)$$

where $f(v_i)$ is calculated using Equation (4.1) and $P(v_i)$ is calculated by using Equation (4.8)

The wind energy potential can now be investigated using two criteria [41]:

- Annual mean wind speed, \underline{v} : 1) nearly good (6.5 m/s), 2) good (7.5 m/s), and 3) very good (8.5 m/s).
- Wind power density, $P(v)$:
 - 1) Moderate: $P(v) < 100 \text{ W/m}^2$,
 - 2) Good: $100 \text{ W/m}^2 < P(v) < 300 \text{ W/m}^2$,
 - 3) Very good: $300 \text{ W/m}^2 < P(v) < 700 \text{ W/m}^2$, and
 - 4) Excellent: $P(v) > 700 \text{ W/m}^2$.

The FTA is the most common analytical method for reliability evaluation which determines the root causes of failures. An undesirable failure or event is called the “top event” in the “tree”. Potential causes that lead to failure are called “branches”. FTA is a graphical representation of the system which shows the relationships between the “basic events” and the top event by using gates such as AND gates, and OR gates. The “OR” gate has an output if either of the inputs are true while the “AND” gate has an output if all of the inputs are true [91, 92].

The majority of wind turbines are based on the DFIG technology because of its efficiency. This type of turbine was firstly installed in 2004. The Vestas V90-2MW system is an upwind turbine with electrically driven yaw and three blades. Its rotor has a weight of 38 tons, a nominal rotational speed of 14.9 r/min, and a diameter of 90 m. In order to perform the optimum power output, the pitch control system with individual pitching capability for each blade consistently adapts the blade angle to the wind direction. Additionally, it serves to control speed, turbine stops and starts-up by aerodynamic braking. A disk brake is also installed on the high-speed shaft [60].

All Vestas V90-2MW systems apply hybrid gearbox with two parallel-shaft stages and one planetary. The torque is then transmitted to the turbine generator through a composite coupling. A converter is used to control the current in the rotor circuit of the turbine generator, and allows to control the reactive power which serves for smooth connection to the electric power system. In particular, the rotor speed of the turbines based on the DFIG technology vary by 30% above and below synchronous speed.

The Vestas V90-2MW systems can provide up to 2 MW of electric power at 690 V and 50 Hz to the grid based on the wind speeds of 4 to 25 m/s and in a standard operating temperature

ranges of -20° , and $+30^\circ$ [60]. The main components of the Vestas V90-2MW systems consist of a tower structure, rotor (blades and pitch control), mechanical gear, electrical generator, yaw mechanism, sensors and control, brake system, transformer, as shown in Figure 4.4 [49].

For reliability modeling of the wind turbine using the FTA technique, the state and behavior of the wind turbine are represented by logic diagrams. The system has a top event inside a box which is defined as an event leading to the entire system failure. A system might have more than one top event [93]. The FTA representation of the wind turbine is shown in Figure 4.5. After this step, the tree is converted into mathematical equations by using minimal cut sets. A minimal cut set causes the system to become unavailable due to the components' failures. The minimal cut sets of the wind turbine fault tree is given by

$$TopEvent = BPC + GX + BS + YS + GEN + CON + CS + S + TR \quad (4.9)$$

where, BPC, GX, BS, YS, GEN, CON, CS, S, and TR are the blade and pitch control system, the gearbox, the brake system, the yaw system, the generator, the converter, the control system, sensors, and the transformer, respectively. It can be seen that there are 9 minimal cut sets for the wind turbine and these cause the wind turbine become unavailable.

The reliability of a series system with n independent components can be given as [93]:

$$R_{system} = \prod_{i=1}^n R_i \quad (4.10)$$

where R_i is the reliability of the i th component.

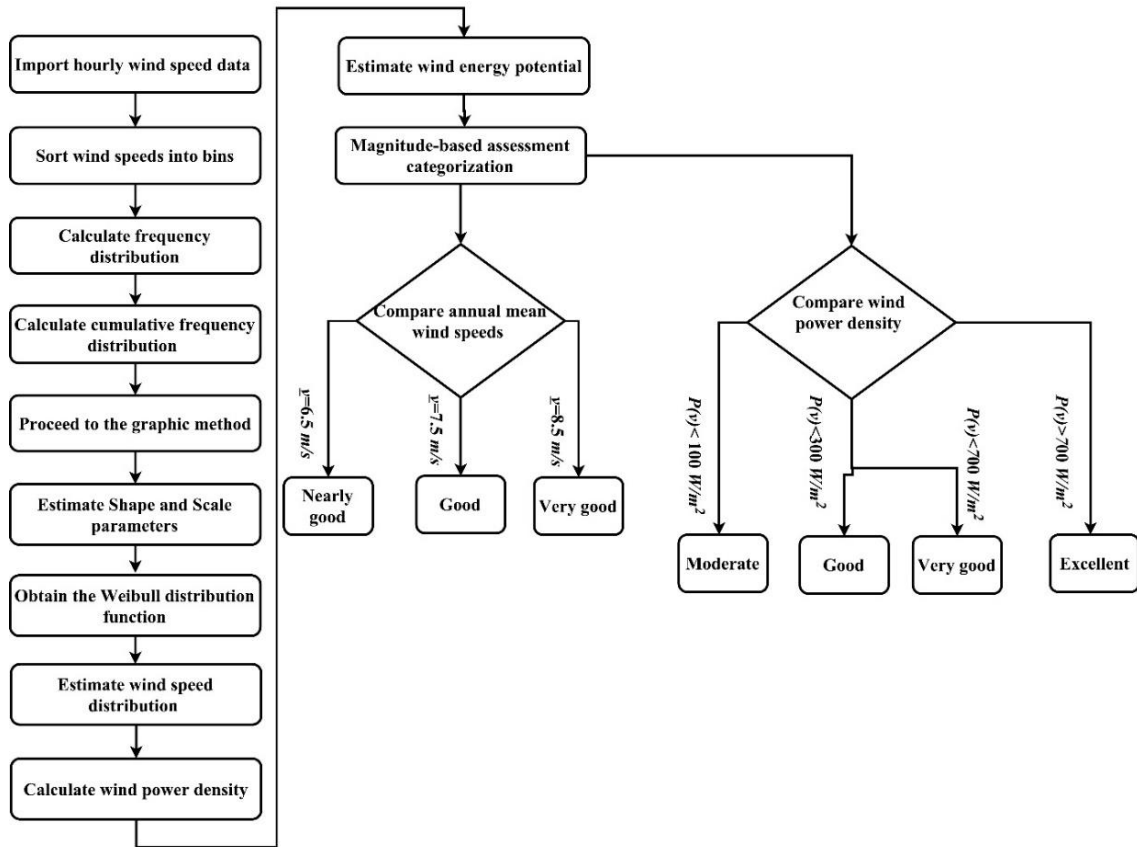


Figure 4.3: The flowchart for estimating wind energy potential [48].

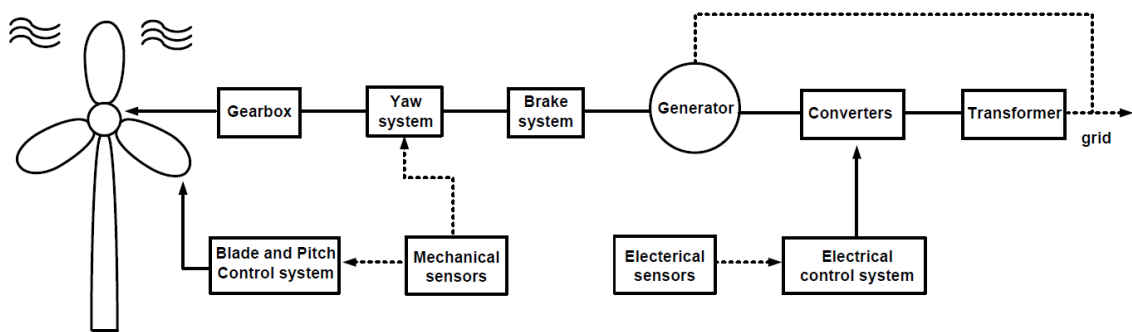


Figure 4.4: The structure of DFIG-based wind turbine [49].

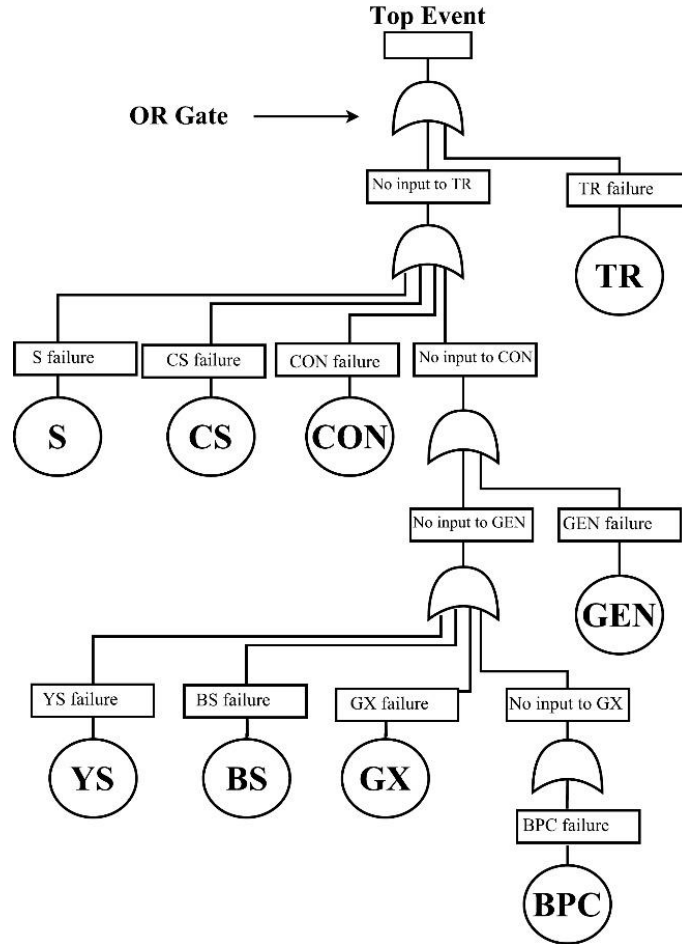


Figure 4.5: The fault tree of a wind turbine system [48].

All wind turbine components are in series because the wind turbine failure is caused by the failure of influential components which are categorized into two groups: 1) Tower, pitch control and blades, generator, control system, gearbox, transformer, and converters. Failures of any of these components cause a full outage of the wind turbine hence the zero production level; 2) sensors, yaw system, and brake system. Failure of either of them does not necessarily cause wind turbine complete outage but might disrupt wind turbine operation. Thus, outages associated with the latter

group are considered as the same as the first group. That is why components of a wind turbine are considered to be in series [49].

Using the definition of the reliability modeling of a series system, the reliability of the wind turbine system, $R_c(t)$, can be estimated by

$$R_c(t) = R(BPC) \times R(GX) \times R(BS) \times R(YS) \times R(GEN) \times R(CON) \times R(CS) \times R(S) \times R(TR) \quad (4.11)$$

where, $R(BPC)$, $R(GX)$, $R(BS)$, $R(YS)$, $R(GEN)$, $R(CON)$, $R(CS)$, $R(S)$, and $R(TR)$ represent the reliability of the blade and pitch control system, gearbox, brake system, yaw system, generator, converter, control system, sensors, and transformer, respectively. If the failure rate of a component is constant, the exponential distribution can be used to calculate the reliability of the system which is a special case of the Weibull distribution when the shape factor is 1.

The reliability of a component using the exponential distribution is given by [93]:

$$R(t) = e^{-\lambda t} \quad (4.12)$$

where λ is the failure rate of a component, t is the time period for the reliability assessment.

The probability density function can also be given by [48]

$$f(t) = \lambda e^{-\lambda t} \quad (4.13)$$

The failure rate function of a component can be calculated as [48]

$$\lambda(t) = \lambda \quad (4.14)$$

By substituting Equation (4.13) into Equation (4.12) for all components, the reliability of a wind turbine system, $R_c(t)$, can be estimated by [48]

$$\begin{aligned}
 R_c(t) &= e^{-\lambda_{BPC}t} \times e^{-\lambda_{GX}t} \times e^{-\lambda_{BS}t} \times e^{-\lambda_{YS}t} \times e^{-\lambda_{GEN}t} \times e^{-\lambda_{CON}t} \times e^{-\lambda_{CS}t} \times e^{-\lambda_S t} \times e^{-\lambda_{GX}t} \\
 &= e^{-(\lambda_{BPC} + \lambda_{GX} + \lambda_{BS} + \lambda_{YS} + \lambda_{GEN} + \lambda_{CON} + \lambda_{CS} + \lambda_S + \lambda_{GX})t}
 \end{aligned}
 \tag{4.15}$$

where, λ_{BPC} , λ_{GX} , λ_{BS} , λ_{YS} , λ_{GEN} , λ_{CON} , λ_{CS} , λ_S , and λ_{GX} are the failure rate of the blade and pitch control system, gearbox, brake system, yaw system, generator, converter, control system, sensors, and transformer, respectively. The equivalent system failure rate, λ_{eq} , is introduced which can be expressed as [48]

$$\lambda_{eq} = \lambda_{BPC} + \lambda_{GX} + \lambda_{BS} + \lambda_{YS} + \lambda_{GEN} + \lambda_{CON} + \lambda_{CS} + \lambda_S + \lambda_{GX}
 \tag{4.16}$$

Therefore, Equation (4.16) can be rewritten, and the reliability of wind turbines can be calculated by [48]

$$R_c(t) = e^{-\lambda_{eq}t}
 \tag{4.17}$$

where t is the time period for the reliability assessment.

Even though the annual O&M costs contribute to a significant amount of the overall costs of a wind energy project, its calculations are uncertain because of unavailability of enough operating information from the field [94, 95]. According to the field survey, the downtime and O&M costs increase with the wind farm aging. The current practice of estimating annual O&M costs are

varying from 1.5% to 3% of capital costs of the wind energy project with an annual escalation of 5% [83]. However, the accuracy of this approach is unknown.

An Excel spreadsheet for all major costs contributors of different operating wind energy projects was developed by NREL in [95]. This tool is based on the real historical operating data of wind energy projects which can be highly useful for wind energy projects planners, however, this tool is not accessible by the public. In this study, a generic formula for calculating O&M costs is proposed which is based on the historical field data and major costs involved with different wind energy projects in [95].

The proposed formula is very simple to use, empirical in nature. The accuracy of the proposed formula is also verified by comparing the results of the NREL tool in [95]. The major cost contributors for O&M costs consist of [95]: 1) Parts replacements (such as hardware, additional labor, and crane); 2) Wage-based labor; 3) Salaried labor; 4) Consumable; 5) Equipment; 6) Site Maintenance. The only major cost contributor which increases significantly during the lifetime of a wind turbine is “parts replacements” which contributes approximately 25% of the first year O&M cost. Other costs are remained constant over the life span of the wind turbine and contributed 75% of the first year O&M cost [95].

For clarification, “parts replacements” and other costs are named as “Increased Costs” and “Fixed Costs”, respectively. The major costs contributors by NREL also matches the O&M costs of German wind turbines as an average between 1997-2001 in [96]: 1) 26% service and spare parts; 2) 13% insurance; 3) 21% administration; 4) 18% land rent; 5) 5% power from the grid; and 6)

17% miscellaneous [96]. Hence, the major cost contributors available by [95] are taken into account in order to develop the proposed formula for O&M costs calculations.

According to the survey in [95], “Increased Costs” will increase to be about 10.88 times of its Year 1 value at the end of 20 year services. This increment has a linear trend. Thus, “Increased Costs” are treated as considering the Year 1 parts replacements cost to be 25% of the first year O&M cost, and increases linearly to 10.88 times of its Year 1 value by Year 20. The sum of “Fixed Costs” are equal to 75% of the first year O&M cost, and remains constant every year over the operating time of the project [48].

The summation of fixed costs and increased costs will result in the total annual O&M costs per turbine. The proposed generic formula for the annual O&M costs (AOMC) calculations per turbine is very simple to use because it is purely based on statistical cost data that can be calculated at any given year (Year N) by [48]

$$\begin{aligned}
 AOMC &= \textit{Fixed Costs} + \textit{Increased Costs} \\
 &= (\textit{initial O\&M Cost at Year1}) \times 0.75 + (\textit{initial O\&M Cost at Year1}) \times [0.25 + 0.13(N-1)] \\
 &= (\textit{initial O\&M Cost at Year1}) \times [1 + 0.13(N-1)]
 \end{aligned}
 \tag{4.18}$$

where, the initial O&M cost at Year 1 is used in the cost calculation as the starting point, N is the Nth year in service for the wind turbine. In Equation (4.19), the value 0.75 represents that the fix costs are 75% of the initial O&M cost at Year 1, while the value 0.25 represents that the increased costs are 25% of the initial O&M cost at Year 1. The value 0.13 is derived based on that the increased costs are 10.88 times of its Year 1 value by Year 20. In this formula, failure rates of

wind turbine components are already included and the failure rates will not be considered separately.

The O&M cost at Year 1 is assumed to be 2% of the capital investment costs. The annual O&M costs calculated using the proposed generic formula for 20 years life span of a wind turbine are shown in Table 4.1. The Present Practice method is also used to compare the results of the proposed formula. The Present Practice method is based on the assumption of considering initial O&M cost at Year 1 to be 2% of the capital investment costs with annual escalation of 5%, as shown in Table 4.1. Figure 4.6 shows the comparison between the proposed formula and the Present Practice. A large discrepancy between the two methods can be seen, where the proposed formula has much higher annual O&M costs than the Present Practice method.

The annual O&M costs for five different wind turbines rated at 750 W, 1000 W, 1500 W, 2000 W, and 2500 W were calculated by the proposed formula and compared with the results obtained by [95] in order to verify the accuracy of the proposed method. It can be noticed from Figure 4.7 that there is a good match between the proposed formula and the developed tool in [95], which emphasize the accuracy of the proposed formula.

The major cost during the operating time of a wind energy project is O&M costs which must be accurately quantified for successful financial planning for future projects as well as reducing O&M costs during the operation time of current wind energy projects. Thus, both developers for future projects and current operators can benefit from a reliable baseline for O&M costs. This can be formed using operating historical data from different wind turbines in wind farms and environmental conditions. Standard reporting schemes among institutions and organizations must

be established in order to evaluate and collect current field data. It is also recommended that a standard reporting format should be used to ensure consistency and adequate depth [94].

The Weibull distribution based on the power curve data of the Vestas V90-2MW (IEC IIIA) wind turbine and hourly wind speed data of St. John’s is calculated by the following steps [48]:

- 1) Importing hourly wind speed data;
- 2) Sorting hourly wind speeds into bins;
- 3) Calculating the frequency distribution;
- 4) Obtaining cumulative frequency distribution from Step 3;
- 5) Calculating equations, $\ln(v)$ and $\ln(-\ln(1 - F(v)))$;
- 6) Calculating the Weibull parameters using Equations (4.4) and (4.5).

Table 4.1: 1the Calculated annual O&M costs per Turbine Using the proposed Method in This Paper and the Present Practice [48].

Nth year in service	Annual O&M Cost per turbine using the proposed method (in percent of capital investment per annum),%	Annual O&M Cost per turbine using Present Practice method (in percent of capital investment per annum), %
1	2	2
2	2.26	2.1
3	2.52	2.205
4	2.78	2.315
5	3.04	2.431
6	3.3	2.552
7	3.56	2.68
8	3.82	2.814
9	4.08	2.955
10	4.34	3.102
11	4.6	3.258
12	4.86	3.421
13	5.12	3.592
14	5.38	3.771
15	5.64	3.96
16	5.9	4.158

17	6.16	4.366
18	6.42	4.584
19	6.68	4.813
20	6.69	5.054

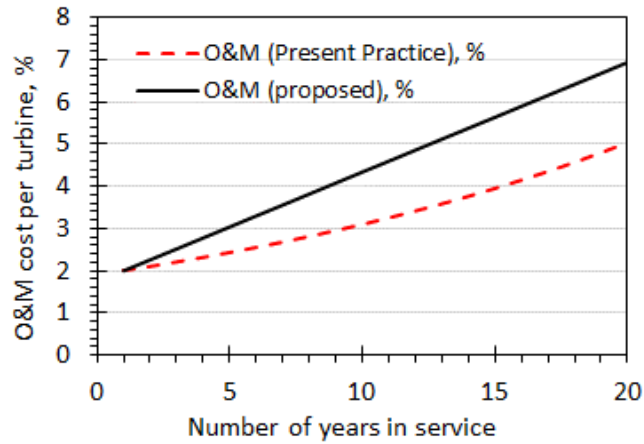
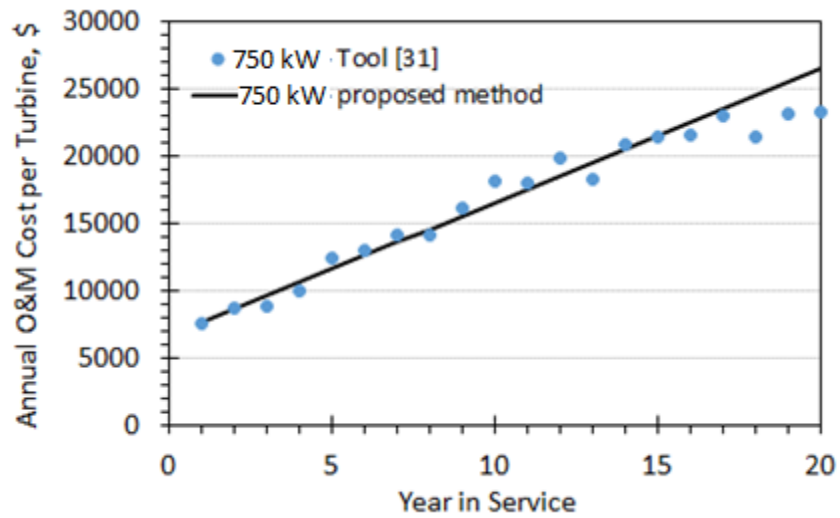
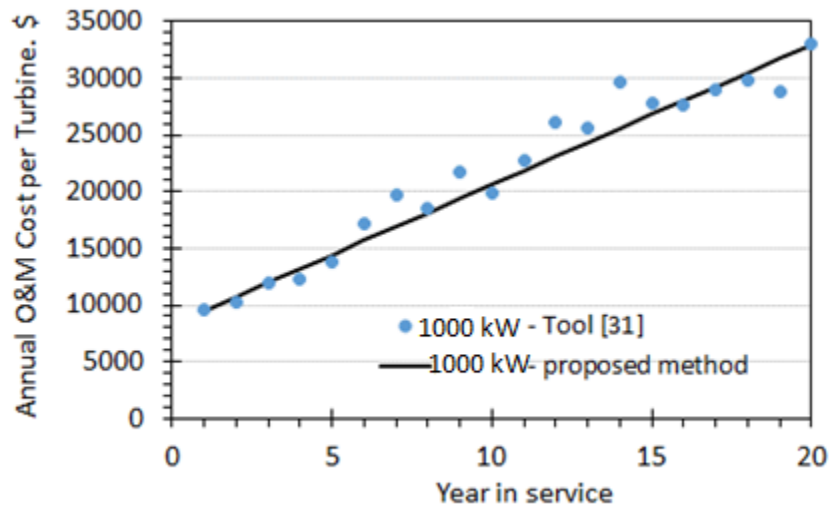


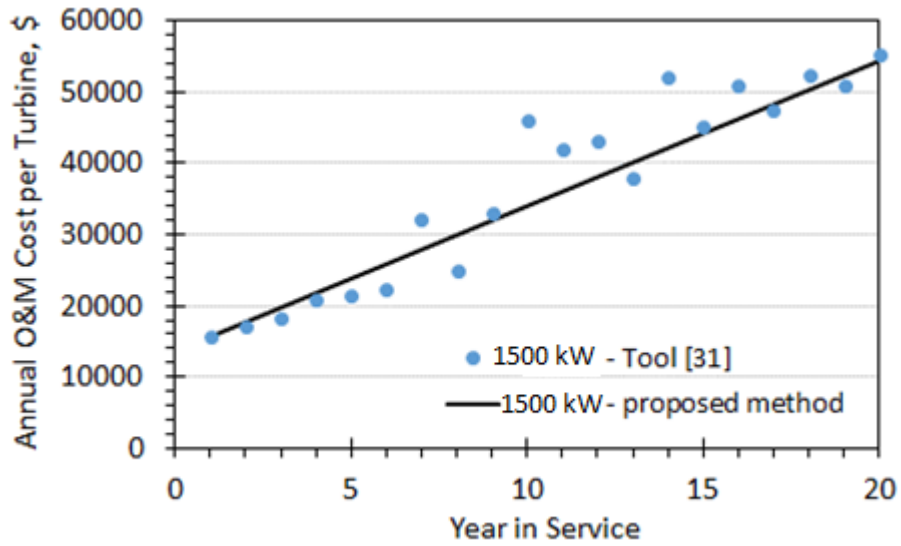
Figure 4.6: Comparison of the calculated annual O&M costs in percent of the capital investment using the proposed method and the Present Practice [48].



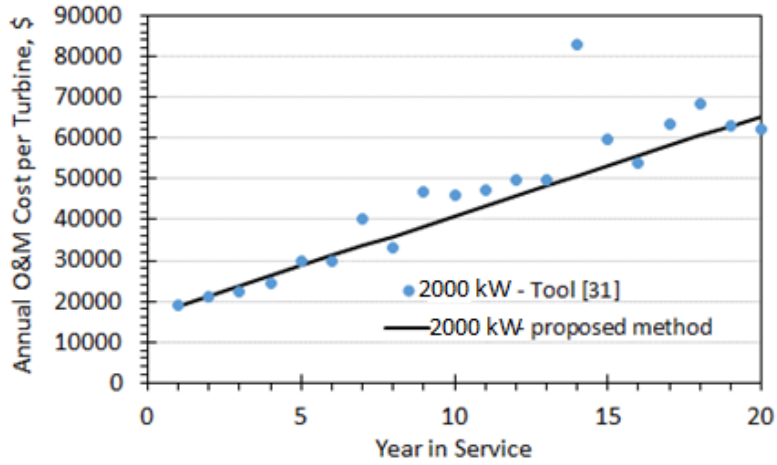
(a)



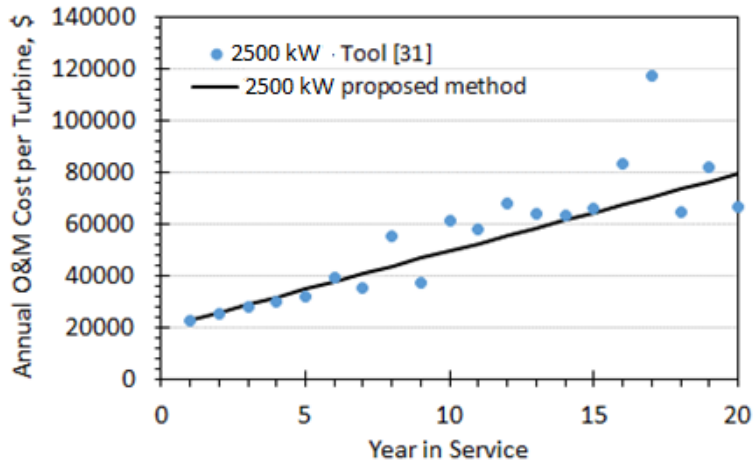
(b)



(c)



(d)



(e)

Figure 4.7: Comparison of the calculated annual O&M cost per turbine in dollars using the proposed method and the tool developed in [31]: (a) 750 kW wind turbine (the initial O&M cost at Year 1 = \$7,633); (b) 1000 kW wind turbine (the initial O&M cost at Year 1 = \$9,501); (c) 1500 kW wind turbine (the initial O&M cost at Year 1 = \$15,683); (d) 2000 kW wind turbine (the initial O&M cost at Year 1 = \$18,858); (e) 2500 kW wind turbine (the initial O&M cost at Year 1 = \$23,016) [48].

Table 4.2 shows the Weibull parameters, annual mean wind speeds, and wind power density calculated for both the measurement height and hub height of the wind turbine. The Weibull distribution is shown in Figure 4.8 which shows the comparison between the wind speed distribution for the measurement height, hub height, and real wind speeds. This will be used for wind energy potential assessment for a wind project in St. John's.

The R^2 value for the Weibull distribution at measurement height vs. wind measurement data is $R^2 = 0.9290$ which indicates a good curve fitting because it is very close to 1. The power density at the measurement height and hub height is 189.72 W/m^2 , and 180.63 W/m^2 , respectively.

Table 4.2: Weibull Shape and Scale Parameters k and c , Annual Mean Wind Speed at 140.5 m elevation and 125 m hub height at St. John's [48].

Parameters	140.5m (elevation of measurement)	125m (hub height of the wind turbine)
Weibull shape parameter k	2.0736	2.051
Weibull scale parameter c	7.6439	7.5198
Annual mean wind speed, m/s	6.76	6.65
The wind power density, W/m^2	189.72	180.63

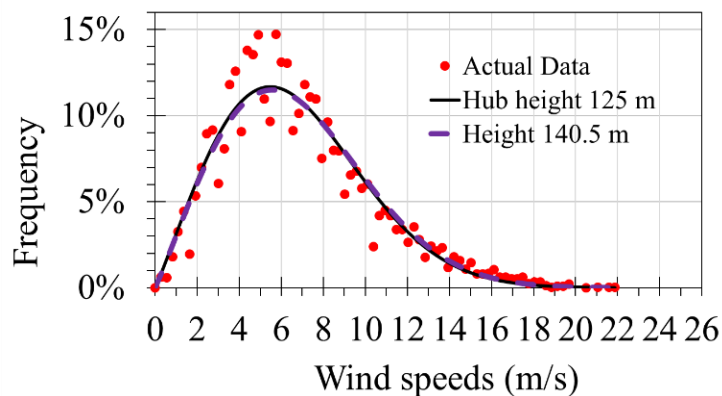
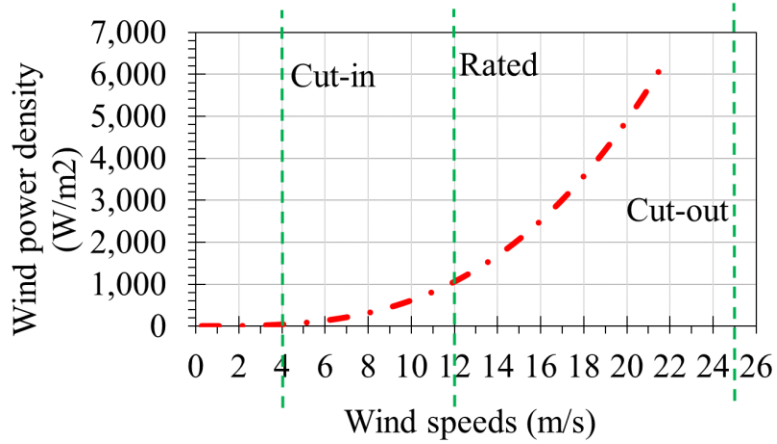


Figure 4.8: The Weibull distribution of wind speed at St. John's at 140.5 m height and the hub height 125 m, and the actual wind measurement data at 140.5 m [48].

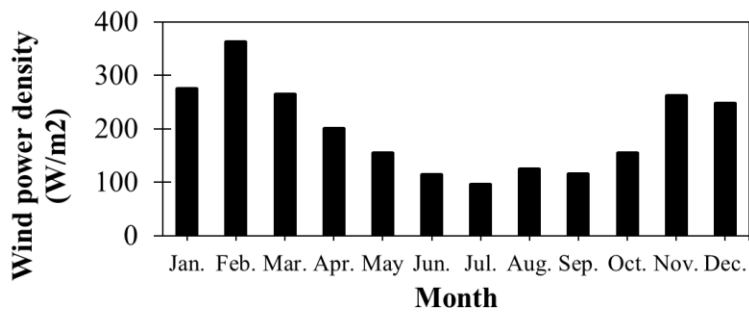
The annual mean wind speed at the measurement height and hub height of the wind turbine is 6.76 m/s, and 6.65 m/s, respectively. The annual mean wind speed and power density at wind turbine hub height will be used for wind energy potential assessment. The calculated wind power density as a function of wind speeds is shown in Figure 4.9 (a). The power density for each month in St. John's for the period of Jan. 2015 to Dec. 15 is also calculated, as shown in Figure 4.9 (b). It can be noticed that the power density is higher during the winter time (above 250 W/m²), and it reaches its highest amount in Feb. 2015 (over 350 W/m²).

Wind energy density calculations are shown in Figure 4.10 which indicates high wind speeds do not necessary contribute on high wind energy production. The wind energy is increased as the wind speed increased and it reached to its highest value of 39207.13 kWh/m² at the wind speed 10.5 m/s. Generally, small-scale wind turbines have a low rated wind speed value. Thus, large-scale wind turbine is a suitable option for St. John's, especially wind turbines with the rated wind speed around 10.5 m/s which results in highest wind energy.

Vestas V90-2MW is rated as 12 m/s wind speed, which is close to the wind speed of 10.5 m/s, thus, the wind turbine under study is a good choice for St. John's. The wind energy potential is evaluated using two criteria: 1) Annual mean wind speeds which is 6.65 m/s at the wind turbine hub height, so St. John's can be classified as "nearly good". 2) Wind power density which is 180.63 W/m² at the wind turbine hub height, so St. John's can be classified as a "good" location ($100\text{W/m}^2 < P(v) < 300\text{W/m}^2$). Hence, it is suitable to build a wind farm at St. John's.



(a)



(b)

Figure 4.9: The wind power density calculated using wind speed at hub height (125 m): (a) wind power density vs. the wind speed, (b) wind power density vs. the month.

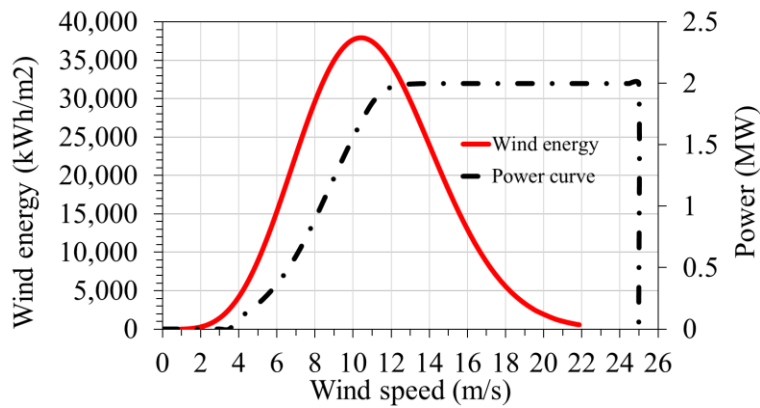


Figure 4.10: The wind energy curve and the chosen wind turbine power curve of the wind turbine system.

The wind turbine components' failure rates are shown in Table 4.3 which were used for reliability calculations using Equation (18), as shown in Table 4.4. It can be seen that the reliability of the wind turbine is decreased over time and the designed lifetime of the wind energy project is about 20 years as the reliability reached 0 value. The AOMC is also calculated using the proposed formula in Equation (4.19) as shown in Figure 4.11. The current practice is also used to calculate the AOMC to verify the proposed method. The proposed analytical method for annual O&M costs and the two-step procedure in this study will provide a practical and comprehensive approach for wind power project assessment and design.

Table 4.3: Components failure rates for the DFIG wind turbine [49].

Components	Failure rate (occ/yr)
Blade and pitch control system	0.052
Yaw system	0.026
Gearbox	0.045
Brake system	0.005
Generator	0.021
Converters	0.067
Tower	0.006
Control system	0.050
Sensors	0.054
Transformer	0.020

Table 4.4: The Reliability Evaluation of the Wind Turbine System [48].

Time (years)	Reliability, $R_c(t)$ (%)	Time (years)	Reliability, $R_c(t)$ (%)
1	70.75	11	2.22
2	50.06	12	1.57
3	35.42	13	1.11
4	25.06	14	0.788
5	17.73	15	0.557
6	12.54	16	0.394
7	8.87	17	0.279
8	6.28	18	0.197
9	4.44	19	0.14
10	3.14	20	0.098

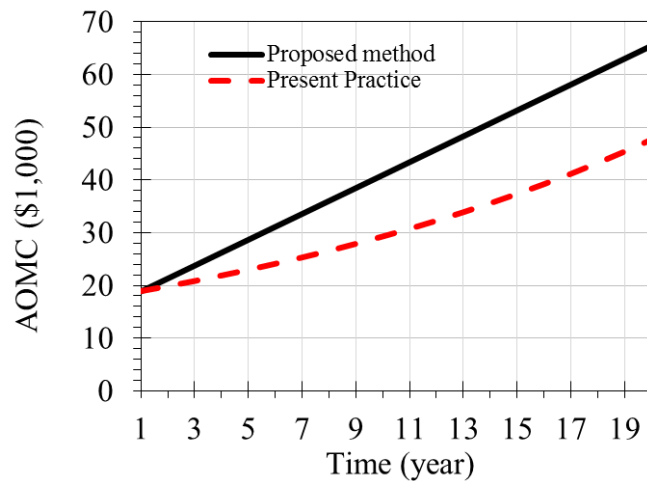


Figure 4.11: The annual O&M costs per turbine calculated using the proposed method and the present practice in the case study [48].

4.3. Hybrid System

Renewable energy systems are preferred option to supply power in rural communities due to their advantages on improving security of energy supply and reducing environmental impact. It is also unfeasible for rural communities to access the main power grid because of high costs of grid

extension. One drawback of renewable energy systems is that their power output fluctuates significantly over time. In addition to the development of advanced control systems, battery energy storage systems can also be used to smooth out these fluctuations [97]. Using at least two energy sources ensure the stability of power supply [98].

In addition, hybrid PV and wind energy systems have gained a great interest of several utility companies among other hybrid combinations of renewable energy systems [99]. Stored hydrogen can also be a significant energy storage system for independency of fossil fuels and sustainable developments [100]. In fact, an optimal cost structure, high efficiency, and reliable configuration for supplying power can be achieved by a hybrid fuel cells/PV/wind energy system with hydrogen energy storage system [101].

As a recent development and research project led by Newfoundland and Labrador Hydro [102], a hybrid standalone power system, which consists of wind, diesel, and hydrogen energy storage system, is installed in a remote area at Ramea Island in Newfoundland and Labrador, Canada. It is expected that this configuration can supply enough energy to Ramea Island communities, thereby shutting down all diesel generators during low load demand periods [102]. Battery banks have been commonly used as an energy storage system [103]. Hence, both battery and hydrogen will be investigated as possible energy storage options in this study.

Cost optimization of renewable energy systems is defined as obtaining optimal number of components in which the load is met, and it is cost-effective and reliable [79]. The cost optimization is an important task for implementing hybrid energy systems efficiently and economically. The objective function is minimization of total annual costs [104].

A total of 37 methodologies and computer software tools for cost optimization of hybrid power systems was surveyed in [104, 105], it was recommended that the HOMER (Hybrid Optimization of Multiple Energy Resources) developed by NREL [106] was the most popular tool for cost optimization of hybrid power systems due to its advantages among other available tools. HOMER is based on the NPC method which has the ability of modeling, economic analysis, optimum sizing, and simulation of hybrid power systems [107, 108].

In this section, a stand-alone hybrid system is proposed for supplying power in a remote area. The electrical schematic of the proposed configuration is shown in Figure 4.12. Wind energy system and PV system are the two types of renewable energy systems which are connected to a DC bus. In this configuration, battery energy system smooths out the renewable energy power output fluctuations in the DC bus.

The proposed configuration was assumed to be based on using a multiport converter in the DC bus which PV, wind turbines, fuel cells, and energy storage systems are connected to a DC bus [109]. Separate converters are required in conventional configurations and independent control of the converters for each source and energy storage system will result in the complexity of the system as well as increasing the costs. Multiport converters have several advantages such as simple structure, less devices, high efficiency, and cost effective in comparison with conventional configurations [110].

There is no available option to include a multiport converter in the HOMER software, hence it was assumed that wind turbines generate DC power, PV systems, wind turbine, fuel cell, and battery are well controlled by the multiport converter to provide adequate power to the load. This

configuration was assumed in the proposed system because most utilities are moving towards using multiport converters in hybrid renewable energy systems [109, 110].

An inverter is also used for converting power from DC to AC to supply the AC loads. The surplus power from this configuration will be stored in the hydrogen tank and battery energy storage system. The process of storing surplus power as the form of hydrogen energy storage system has done by two main equipment as an electrolyzer and a fuel cell. Electrical energy is converted into chemical energy as hydrogen by the electrolyzer, where chemical energy such as fuel is converted into electrical energy by the fuel cell [97].

The principle of the NPC method in the HOMER software is finding out the optimal number of components to meet the load demand and the annual total costs which consist of capital, component replacement, and O&M costs are minimized [107]. Capital costs are the costs for purchasing all components at the beginning of the project. Replacement costs are associated with replacing components at the end of their operating lifetime which is treated in the capital costs [108].

The NPC method ranks several feasible system configurations and number of components that can meet the load demand with the lowest total costs [107]. The procedure of the optimization based on the NPC method is shown in Figure 4.13. The main part of the procedure and the objective function is determining number of units of all components during the designed life of the project. Number of units of components are selected based on type and capacity of each component. Objective function is the total costs that must be minimized considering several constraints such as meeting the load demand.

The cost inputs in the HOMER are capital, O&M, and replacement costs of each component. It then estimates the total costs for several feasible combinations of the system which are number of units of components such as PV system and wind turbines. The first ranked feasible combination is the number of units of components which lead to the lowest total costs. Other feasible combinations can also satisfy the constraints and the load but total costs are not minimum [97].

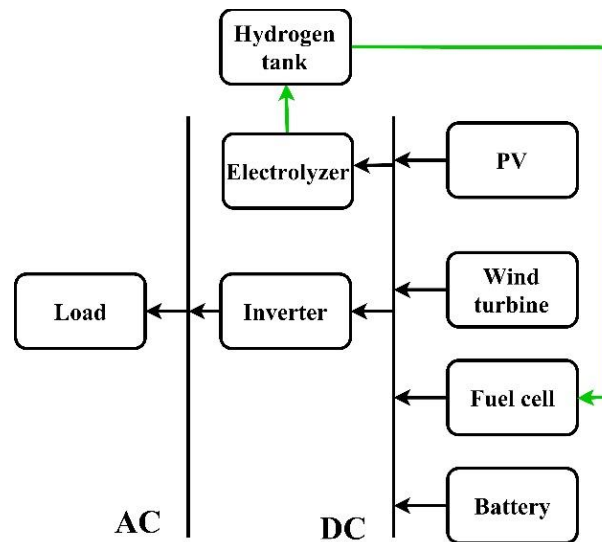


Figure 4.12: The electric system configuration of the proposed system [97].

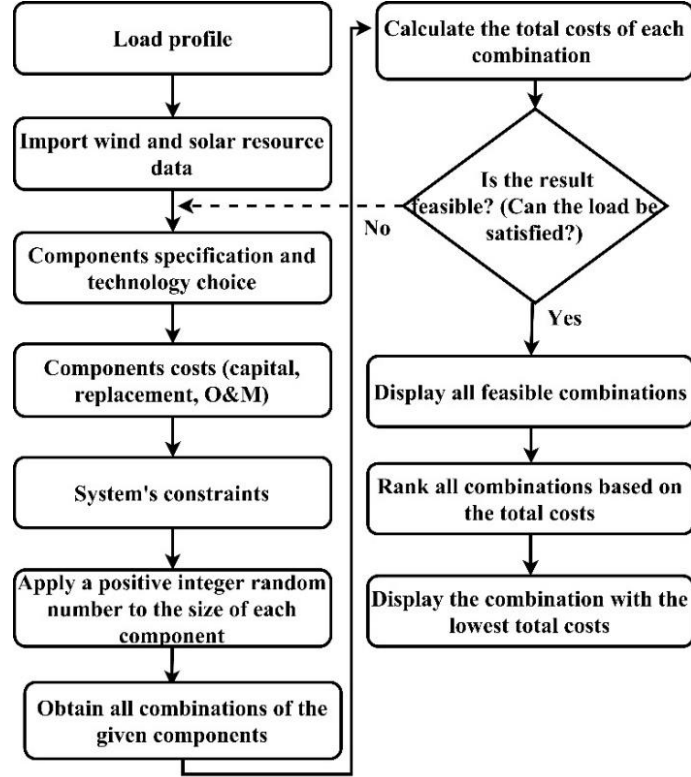


Figure 4.13: The procedure of the NPC optimization method [97].

The capital costs (C_C) of the system can be given by [107]:

$$C_C = CRF \times \left(\begin{array}{l} N_W \times C_W + N_E \times C_E + N_H \times C_H \\ + N_F \times C_F + N_{PV} \times C_{PV} + N_B \times C_B \\ + N_{CN} \times C_{CN} \end{array} \right) \quad (4.19)$$

where N_W , N_E , N_H , N_F , N_{PV} , N_B , and N_{CN} are the number of units of wind turbines, electrolyzer, hydrogen tank, fuel cell, PV system, batteries, and inverter, respectively. C_W , C_E , C_H , C_F , C_{PV} , C_B , and C_{CN} denote the capital and replacement costs of wind turbines, electrolyzer, hydrogen tank, fuel cell, PV, battery system, and inverter, respectively.

The capital recovery factor (CRF) in Equation (4.20) is used to calculate the present value during the designed life of a project [12]. Present value is the amount of money today which, if invested at a specific interest rate, will increase in the future [108]. CRF can be given by [107]

$$CRF = \frac{I(1+I)^L}{(1+I)^L - 1} \quad (4.20)$$

where I is the interest rate and L is the life span of the project.

The operation and maintenance cost (M_C) of the system can be calculated by [107]

$$M_C = \left(\begin{array}{l} M_W \times E_W + M_E \times E_E + M_H \times E_H + M_F \times E_F \\ + M_{PV} \times E_{PV} + M_B \times E_B + M_{CN} \times E_{CN} \end{array} \right) \times 365 \quad (4.21)$$

where M_W , M_E , M_H , M_F , M_{PV} , M_B , and M_{CN} are the maintenance cost of wind turbines, electrolyzer, hydrogen tank, fuel cell, PV system, batteries, and inverter, respectively. E_W , E_E , E_H , E_F , E_{PV} , E_B , and E_{CN} denote the energy generated by wind turbines, electrolyzer, hydrogen tank, fuel cell, PV, battery system, and inverter, respectively.

The objective function is minimizing total system cost C_T of the proposed configuration, which can be mathematically expressed as [107]

$$\min C_T = C_C + M_C. \quad (4.22)$$

The constraints of the objective function which are considered in the HOMER software are [107]

$$\begin{cases} N_{PV} = Integer, & 0 \leq N_{PV} < N_{PV}^{Max} \\ N_W = Integer, & 0 \leq N_W < N_W^{Max} \\ N_{BT} = Integer, & 0 \leq N_{BT} < N_{BT}^{Max} \end{cases} \quad (4.23)$$

where N_{PV}^{Max} , N_W^{Max} , and N_{BT}^{Max} are the maximum available number of units of PV panels, wind turbines, and batteries, respectively.

The proposed hybrid system and the economic assessment is investigated for a city called Ardabil in north-western of Iran. The wind speed and solar radiation data for Ardabil's Airport with the latitude of 38.2537° N, and longitude of 48.3000° E were collected from the National Aeronautics and Space Administrative, NASA for the period of January 2014-December 2014 [111]. The wind speed measurement height is 24 m. The annual solar radiation and average wind speeds are $4.08 \text{ kWh/m}^2/\text{day}$, and 7.05 m/s , respectively [111]. The monthly variations of wind speed and solar radiation are shown in Figures 4.14 and 4.15. The technical characteristics and costs of each component are shown in Table 4.5 [101, 112].

The wind turbines, PV system, and inverter are rated at 7.5 kW , 5kW , and 70 kW , respectively. The nominal voltage and nominal capacity of the battery are 6 v , and 1156 Ah , respectively. The electrolyzer and fuel cell are rated at 10 kW and the hydrogen tank size is 10 kg . The HOMER software estimates number of units of each component to meet the load even though each component is rated at a specific value. The load of the system consists of 50 houses with 2 kW peak load in each house, thereby total peak load of 100 kW . Load varies during one year period and the maximum load demand occurs at night since most of consumers are not at home during morning. This load variation has been done in the HOMER software. The hourly and average monthly load variation are shown in Figures 4.16 and 4.17.

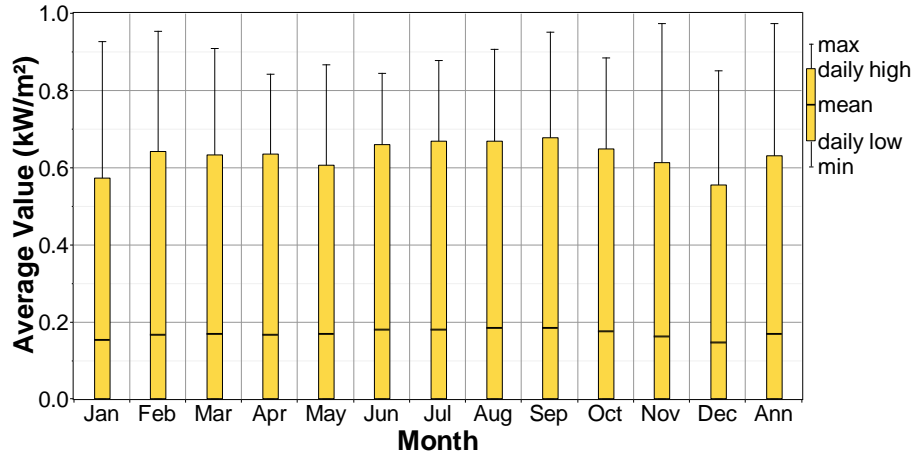


Figure 4.14: Monthly average variation of the solar radiation [111].

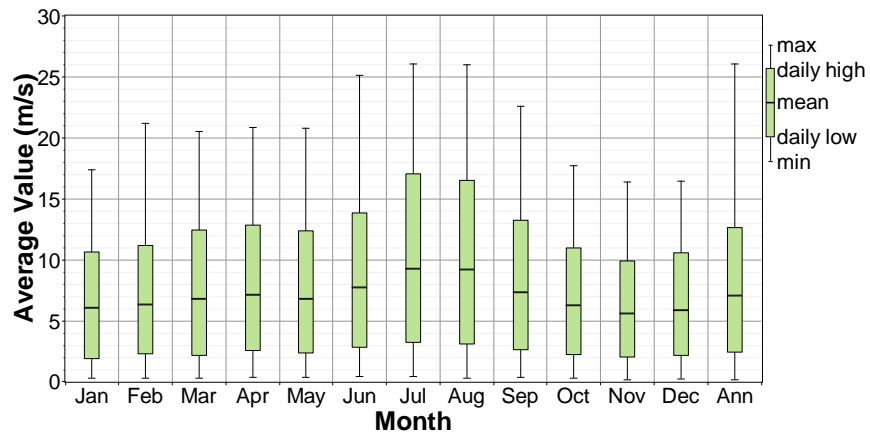


Figure 4.15: Monthly average variation of the wind resource [111].

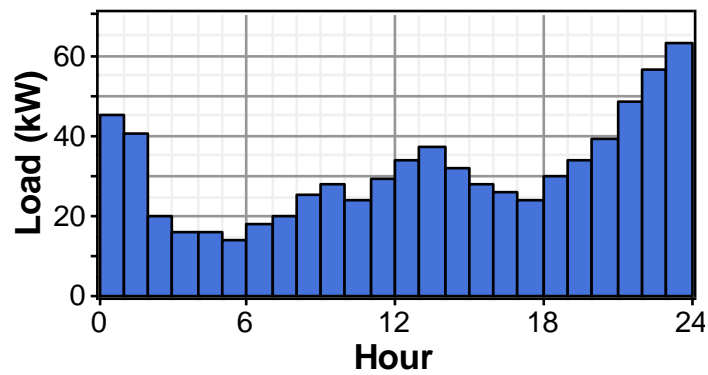


Figure 4.16: Hourly variation of the load [97].

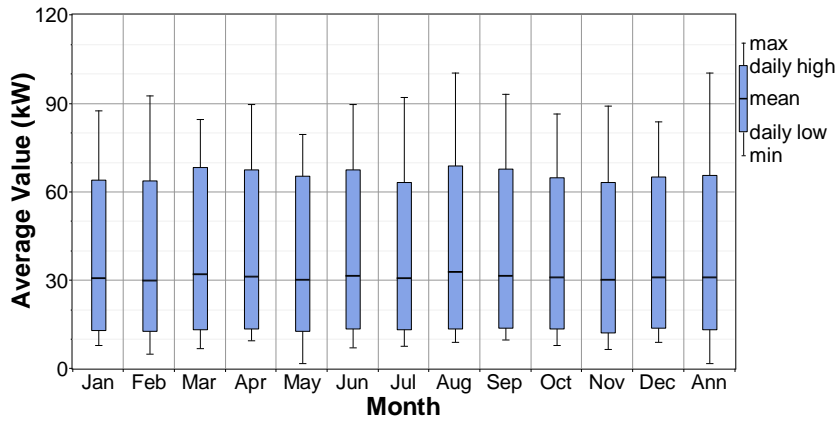


Figure 4.17: Monthly average variation of the load [97].

Table 4.5: Costs and Technical specifications of the system ([101], [112]).

Component	Parameter	Quantity
Wind turbine	Nominal size (kW)	7.5
	Capital (\$/kW)	3500
	Replacement (\$/kW)	2800
	O&M (\$/kW)	95
	Lifetime (years)	25
	Hub height (m)	20
	PV system	Size (kW)
Capital (\$/kW)		6500
Replacement (\$/kW)		6500
O&M (\$/kW)		65
Lifetime (years)		25
Battery		Nominal capacity (Ah)
	Nominal voltage (V)	6
	Number of cells	4

	Minimum state of charge (%)	30
	Lifetime (years)	12
	Capital (\$)	1200
	Replacement (\$)	1000
	O&M (\$/year)	15
Fuel cell	Size (kW)	10
	Capital (\$/kW)	4080
	Replacement (\$/kW)	4080
	O&M (\$/kW)	\$0.1/h
	Lifetime (operating hours)	30,000
Inverter	Size (kW)	70
	Capital (\$/kW)	1000
	Replacement (\$/kW)	1000
	O&M (\$/kW)	100
	Lifetime (years)	15
Electrolyzer	Size (kW)	10
	Capital (\$/kW)	5000
	Replacement (\$/kW)	5000
	O&M (\$/kW)	100
	Lifetime (years)	15
Hydrogen tank	Size (kg)	10
	Capital (\$/kg)	\$574.22/kg
	Replacement (\$/kg)	\$574.22/kg
	O&M (\$/kg)	2,000
	Lifetime (years)	20

*\$=USD.

The optimum combination of the components that can meet the load demand at the lowest costs is obtained using the NPC method in the HOEMR software. The input for the HOMER software were wind speed, solar radiations, components' technical characteristics, components' costs, and load. Around 70000 simulation cases including optimal case and non-optimal cases were carried out in the HOMER. The optimal case and one of the non-optimal cases as an example are shown in Table 4.6.

The optimal case is the first ranked solution of the system and non-optimal case of the one that can meet the load demand but it is not a cost-effective choice. By comparing the two cases, it can be noticed that the budget is overestimated by approximately 20% if the proposed hybrid power system would be configured by the number of units of components in the non-optimal case.

A summary of the cash flow and total costs were also obtained by the HOMER, as shown in Table 4.7. In this table, the cost recovery is the amount of money that remained in each component at the end of the designed life of the project. It can be noticed that the cost recovery of the battery system and wind turbines are higher which means they have higher influence on decreasing the total costs of the system. Hence, these components must be considered in the proposed system [97].

Table 4.6: The Optimal and Non-optimal Case of the Proposed Configuration [97].

Item	Optimal Case	Non-Optimal Case
PV capacity (kW)	15	25
Wind turbine capacity (kW)	112.5	165
Fuel cell capacity (kW)	30	20

Operating hours of fuel cell (hours)	102	215
Electrolyzer capacity (kW)	10	10
Hydrogen tank (kg)	10	10
Number of batteries	100	50
Inverter capacity (kW)	70	70
Total costs (\$)	939,905	988,004

Table 4.7: The Optimal Case of the Proposed Configuration [97].

Component	Capital (\$)	Replacement (\$)	O&M (\$)	Cost recovery (\$)	Total (\$)
PV	95,000	26,192	7,670	-14,679	114,183
Wind turbine	291,000	70,156	14,381	-39,319	336,219
Fuel cell	21,000	0	156	-4,715	16,442
Battery	200,000	133,911	63,917	-38,445	359,383
Inverter	74,667	23,281	1,193	-13,048	86,093
Electrolyzer	11,667	7,252	2,770	-971	20,717
Hydrogen tank	4,167	1,299	2,131	-728	6,868
System	697,500	262,091	92,218	-111,904	939,905

The simulation of each component has also been investigated for the optimal case of the system. It can be seen from Figure 4.18 that when there is not enough wind or PV generation, batteries were discharged to meet the load. If the total renewable energy power output is higher than the load, the hydrogen tank will be filled by the surplus electricity that is from the renewable energy and converted into the hydrogen, as shown in Figure 4.19.

The impacts of surplus electricity on charging batteries is also shown in Figure 4.20. It shows that the batteries are charged when the load is already met by the renewable energy system and there is a surplus electricity that can be stored in battery energy system [97].

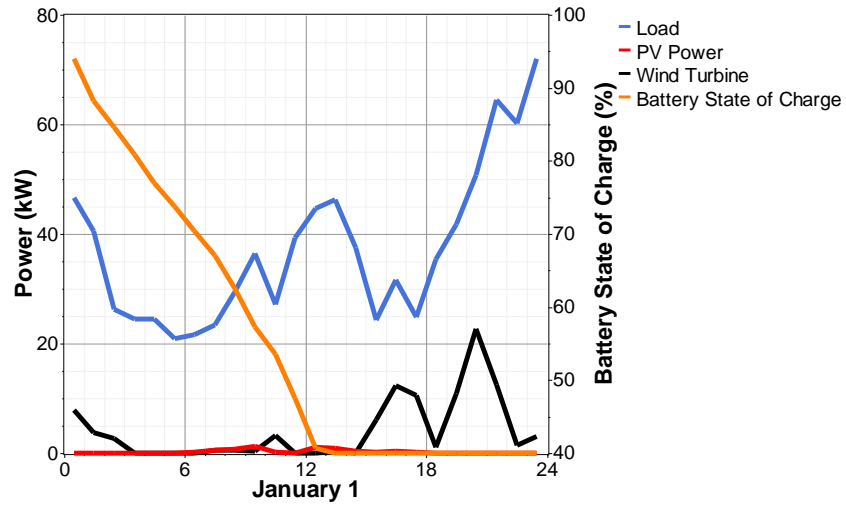


Figure 4.18: Discharge of batteries in low renewable energy availability [97].

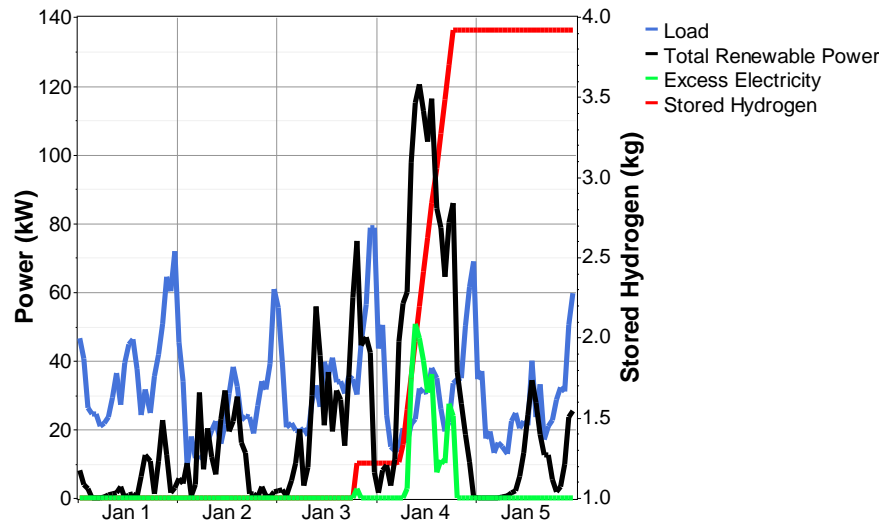


Figure 4.19: The effects of surplus electricity on the hydrogen tank [97].

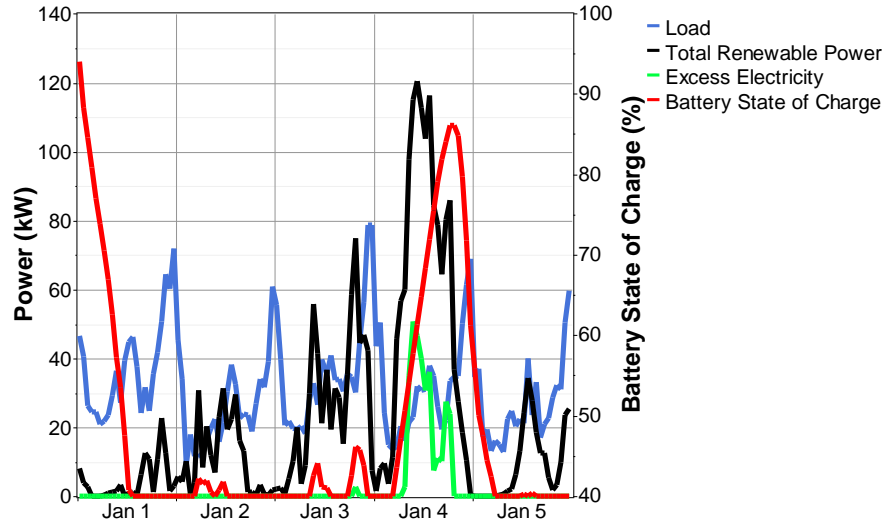


Figure 4.20: The effects of surplus electricity on the battery system [97].

Two additional cases for cost assessment were investigated which are: 1) the energy storage is only Battery; 2) the energy storage is only fuel cell and hydrogen system. The results are shown in Table 4.8 which were obtained by the same process in previous cost assessment cases of the hybrid power system. These two cases were compared with the optimal case of the proposed configuration which both battery and hydrogen tank were considered for energy storage.

It is found when the energy storage is only battery, the PV capacity is decreased by 5 kW, thereby meeting the load with less PV capacity and 4% cheaper than the proposed configuration. However, the surplus electricity for the proposed configuration, and when the energy storage is only battery, are 32.5%, and 25%, respectively. The surplus electricity of the proposed configuration is less because batteries are already charged with the surplus electricity and the load is already met by this configuration, hence, the rest of remaining energy appears as surplus electricity.

As far as the total costs are considered, when the energy storage is only battery, only 4% of costs were decreased in comparison with the proposed configuration. However, the overall performance of the system was significantly improved when both batteries and hydrogen system are considered as energy storage option because of less surplus electricity in the system. In conclusion, only battery system is a cost-effective choice but cannot be considered as efficient as the proposed configuration.

The most uneconomical case is for the system with only fuel cell and hydrogen as energy storage option since the costs were increased by 49% in comparison with the proposed configuration. Because number of units of wind turbines and PV system, due to their resource variability, must be high to satisfy the load. The surplus electricity is also much higher (52%) than the proposed configuration. Hence, this configuration is neither cost-effective nor efficient solution [97].

Table 4.8: The Optimal Case of the System [97].

Item	Value		
	Proposed configuration	Only battery	Only fuel cell and hydrogen
PV capacity (kW)	15	10	70
Wind turbine capacity (kW)	112.5	112.5	337.5
Fuel cell capacity (kW)	30	--	30
Operating hours of fuel cell (hours)	102	--	2796
Electrolyzer capacity (kW)	10	--	80
Hydrogen tank (kg)	10	--	70
Number of batteries	100	100	--

Inverter capacity (kW)	70	70	70
Surplus electricity (%)	25	32.5	52
Total costs (\$)	939,905	895,878	1,849,846

The main contribution of this section is to evaluate the feasibility of a hybrid power system with two energy storage system options as hydrogen tank and battery. The HOMER software which is based on the NPC method was used for the simulation and cost evaluation of the proposed configuration.

The optimal case was obtained which gives information on number of units of components in the system to meet the load with the lowest costs. Cost assessment was also investigated when only battery and only hydrogen tank were considered as energy storage options. It was found that the most uneconomical solution for the system is when only hydrogen tank is used as energy storage option.

The most cost-effective solution is when both hydrogen tank and batteries were considered as the energy storage system. The analysis of this section is useful for power system designers and planners in remote areas to determine optimal number of units of components before starting the project [97].

4.4. Conclusion

The main objective of this chapter is to investigate a standalone system design for wind generation and hybrid renewable energy systems. In the first section, a method and a corresponding two-step procedure are used for a wind power generation system design by wind energy potential

evaluation, reliability and costs assessment. The wind energy potential is investigated through the Weibull two-parameter model using the hourly wind speed data of a site in St. John's. An analytical method based on the fault tree analysis (FTA) and minimal cut sets is developed for the system reliability evaluation. A generic annual operation and maintenance (O&M) costs calculation formula is proposed based on the field data from NREL.

In the second section, a stand-alone hybrid renewable energy system is proposed, which consists of solar PV, wind turbine, and energy storage with the combination of battery and hydrogen. Cost optimization based on the net present cost (NPC) method is used for finding optimal sizing of individual components. The proposed stand-alone hybrid renewable energy system is suitable for supplying electricity in remote areas without access to the main grid.

Chapter 5: Proposed Guideline for Generation Planning Using Analytical Approach

5.1. Proposed Guideline

Chapter 5 proposes a guideline for generation planning with wind energy using the analytical approach. The MW capacity of conventional generators that can be replaced by wind energy systems while maintaining the same risk criteria is obtained and investments costs were determined.

In this thesis, the importance of reliability evaluation in generation planning was discussed in Chapters 1 and 2. Reliability has been viewed in two aspects, adequacy and system security. The main goal in generation adequacy evaluation is to determine the ability of generation units to satisfy a total load demand, where the transmission system is assumed to be 100% reliable. Hence, generation units and loads are the two main components that have to be modeled for the generation adequacy evaluation. Then, the generation adequacy was evaluated by a commonly used method called the loss of load approach. A general overview of the proposed generation adequacy evaluation is shown in Figure 5.1. As it can be seen generation adequacy has been done in four major steps: Step 1: Input data; Step 2: modeling generators; Step 3: load model; and Step 4: generation adequacy and cost calculation. These steps have been discussed in details in Figure 5.2.

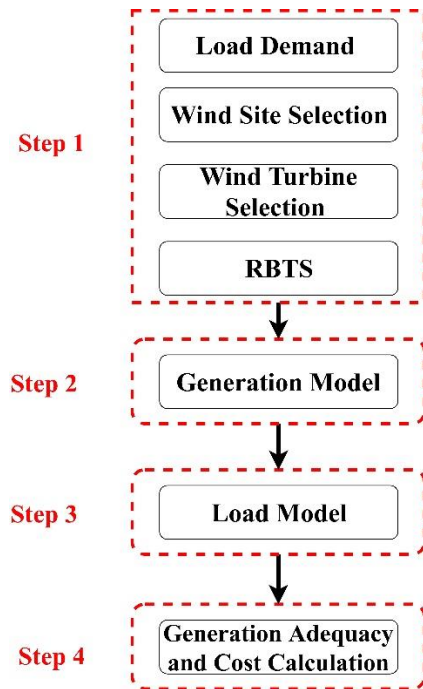


Figure 5.1: Proposed generation adequacy and cost evaluation.

Step 1 involves with input data required for the generation adequacy evaluation, which consists of wind site selection, historical hourly wind speed data, wind turbine specifications, a test system, conventional generators specifications, hourly load demand data, and risk criteria. After a wind site selected, historical hourly wind speeds can be obtained for the wind site by Climate Data - Climate - Environment Canada. Wind turbine specifications include wind turbine rated power, power curve characteristics, cut-in wind speed, cut-out wind speed, rated wind speed, and hub height of the wind turbine.

A test system can also be used for the generation adequacy evaluation. IEEE RBTS has been considered in this thesis. Conventional generators specifications include the number of generators, generators rated power, and FOR of each generator. Hourly load data and conventional generators

data are for the RBTS obtained from [113]. The risk criteria is a very important factor in generation adequacy.

One of the main objectives in generation planning with wind energy is replacing conventional generators with wind energy while maintaining the same risk criteria. One event in ten years is the industry-accepted risk standard by utilities which translates to LOLE of 0.1 days/year. One event in ten years risk criteria means that the power electric system meets the load demand such that the demand exceeds power generation only once in ten year period [114]. The risk criteria is also expressed in hours per year. Hence, one day in ten years risk criteria is treated as LOLE of 2.4 h/year [114]. LOLE in hours/year is a more precise risk criteria since an event might not last 24 hours ($2.4 \text{ hours}/0.1 \text{ days} = 24 \text{ hours}$) and it calculates outages in hours rather than days [115]. The risk criteria for the RBTS is LOLE of 1.05 h/year [72], which has been used in our study.

Step 2 involves with modeling conventional generators and wind energy system. In the generation adequacy evaluation, a generator model is represented in the form of arrays of capacity levels with the probability of each capacity level. In this thesis, the COPT model is used. Conventional generators are generally assumed in a two-state model, while wind energy systems are represented by a multi-state model. For wind generation system modeling, measured wind speeds are converted into wind speeds seen by the hub height of the wind turbine. If the wind speed measurement height is different than the hub height of the wind turbine, the power-law wind speed model should be used to convert measured historical hourly wind speed data to wind speeds experienced by the wind turbine hub height.

Wind speeds are then predicted by the ARMA model. After predicting wind speeds, the nonlinear relationship between wind speed and power output of wind turbine is represented by the power curve of wind turbine to generate hourly wind power output as a function of hourly predicted wind speeds using wind turbine power curve. The COPT of the wind energy system is then built. The COPT model can be obtained using the steps explained in Chapter 2.2. The number of COPT states is critical in generation adequacy evaluation because more states generally means a better modeling accuracy and a higher computation overhead. The FCM method can be used to reduce the number of COPT states with wind energy.

In Step 3, load model is constructed. A load model represents the system load level variation with respect to time for a specific period of time. The basic period of time for power system planning is one year [30]. Since the risk will be evaluated for a specific year, hourly load data for only that specific year is required. Different load models can be used for the generation adequacy evaluation depending on the availability of load demand data. The LDC model is the most frequently used load model in generation adequacy which has been used in this research and adopted from [113]. This load data is for the RBTS obtained from [113].

In Step 4, generation model constructed in Step 2 is combined with the load model to evaluate generation adequacy. Once generation and load models are determined, loss of load approach can be used to obtain risk index (LOLE). In loss of load method, the generation system is represented by the COPT and the load is represented by LDC. The “LOLE” index gives the information about the expected number of hours in the given time period; in which the hourly load exceeds the available capacity.

The capacity of wind farm replacing conventional generators can then be obtained by removing MW capacity of conventional generator from the RBTS and increasing MW capacity of wind farm until the risk criteria of LOLE=1.05 hours/year is obtained. After the generation adequacy is evaluated, investment costs of wind farm can be calculated. For cost calculations, investment cost of only one wind turbine is required as an input. Then, the investment costs of wind farm can be calculated by multiplying MW capacity required of wind farm obtained from generation adequacy and investment cost of a wind turbine [116]. The main goal is to obtain the minimum investment in which the risk criterion is not violated.

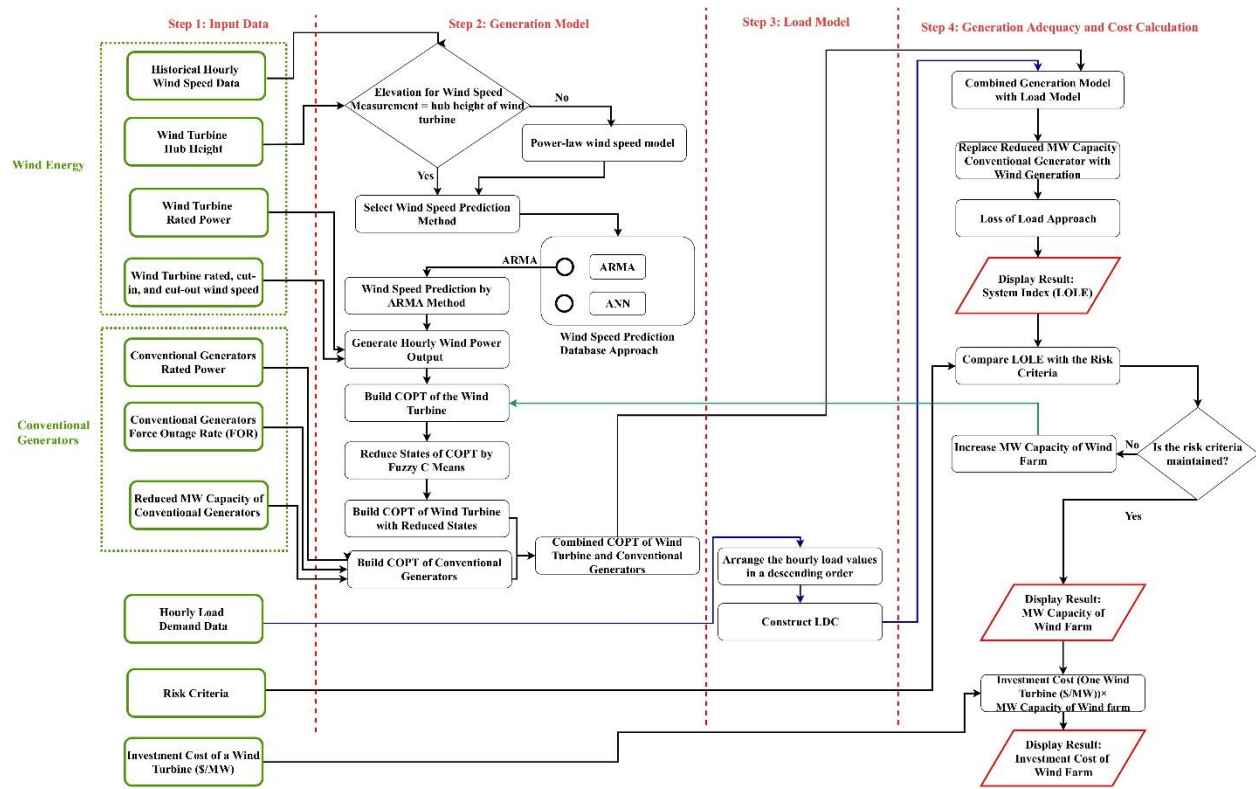


Figure 5.2: Proposed procedure for generation adequacy and cost evaluation with wind energy.

5.2. Cost Analysis

The cost calculation method is adopted from [116]. Wind farm investment cost can be obtained by multiplication of investment cost of a single wind turbine (\$/MW or \$/kW) and MW capacity of wind farm required to replace conventional generators. This method is clarified using a case study as follow.

The investment costs of the wind turbine and gas turbine are \$1200/kW, and \$700/kW, respectively [116]. The cost calculations of gas turbine will be done for comparison purpose. Generation adequacy and cost calculations are done for one year scenario with an annual peak load of 200 MW.

The main goal is to find the most suitable wind farm MW capacity to replace part of conventional generation in a large power grid where the costs are minimized and the risk criteria is maintained. Reliability index with wind farm capacity additions are shown in Table 5.1. It can be seen that the reliability criterion cannot be satisfied until 18 wind turbines are added to the system. The minimum investment to supply the incremental load at the risk criterion of LOLE = 1.05 hour/year is therefore 18 wind turbines for the wind farm in St. John's. Hence, wind farm capacity is $18 \times 2\text{MW} = 36\text{MW}$.

For comparison, reliability index with the addition of gas turbine rather than wind turbines is calculated, as shown in Table 5.2. The capacity of gas turbine is 5MW. With three additional gas turbine the LOLE is 0.9036 hours/year and the risk is acceptable. Hence, the minimum investment is three gas turbines with a total additional capacity of 15 MW. The investment costs of adding gas turbine or wind farm into the system are shown in Table 5.3. It can be noticed that gas turbine is

the most effective plan in terms of investment costs. However, as mentioned by [116], the operating costs of wind energy systems are usually much lower than gas turbines. Operating and maintenance costs of wind energy and gas turbine are calculated as \$1.0372 million, and \$6.57 million, respectively. Hence, if the objective is to find out the total costs including investment, operating and outage costs, wind energy systems are a good option for some particular areas rather than gas turbine.

Table 5.1: Generation adequacy evaluation.

Number of wind turbines	LOLE (hours/year)
1	3.167
2	2.833
3	2.518
4	2.240
5	2.002
6	1.819
7	1.669
8	1.550
9	1.451
10	1.355
11	1.285
12	1.234
13	1.186
14	1.140
15	1.106
16	1.079
17	1.061
18	1.047

19	1.036
20	1.025
21	1.018

Table 5.2: Gas turbine generator additions.

Number of gas turbine	Total Capacity (MW)	LOLE (hours/year)
0	240	3.562
1	245	2.347
2	250	1.430
3	255	0.9036
4	260	0.5316

Table 5.3: Investment comparison with WTG and gas turbines.

Alternative	Additional Capacity (MW)	Investment (\$)	O&M costs (\$)
Wind farm	36	43.2 million	1.0372 million
Gas turbine	15	10.5 million	6.57 million

5.3. Conclusion

In this chapter, a procedure and guideline for generation planning with wind power integration using the analytical approach is proposed. The cost analysis is also provided in the guideline.

Chapter 6: Conclusion and Future Work

This thesis focuses on analytical approach based generation planning with wind energy. An analytical method for generation adequacy with wind energy system was described in Chapter 3. Three steps are required for generation adequacy of wind energy systems which are load model, generator model, and risk model. Each of model was discussed in Chapter 3. The LDC over one year was used for load model. ARMA model which is the most frequently used model and it is suitable for generation adequacy evaluations was used for predicting wind speeds. The multi-state COPT model was used for conventional and wind energy generation model. After determining the load and generator model, the risk was determined using a recursive technique.

Standalone system designs for wind generation system design and hybrid renewable energy systems were investigated in Chapter 4. In the first part of this chapter, wind energy potential for a site in St. John's was investigated. Reliability was also evaluated by FTA and minimal cut sets. Following this, a generic cost formula was proposed by using the field data from NREL. A standalone hybrid renewable energy system consist of wind turbine, PV, and energy storage system with the combination of hydrogen and battery was proposed in the second part of this chapter. The costs of the proposed system were evaluated using NPC method. The main objective was determining optimal number of each component so that the load can be satisfied with the lowest costs.

The main objective of Chapter 5 was linking all of the technical aspects discussed through Chapters 1-4 for power system planning with wind energy. For this aim, a guideline and procedure for generation planning using analytical approach was proposed. The MW capacity of conventional generators required for replacing conventional generators while the same risk criteria

is maintained was determined. The minimum investment cost to supply the load at the risk criterion was also determined.

The main research contributions of this thesis are:

- Modeling of generation adequacy evaluation of conventional generators and wind energy systems using an analytical approach;
- Wind speed prediction by two methods ARMA and Neural Networks.
- An improved method using Fuzzy C means algorithm to obtain a number of states of wind turbine in the generation adequacy evaluation.
- Standalone system design for wind generation and hybrid renewable energy systems.
- Develop a procedure and guideline for generation planning with wind power integration using the analytical approach.

It is hoped that the explanations and results of this thesis will assist power system planners to evaluate economic and reliable with wind power.

The future work are listed as follows:

- Using different types of wind speed prediction modeling techniques such as MCMC and comparing with ARMA model;
- Energy storage system can be used in order to overcome fluctuation nature of wind generation system. This will reduce further the usage of conventional generators. Generation adequacy and cost analysis can be investigated considering both wind energy and energy storage system in replacing conventional generators while maintaining the same risk criteria.

- Generation adequacy using Monte Carlo simulation which is effective for large-scale systems with large number of components.

References

- [1] Arriaga, M., Caizares, C. A., & Kazerani, M. (2016). Long-term renewable energy planning model for remote communities. *IEEE Transactions on Sustainable Energy*, 7(1), 221-231.
- [2] Arriaga Marin, M. (2015). Long-term renewable energy generation planning for off-grid remote communities, PhD thesis, University of Waterloo.
- [3] Tan, Y., Meegahapola, L., & Muttaqi, K. M. (2014). A review of technical challenges in planning and operation of remote area power supply systems. *Renewable and Sustainable Energy Reviews*, 38, 876-889.
- [4] Renewables Global Status Report 2017. Available online: http://www.ren21.net/wp-content/uploads/2017/06/17-8399_GSR_2017_Full_Report_0621_Opt.pdf.
- [5] Long, H., Eghlimi, M., & Zhang, Z. (2017). Configuration Optimization and Analysis of a Large Scale PV/Wind System. *IEEE Transactions on Sustainable Energy*, 8(1), 84-93.
- [6] Grid integration of large-capacity Renewable Energy sources and use of large-capacity Electrical Energy Storage. Available Online: www.iec.ch/whitepaper/pdf/iecWP-gridintegrationlargecapacity-LR-en.pdf.
- [7] Patel, J. (2006). Reliability/cost evaluation of a wind power delivery system (Doctoral dissertation, University of Saskatchewan Saskatoon).
- [8] Moeini-Aghtaie, M., Abbaspour, A., & Fotuhi-Firuzabad, M. (2012). Incorporating large-scale distant wind farms in probabilistic transmission expansion planning—Part I: Theory and algorithm. *IEEE Transactions on Power Systems*, 27(3), 1585-1593.

- [9] NREL. Wind and solar energy curtailment: experience and practices in the United States. National Renewable Energy Laboratory; Mar. 2014. Available at: <http://www.nrel.gov/docs/fy14osti/60983.pdf>.
- [10] Li, H., Lu, Z., Qiao, Y., & Wang, N. (2017). A Non-sequential Probabilistic Production Simulation Method for Wind Energy Curtailment Evaluation Considering the Seasonal Heat Supply Constraints. *IEEE Transactions on Sustainable Energy*.
- [11] Ugranli, F., & Karatepe, E. (2016). Transmission Expansion Planning for Wind Turbine Integrated Power Systems Considering Contingency. *IEEE Transactions on Power Systems*, 31(2), 1476-1485.
- [12] Tomasson, E., & Soder, L. (2017). Generation Adequacy Analysis of Multi-Area Power Systems with a High Share of Wind Power. *IEEE Transactions on Power Systems*.
- [13] Nguyen, N., & Mitra, J. (2017). Reliability of Power System with High Wind Penetration under Frequency Stability Constraint. *IEEE Transactions on Power Systems*.
- [14] Aien, M., Hajebrahimi, A., & Fotuhi-Firuzabad, M. (2016). A comprehensive review on uncertainty modeling techniques in power system studies. *Renewable and Sustainable Energy Reviews*, 57, 1077-1089.
- [15] Talari, S., Shafie-khah, M., Osório, G. J., Aghaei, J., & Catalão, J. P. (2017). Stochastic modelling of renewable energy sources from operators' point-of-view: A survey. *Renewable and Sustainable Energy Reviews*.

- [16] Oree, V., Hassen, S. Z. S., & Fleming, P. J. (2017). Generation expansion planning optimisation with renewable energy integration: A review. *Renewable and Sustainable Energy Reviews*, 69, 790-803.
- [17] Santos, S. F., Fitiwi, D. Z., Bizuayehu, A. W., Shafie-Khah, M., Asensio, M., Contreras, & Catalão, J. P. (2017). Impacts of Operational Variability and Uncertainty on Distributed Generation Investment Planning: A Comprehensive Sensitivity Analysis. *IEEE Transactions on Sustainable Energy*, 8(2), 855-869.
- [18] Seifi, Hossein, and Mohammad Sadegh Sepasian. *Electric power system planning: issues, algorithms and solutions*. Springer Science & Business Media, 2011.
- [19] Choi, J., Mount, T. D., Thomas, R. J., Billinton, R. Probabilistic reliability criterion for planning transmission system expansions. *IEE Proceedings-Generation, Transmission and Distribution*, 153(6), 719-727, 2006.
- [20] Arman, S. I. (2016). *Bulk System Adequacy Assessment Incorporating Wind and Solar Energy* (Master Of Science Thesis).
- [21] Chowdhury, A. A., & Koval, D. O. (2001). Deregulated transmission system reliability planning criteria based on historical equipment performance data. *IEEE Transactions on Industry Applications*, 37(1), 204-211.
- [22] Hemmati, R., Hooshmand, R. A., & Khodabakhshian, A. (2013). State-of-the-art of transmission expansion planning: Comprehensive review. *Renewable and Sustainable Energy Reviews*, 23, 312-319.

- [23] Li, W., & Choudhury, P. (2007). Probabilistic transmission planning. *IEEE power and energy magazine*, 5(5), 46-53.
- [24] Huang, D. (2010). Bulk electric system reliability evaluation incorporating wind power and demand side management. Doctor of Philosophy Thesis, University of Saskatchewan.
- [25] Ren, Z., Li, W., Billinton, R., & Yan, W. (2016). Probabilistic power flow analysis based on the stochastic response surface method. *IEEE Transactions on Power Systems*, 31(3), 2307-2315.
- [26] Prusty, B. R., & Jena, D. (2016). A critical review on probabilistic load flow studies in uncertainty constrained power systems with photovoltaic generation and a new approach. *Renewable and Sustainable Energy Reviews*.
- [27] Aien M, Fotuhi-Firuzabad M, Aminifar F. Probabilistic load flow in correlated uncertain environment using unscented transformation. *IEEE Trans Power Syst* 2012;27(4):2233-41.
- [28] Almutairi, A. (2014). Evaluating Wind Power Generating Capacity Adequacy Using MCMC Time Series Model. Master Thesis, University of Waterloo.
- [29] Allan, R., & Billinton, R. (2000). Probabilistic assessment of power systems. *Proceedings of the IEEE*, 88(2), 140-162.
- [30] Billinton, R., Karki, R., Gao, Y., Huang, D., Hu, P., & Wangdee, W. (2012). Adequacy assessment considerations in wind integrated power systems. *IEEE Transactions on Power Systems*, 27(4), 2297-2305.

- [31] Liang, X., & Bagen, B. (2015). Probabilistic planning and risk analysis for renewable power generation system. In Proceedings of CIGRE Canada Conference, Winnipeg, Manitoba (Vol. 31).
- [32] Almutairi, A., Ahmed, M. H., & Salama, M. M. A. (2015). Probabilistic generating capacity adequacy evaluation: Research roadmap. *Electric Power Systems Research*, 129, 83-93.
- [33] Almutairi, A., Ahmed, M. H., & Salama, M. M. A. (2014, November). Inclusion of Wind Generation Modeling into the Conventional Generation Adequacy Evaluation. In *Electrical Power and Energy Conference (EPEC), 2014 IEEE* (pp. 122-127). IEEE.
- [34] Billinton, R., & Huang, D. (2011). Incorporating wind power in generating capacity reliability evaluation using different models. *IEEE Transactions on Power Systems*, 26(4), 2509-2517.
- [35] Karki, R., Hu, P., & Billinton, R. (2006). A simplified wind power generation model for reliability evaluation. *IEEE transactions on Energy conversion*, 21(2), 533-540.
- [36] Abdullah, M. A., Muttaqi, K. M., Agalgaonkar, A. P., & Sutanto, D. (2014). A noniterative method to estimate load carrying capability of generating units in a renewable energy rich power grid. *IEEE Transactions on Sustainable Energy*, 5(3), 854-865.
- [37] Vallee, F., Lobry, J., & Deblecker, O. (2008). System reliability assessment method for wind power integration. *IEEE Transactions on Power Systems*, 23(3), 1288-1297.
- [38] Sarkar, S., & Ajarapu, V. (2011). MW resource assessment model for a hybrid energy conversion system with wind and solar resources. *IEEE transactions on sustainable energy*, 2(4), 383-391.

- [39] Almutairi, A., Ahmed, M. H., & Salama, M. M. A. (2016). Use of MCMC to incorporate a wind power model for the evaluation of generating capacity adequacy. *Electric Power Systems Research*, 133, 63-70.
- [40] Aries, N., Boudia, S. M., & Ounis, H. (2018). Deep assessment of wind speed distribution models: A case study of four sites in Algeria. *Energy Conversion and Management*, 155, 78-90.
- [41] Dabbaghiyan, A., Fazelpour, F., Abnavi, M. D., & Rosen, M. A. (2016). Evaluation of wind energy potential in province of Bushehr, Iran. *Renewable and Sustainable Energy Reviews*, 55, 455-466.
- [42] Ayodele, T. R., & Ogunjuyigbe, A. S. O. (2016). Wind energy potential of Vesleskarvet and the feasibility of meeting the South African' s SANAE IV energy demand. *Renewable and Sustainable Energy Reviews*, 56, 226-234.
- [43] Leite, A. P., Borges, C. L., & Falcao, D. M. (2006). Probabilistic wind farms generation model for reliability studies applied to Brazilian sites. *IEEE Transactions on Power Systems*, 21(4), 1493-1501.
- [44] Sulaeman, S., Benidris, M., Mitra, J., & Singh, C. (2017). A wind farm reliability model considering both wind variability and turbine forced outages. *IEEE Transactions on Sustainable Energy*, 8(2), 629-637.

- [45] Guo, Y., Gao, H., & Wu, Q. (2017). A meteorological information mining-based wind speed model for adequacy assessment of power systems with wind power. *International Journal of Electrical Power & Energy Systems*, 93, 406-413.
- [46] Karki, R., Hu, P., & Billinton, R. (2006). A simplified wind power generation model for reliability evaluation. *IEEE transactions on Energy conversion*, 21(2), 533-540.
- [47] Ding, Y., Wang, P., Goel, L., Loh, P. C., & Wu, Q. (2011). Long-term reserve expansion of power systems with high wind power penetration using universal generating function methods. *IEEE Transactions on Power Systems*, 26(2), 766-774.
- [48] Miao, S., Xie, K., Yang, H., Tai, H. M., & Hu, B. (2017). A Markovian wind farm generation model and its application to adequacy assessment. *Renewable Energy*, 113, 1447-1461.
- [49] Ghaedi, A., Abbaspour, A., Fotuhi-Firuzabad, M., & Moeini-Aghtaie, M. (2014). Toward a comprehensive model of large-scale DFIG-based wind farms in adequacy assessment of power systems. *IEEE Transactions on Sustainable Energy*, 5(1), 55-63.
- [50] Zubo, R. H., Mokryani, G., Rajamani, H. S., Aghaei, J., Niknam, T., & Pillai, P. (2017). Operation and planning of distribution networks with integration of renewable distributed generators considering uncertainties: A review. *Renewable and Sustainable Energy Reviews*, 72, 1177-1198.
- [51] Sharifzadeh, M., Lubiano-Walochik, H., & Shah, N. (2017). Integrated renewable electricity generation considering uncertainties: The UK roadmap to 50% power generation from wind and solar energies. *Renewable and Sustainable Energy Reviews*, 72, 385-398.

- [52] Dolatabadi, A., Mohammadi-ivatloo, B., Abapour, M., & Tohidi, S. (2017). Optimal Stochastic Design of Wind Integrated Energy Hub. *IEEE Transactions on Industrial Informatics*.
- [53] Hajipour, E., Bozorg, M., & Fotuhi-Firuzabad, M. (2015). Stochastic capacity expansion planning of remote microgrids with wind farms and energy storage. *IEEE Transactions on Sustainable Energy*, 6(2), 491-498.
- [54] De Giorgi, M. G., Ficarella, A., & Tarantino, M. (2011). Error analysis of short term wind power prediction models. *Applied Energy*, 88(4), 1298-1311.
- [55] Billinton, R., Chen, H., & Ghajar, R. (1996). Time-series models for reliability evaluation of power systems including wind energy. *Microelectronics Reliability*, 36(9), 1253-1261.
- [56] Lino, Angel Andres Recalde. "Reliability Evaluation of Distribution Networks With Wind Turbines And Pv Panels." Master Degree Thesis, The University of Queensland, 2013.
- [57] M. Hurvich, and C. Tsai, "Bias of the corrected AIC criterion for underfitted regression and time series models," *Biometrika*, vol. 78, no. 3, pp. 499-509, 1991.
- [58] A. Ahadi, X. Liang, and W. Li, "An Analytical Method for Wind Energy Potential, Reliability, and Cost Assessment for Wind Generation Systems", *Industrial and Commercial Power Systems Technical Conference (I&CPS), 2017 IEEE/IAS 53rd*. May 2017.
- [59] "Historical Climate Data- Climate- Environment Canada". Retrieved from <http://Climate.weather.gc.ca/> [accessed 2016.09.13].
- [60] Vestas Wind Systems. Retrieved from <https://www.vestas.com/> [accessed 2016.09.14].

- [61] Allouhi, A., Zamzoum, O., Islam, M. R., Saidur, R., Kousksou, T., Jamil, A., & Derouich, A. (2017). Evaluation of wind energy potential in Morocco's coastal regions. *Renewable and Sustainable Energy Reviews*, 72, 311-324.
- [62] Shu, Z. R., Li, Q. S., & Chan, P. W. (2015). Investigation of offshore wind energy potential in Hong Kong based on Weibull distribution function. *Applied Energy*, 156, 362-373.
- [63] Ata, R. (2015). Artificial neural networks applications in wind energy systems: a review. *Renewable and Sustainable Energy Reviews*, 49, 534-562.
- [64] Da Silva, I. N., Spatti, D. H., Flauzino, R. A., Liboni, L. H. B., & dos Reis Alves, S. F. (2016). *Artificial Neural Networks: A Practical Course*. Springer.
- [65] Yu, H., & Wilamowski, B. M. (2011). Levenberg–Marquardt training, industrial electronics handbook, vol 5—Intelligent systems. CRC Press, Boca Raton.
- [66] Ticknor, J. L. (2013). A Bayesian regularized artificial neural network for stock market forecasting. *Expert Systems with Applications*, 40(14), 5501-5506.
- [67] Møller, M. F. (1993). A scaled conjugate gradient algorithm for fast supervised learning. *Neural networks*, 6(4), 525-533.
- [68] Falas, T., & Stafylopatis, A. (2002, November). Temporal differences learning with the scaled conjugate gradient algorithm. In *Neural Information Processing, 2002. ICONIP'02. Proceedings of the 9th International Conference on* (Vol. 5, pp. 2625-2629). IEEE.
- [69] Gao, Y. (2006). Adequacy assessment of electric power systems incorporating wind and solar energy (Master of Science thesis), University of Saskatchewan.

- [70] R. Billinton and et al, "A Reliability Test System for Educational Purposes Basic Data", IEEE Transactions on Power Systems, Vol. PWRS-3, No. 4, August 1989, pp. 1238-1244.
- [71] Karki, R., & Billinton, R. (2001). Reliability/cost implications of PV and wind energy utilization in small isolated power systems. IEEE Transactions on Energy Conversion, 16(4), 368-373.
- [72] Billinton, R., & Bai, G. (2004). Generating capacity adequacy associated with wind energy. IEEE transactions on energy conversion, 19(3), 641-646.
- [73] Amir Ahadi, and Xiaodong Liang, "Generation Adequacy Evaluation Using Fuzzy C–Means Method – A Case Study", accepted by 31st Annual IEEE Canadian Conference on Electrical and Computer Engineering (CCECE 2018), Québec City, Québec, Canada, May 13-16, 2018.
- [74] Bezdec, J.C., Pattern Recognition with Fuzzy Objective Function Algorithms, Plenum Press, New York, 1981.
- [75] Ahadi, A., Reza, S. E., & Liang, X. (2017, March). Probabilistic reliability evaluation for power systems with high penetration of renewable power generation. In Industrial Technology (ICIT), 2017 IEEE International Conference on (pp. 464-468). IEEE.
- [76] K. Abed, A. El-Mallah, "Capacity factor of wind turbines," Energy, vol. 22, no. 5, pp.487-491, 1997.

- [77] B. Falahati, A. Kargarian, and Y. Fu, "Timeframe capacity factor reliability model for isolated microgrids with renewable energy resources," 2012 IEEE Power and Energy Society General Meeting pp. 1-8.
- [78] NREL Transparent Cost Database. Available from: <http://en.openei.org/apps/TCDB/#blank>.
- [79] Das, B. K., Hoque, N., Mandal, S., Pal, T. K., & Raihan, M. A. (2017). A techno-economic feasibility of a stand-alone hybrid power generation for remote area application in Bangladesh. *Energy*.
- [80] Billinton, R. (2005). Evaluation of different operating strategies in small stand-alone power systems. *IEEE Transactions on energy conversion*, 20(3), 654-660.
- [81] Xie, K., & Billinton, R. (2011). Determination of the optimum capacity and type of wind turbine generators in a power system considering reliability and cost. *IEEE Transactions on Energy Conversion*, 26(1), 227-234.
- [82] Jordan Lofthouse, Randy T Simmons, and Ryan M. Yonk, "Reliability of Renewable Energy: Wind", The Institute of Political Economy (IPE) at Utah State University, <http://www.strata.org/reliability-of-renewable-energy-wind/>, visited at 10:14 am Feb 6, 2017.
- [83] Joshi, D. R., & Jangamshetti, S. H. (2010). A novel method to estimate the o&m costs for the financial planning of the wind power projects based on wind speed—A case study. *IEEE Transactions on Energy Conversion*, 25(1), 161-167.

- [84] Schweizer, J., Antonini, A., Govoni, L., Gottardi, G., Archetti, R., Supino, E., ... & Ozzi, C. (2016). Investigating the potential and feasibility of an offshore wind farm in the Northern Adriatic Sea. *Applied Energy*, 177, 449-463.
- [85] Dahmani, O., Bourguet, S., Machmoum, M., Guerin, P., Rhein, P., & Josse, L. (2017). Optimization and Reliability Evaluation of an Offshore Wind Farm Architecture. *IEEE Transactions on Sustainable Energy*, 8(2), 542-550.
- [86] Pérez, J. M. P., Márquez, F. P. G., Tobias, A., & Papaelias, M. (2013). Wind turbine reliability analysis. *Renewable and Sustainable Energy Reviews*, 23, 463-472.
- [87] Huang, H. S. (2007, November). Distributed genetic algorithm for optimization of wind farm annual profits. In *Intelligent Systems Applications to Power Systems, 2007. ISAP 2007. International Conference on* (pp. 1-6). IEEE.
- [88] Bilbao, M., & Alba, E. (2009, September). Simulated annealing for optimization of wind farm annual profit. In *Logistics and Industrial Informatics, 2009. LINDI 2009. 2nd International* (pp. 1-5). IEEE.
- [89] Akdağ, S. A., & Dinler, A. (2009). A new method to estimate Weibull parameters for wind energy applications. *Energy conversion and management*, 50(7), 1761-1766.
- [90] Ayodele, T. R., & Ogunjuyigbe, A. S. O. (2016). Wind energy potential of Vesleskarvet and the feasibility of meeting the South African' s SANAE IV energy demand. *Renewable and Sustainable Energy Reviews*, 56, 226-234.

- [91] Shi, X., & Bazzi, A. M. (2015, February). Fault tree reliability analysis of a micro-grid using Monte Carlo simulations. In Power and Energy Conference at Illinois (PECI), 2015 IEEE (pp. 1-5). IEEE.
- [92] Anthony, M., Arno, R., Dowling, N., & Schuerger, R. (2013). Reliability analysis for power to fire pump using fault tree and RBD. IEEE Transactions on Industry Applications, 49(2), 997-1003.
- [93] Ahadi, A., Ghadimi, N., & Mirabbasi, D. (2014). Reliability assessment for components of large scale photovoltaic systems. Journal of Power Sources, 264, 211-219.
- [94] Christopher A. Walford, “Wind Turbine Reliability: Understanding and Minimizing Wind Turbine Operation and Maintenance Costs”, Sandia Report prepared by Sandia National Laboratories, Albuquerque, New Mexico 87185 and Livermore, California 94550, March 2006 (<http://prod.sandia.gov/techlib/access-control.cgi/2006/061100.pdf>).
- [95] R. Poore, and C. Walford, “Development of an Operations and Maintenance Cost Model to Identify Cost of Energy Savings for Low Wind Speed Turbines”, National Renewable Energy Laboratory (NREL), 1617 Cole Boulevard, Golden, Colorado 80401-3393, United States, January 2008 (<http://www.nrel.gov/docs/fy08osti/40581.pdf>).
- [96] “Operation and Maintenance Costs of Wind Generated Power”, <https://www.wind-energy-the-facts.org/operation-and-maintenance-costs-of-wind-generated-power.html>. Accessed at 3:17 pm on Feb 20, 2017.

- [97] Ahadi, A., & Liang, X. (2017, March). A stand-alone hybrid renewable energy system assessment using cost optimization method. In Industrial Technology (ICIT), Toronto, ON, Canada 2017 IEEE International Conference on (pp. 376-381). IEEE.
- [98] Ma, T., Yang, H., & Lu, L. (2014). A feasibility study of a stand-alone hybrid solar–wind–battery system for a remote island. *Applied Energy*, 121, 149-158.
- [99] Al Busaidi, A. S., Kazem, H. A., Al-Badi, A. H., & Khan, M. F. (2016). A review of optimum sizing of hybrid PV–Wind renewable energy systems in oman. *Renewable and Sustainable Energy Reviews*, 53, 185-193.
- [100] Tamalouzt, S., Benyahia, N., Rekioua, T., Rekioua, D., & Abdessemed, R. (2016). Performances analysis of WT-DFIG with PV and fuel cell hybrid power sources system associated with hydrogen storage hybrid energy system. *International Journal of Hydrogen Energy*, 41(45), 21006-21021.
- [101] Kalinci, Y., Hepbasli, A., & Dincer, I. (2015). Techno-economic analysis of a stand-alone hybrid renewable energy system with hydrogen production and storage options. *International Journal of Hydrogen Energy*, 40(24), 7652-7664.
- [102] Natural Resources Canada, Wind-Hydrogen-Diesel on Ramea Island [Online]. Available from: <https://www.nrcan.gc.ca/energy/renewable-electricity/wind/7319>, Accessed on October 2016.

- [103] Bahramara, S., Moghaddam, M. P., & Haghifam, M. R. (2016). Optimal planning of hybrid renewable energy systems using HOMER: A review. *Renewable and Sustainable Energy Reviews*, 62, 609-620.
- [104] Connolly, D., Lund, H., Mathiesen, B. V., & Leahy, M. (2010). A review of computer tools for analysing the integration of renewable energy into various energy systems. *Applied Energy*, 87(4), 1059-1082.
- [105] Luna-Rubio, R., Trejo-Perea, M., Vargas-Vázquez, D., & Ríos-Moreno, G. J. (2012). Optimal sizing of renewable hybrids energy systems: A review of methodologies. *Solar Energy*, 86(4), 1077-1088.
- [106] HOMER Energy LLC. Available from: <http://homerenergy.com/index.html>.
- [107] Lambert, T., Gilman, P., & Lilienthal, P. (2006). Micropower system modeling with HOMER. *Integration of alternative sources of energy*, 379-418.
- [108] HOMER Pro Version 3.7 User Manual. Available from: www.homerenergy.com/pdf/HOMERHelpManual.pdf. Accessed on November 2016.
- [109] Zhang, N., Sutanto, D., & Muttaqi, K. M. (2016). A review of topologies of three-port DC–DC converters for the integration of renewable energy and energy storage system. *Renewable and Sustainable Energy Reviews*, 56, 388-401.
- [110] Rehman, Z., Al-Bahadly, I., & Mukhopadhyay, S. (2015). Multiinput DC–DC converters in renewable energy applications—An overview. *Renewable and Sustainable Energy Reviews*, 41, 521-539.

- [111] Surface meteorology and solar energy. Available from: <http://eosweb.larc.nasa.gov/sse/>. Accessed on October 2016.
- [112] Sigarchian, S. G., Paleta, R., Malmquist, A., & Pina, A. (2015). Feasibility study of using a biogas engine as backup in a decentralized hybrid (PV/wind/battery) power generation system—Case study Kenya. *Energy*, 90, 1830-1841.
- [113] R. Billinton, et. al, “A reliability test system for educational purposes-basic data,” *IEEE Transactions on Power Systems*, 4(3), 1238-1244, 1989.
- [114] Pfeifenberger, J. P., Spees, K., Carden, K., & Wintermantel, N. (2013). Resource adequacy requirements: Reliability and economic implications. The Brattle Group. Available Online: <https://www.ferc.gov/legal/staff-reports/2014/02-07-14-consultant-report.pdf>.
- [115] A Probabilistic Method to Assess Power Supply Adequacy for the Pacific Northwest. NW Power And Conservation Council 2011. Available Online: https://www.nwcouncil.org/media/8932/Adequacy_Standard_Background_2008_07a_.pdf.
- [116] Chen, Hua. "Generating system reliability optimization." Published PhD thesis, University of Saskatchewan (2000).
- [117] Amir Ahadi, and Xiaodong Liang, "Wind Speed Time Series Predicted by Neural Network", accepted by 31st Annual IEEE Canadian Conference on Electrical and Computer Engineering (CCECE 2018), Québec City, Québec, Canada, May 13-16, 2018.

Appendix: List of Refereed Publications

- [1] Amir Ahadi, and Xiaodong Liang, "Wind Speed Time Series Predicted by Neural Network", accepted by 31st Annual IEEE Canadian Conference on Electrical and Computer Engineering (CCECE 2018), Québec City, Québec, Canada, May 13-16, 2018.
- [2] Amir Ahadi, and Xiaodong Liang, "Generation Adequacy Evaluation Using Fuzzy C–Means Method – A Case Study", accepted by 31st Annual IEEE Canadian Conference on Electrical and Computer Engineering (CCECE 2018), Québec City, Québec, Canada, May 13-16, 2018.
- [3] Muhammad Sifatul Alam Chowdhury, Md. Arman Uddin, Khandakar Abdulla Al Mamun, Xiaodong Liang, and Amir Ahadi, “Concentrated Solar Power Generation in A Remote Island”, accepted by 31st Annual IEEE Canadian Conference on Electrical and Computer Engineering (CCECE 2018), Québec City, Québec, Canada, May 13-16, 2018.
- [4] Amir Ahadi, Xiaodong Liang, and Weixing Li, “An Analytical Method for Wind Energy Potential, Reliability, and Cost Assessment for Wind Generation Systems”, accepted by 2017 IEEE Industrial and Commercial Power Systems (I&CPS) Conference, pp. 1-11, May 7th - 11th, Niagara Falls, ON, Canada, 2017.
- [5] Amir Ahadi, and Xiaodong Liang, “A Stand-Alone Hybrid Renewable Energy System Assessment Using Cost Optimization Method”, Proceedings of the IEEE Industrial Electronics Society's 18th International Conf. on Industrial Technology (ICIT), pp. 1-6, Toronto, Canada, March 22-25, 2017.
- [6] Amir Ahadi, Syed Enam Reza, and Xiaodong Liang, “Probabilistic Reliability Evaluation for Power Systems with High Penetration of Renewable Power Generation”, Proceedings of

the IEEE Industrial Electronics Society's 18th International Conf. on Industrial Technology (ICIT), pp. 1-5, Toronto, Canada, March 22-25, 2017.